2013

LATEXIN'S ROLE IN REGULATING HEMATOPOIETIC STEM AND PROGENITOR CELLS

Yi Liu
University of Kentucky, glory19831029@gmail.com

STUDENT AGREEMENT:

I represent that my thesis or dissertation and abstract are my original work. Proper attribution has been given to all outside sources. I understand that I am solely responsible for obtaining any needed copyright permissions. I have obtained and attached hereto needed written permission statements(s) from the owner(s) of each third-party copyrighted matter to be included in my work, allowing electronic distribution (if such use is not permitted by the fair use doctrine).

I hereby grant to The University of Kentucky and its agents the non-exclusive license to archive and make accessible my work in whole or in part in all forms of media, now or hereafter known. I agree that the document mentioned above may be made available immediately for worldwide access unless a preapproved embargo applies.

I retain all other ownership rights to the copyright of my work. I also retain the right to use in future works (such as articles or books) all or part of my work. I understand that I am free to register the copyright to my work.

REVIEW, APPROVAL AND ACCEPTANCE

The document mentioned above has been reviewed and accepted by the student's advisor, on behalf of the advisory committee, and by the Director of Graduate Studies (DGS), on behalf of the program; we verify that this is the final, approved version of the student's dissertation including all changes required by the advisory committee. The undersigned agree to abide by the statements above.

Yi Liu, Student

Dr. Gary Van Zant, Major Professor

Dr. Bret Smith, Director of Graduate Studies

LATEXIN'S ROLE IN REGULATING HEMATOPOIETIC STEM AND PROGENITOR CELLS

DISSERTATION

A dissertation submitted in partial fulfillment of the
requirements for the degree of Doctor of Philosophy in the
College of Medicine
at the University of Kentucky

By
Yi Liu

Lexington, Kentucky

Director: Dr. Gary Van Zant, Professor of Medicine and Physiology
Co-Director: Dr. Steve Estus, Professor of Physiology

Lexington, Kentucky

2013

ABSTRACT OF DISSERTATION

LATEXIN'S ROLE IN REGULATING HEMATOPOIETIC STEM AND PROGENITOR CELLS

Previous studies in our lab identified a novel gene, latexin (*Lxn*), that regulates murine hematopoietic stem cells through balancing apoptosis, self-renewal and proliferation. In these dissertation studies, I performed a series of experiments to examine the function of *Lxn* using a *Lxn* conventional knockout mouse, and characterize *Lxn*'s role in the presence of hematopoietic stresses such as ionizing radiation, cytokines induced-mobilization, and hematopoietic malignancy.

The first series of experiments was designed to determine the role of *Lxn* in hematopoiesis under homeostatic conditions. I found that *Lxn-/-* mice exhibited hyperproliferative hematopoiesis, a repopulation advantage and elevated self-renewal capacity which was intrinsic to the *Lxn-/-* hematopoietic cells. Furthermore, I identified a reduction in apoptotic frequency in *Lxn-/-* hematopoietic progenitors, which may account for the expansion seen in the progenitor population.

In a second series of experiments, I discovered a role of *Lxn* in the radio-sensitivity of hematopoietic cells. I found that loss of *Lxn* in mice confers resistance to ionizing radiation. *Lxn*-/- mice showed rapid hematological recoveries after radiation exposure at the stem and progenitor cell (HSPC) level. The ablation of *Lxn* hindered irradiation-induced apoptosis which may underlie the radiation resistance through regulating hematopoietic recovery.

In a third series of experiments, I studied the interaction of *Lxn-/-* stem and progenitor cells with their microenvironment. Using a granulocyte colony-stimulating factor-induced mobilization model, I determined that the ability of HSPCs to mobilize into the bloodstream was significantly increased in *Lxn*-/- mice. The adhesive properties of hematopoietic cells were compromised in *Lxn-/-* animals. Gene expression studies on progenitor cells identified cell-to-ECM interactions were down-regulated upon *Lxn* deletion, implying the enhanced

mobilization efficiency of hematopoietic cells from *Lxn-/-* mice correlated with reduced adhesion of hematopoietic progenitor cells to stroma.

Last, but not least, I performed a series of experiments to study the putative tumor suppressor role of *Lxn* in hematological malignancy. I found that *Lxn* expression was down-regulated in primary tumor and tumor cell lines by promoter methylation. Overexpression of *Lxn* inhibited lymphoma cell growth both in vitro and in vivo. Overexpressed *Lxn* increased apoptosis frequency by suppressing the expression of several anti-apoptotic genes, and therefore reduced the tumor growth.

KEYWORDS: Latexin, hyperproliferative hematopoiesis, radio-resistance, cell retention, apoptosis

Yi Liu
Student's Signature

September 06, 2013
Date

LATEXIN'S ROLE IN REGULATING HEMATOPOIETIC STEM AND PROGENITOR CELLS

By

Yi Liu

Gary Van Zant, Ph.D.
Director of Dissertation

Steve Estus Ph.D.
Co-Director of Dissertation

Bret Smith, Ph.D.
Director of Graduate Studies

September 06, 2013
Date

I would like to dedicate this dissertation to my husband Xiangrong Li, to my parents, Ping He and Bin Liu, and to my dearest friends from University of Kentucky, in appreciation for their unconditional supports and priceless friendships.

ACKNOWLEGEMENT

For this dissertation, I would like to gratefully and sincerely thank Dr. Gary Van Zant for his guidance, patience, and most importantly, his friendship during my graduate studies at University of Kentucky. Life blessed me with the opportunity to meet Dr. Gary Van Zant. He embraced me as an inexperienced lab volunteer and kindly gave me the chance to become a graduate student in his lab. His dedication to scientific research has inspired me to become a qualified scientist. His mentorship is paramount in equipping me with a faith of life-long pursuit of knowledge.

Many thanks to my committee members Dr. Steve Estus, Dr. Charlotte Peterson, and Dr. James Geddes for their encouragement, suggestions, and guidance both in scientific research and my graduate studies. I also would like to thank Dr. Misung Jo for serving as the outside examiner for this dissertation. I am deeply grateful for their insightful comments that helped me complete this dissertation.

The studies described in this dissertation are built upon studies started by Dr. Ying Liang, Dr. Erin Oakley and many other individuals in the Van Zant lab. I would like to express my gratitude to Dr. Ying Liang for her creative work, thoughtful instruction, and priceless friendship. I also would like to thank Dr. Erin Oakley and Dr. Scott Bryson for their suggestions and help in editing this dissertation. Moreover, my appreciation is also given to my colleagues and friends from my Lab: Kyle Rector, Carol Swiderski, Barry Grimes, Amanda Waterstrat and Ailing Li. I am very fortunate to have worked in an amicable lab

where I made lifelong friends.

Last but not least, I want to show my appreciation for my parents, grandparents, and my husband for their faith in me and support for my work. I am deeply grateful for Xiangrong, my considerate husband, unconditional supporter, and best friend. I thank him for going through hard times and wonderful experiences with me.

TABLE OF CONTENTS

LIST OF TABLES

LIST OF FIGURES

CHAPTER 1: INTRODUCTION

1.1 Hematopoiesis and hematopoietic stem cell

Hematopoiesis is the developmental process of blood formation. Blood is composed of as many as eight specialized blood cell types, including granulocytes, lymphocytes, erythrocytes (red blood cells) and thrombocytes (platelets). Different cell types perform distinct biological functions, ranging from nutrient and oxygen supply, blood coagulation, and pathogen defense. Since these blood cells have a limited lifespan, a large pool must be replenished continuously. In a healthy adult, approximately 10^{11}-10^{12} new blood cells are produced daily, by a small number of hematopoietic stem cells (~10^5)(HSCs)[1-3].

HSCs reside in bone marrow (BM) and have the unique capacity to give rise to a large population of mature blood cells of various lineages. Much like stem cells from other tissues, pluripotent differentiation potential and highly conserved self-renewal capacity are common features of HSCs. 1) HSCs reside on top of the hematopoietic hierarchy. A small number of HSCs are able to rapidly accomplish their regenerative task via the generation of very proliferative multi-potent progenitor cells (MPPs). These cells differentiate into lineage-committed progenitor cells such as common lymphoid progenitor (CLP) and common myeloid progenitors (CMP). The lineage committed progenitor cells further differentiate in a series of steps to mature blood cells which have no differentiation potential (Fig. 1.1). In general, along the hematopoietic hierarchy, stem and progenitor cells gradually lose differentiation potential from pluripotent

to unipotent, and this multi-lineage differentiation potential is one of the hallmarks of stem cells. 2) Another unique feature of HSCs is their capacity to self-renewal. The self-renewal is defined as: a stem cell produces one daughter cell which remains as stem cell, and another daughter cell which has more restricted differentiation and proliferative potential. In this way, HSCs maintain the size of the stem cell pool, preventing depletion of HSCs by differentiation. 3) Proliferative capacity is not a unique feature of HSCs. However, the proliferative nature of HSCs may affect other unique features such as in *vivo* HSC self-renewal and differentiation potential [4]. The extensive proliferation history leads to loss of stem cell functional quality which known as replicative senescence[5]. In sum, all three features mentioned above are indispensable for HSCs. The intrinsic balance between proliferation, differentiation and self-renewal is essential for maintaining hematopoietic homeostasis, robustly restoring injured hematopoiesis (blood loss or ionizing radiation induced injury), as well as rapidly responding to pathogen infection.

1.2 Stem cell niche

The hematopoietic stem cell niche is an anatomic location in bone marrow where HSCs remain quiescent, self-regenerate, proliferate or differentiate in response to various extrinsic cues. The first study that described the possible physiological functions of niche cells was conducted in Dr. John Trentin's lab forty years ago[6, 7]. They demonstrated an active role of stromal cells in regulating the differentiation of HSCs. In 1978 Schofield expanded the observations of Trentin and others and proposed a hypothesis in which HSCs reside in specific

microenvironments where HSC fate decisions are made[8]. The microenvironment has been termed "niche"[6, 7]. In recent years, there have been many studies of the HSC niche to identify the cell types that compose the niche and to determine the signals that regulate HSC behavior within the niche.

1.2.1 Endosteal niche and vascular niche

Previous studies revealed two types of hematopoietic stem cell niches: the vascular niche and the endosteal niche (Fig. 1.2). The vascular niche consists of endothelial cells lining sinusoidal vessels. This particular microenvironment has been shown to be critical in supporting the differentiation and proliferation of short-term HSCs and HSC regeneration after injury[9]. The endosteal niche is located on the inner surface of the bone cavity and is comprised of a heterogeneous cell population that includes, endothelial cells, adipocytes, and osteoblasts[10-14] (Fig. 1.2). This niche, in general, is primarily associated with a capacity to provide signals for HSC quiescence. The two niches work cooperatively in a dynamic process that permits HSCs to migrate from a hypoxic endosteal microenvironment, in a relatively inactive state, to sinusoidal vessels, a permissive environment that promotes HSC proliferation and differentiation[15].

1.2.2 Cell types in the bone marrow niche

Amongst the various cell types within the endosteal niche, osteoblasts play an important role in reciprocal communication with primitive stem cells[16, 17]. *In vivo,* HSCs are localized spatially close to osteoblasts[16, 18] (Fig. 1.2). Ablation of osteoblasts resulted in a significant reduction in the hematopoietic cell

population, which indicates a supportive role of osteoblasts in maintaining HSCs[12]. Moreover, other niche components such as neuronal cells and adipocytes have also been shown to be involved in regulating the HSC pool. Nonmyelinating Schwann cells of autonomic nerves have been shown to be a critical determinant in maintaining HSC hibernation by activating latent TGF-beta[13]. Niche adipocytes were discovered as negative regulators of HSCs in a study using a lipoatrophic mouse model and pharmacological inhibition of adipocyte formation[14]**.** While so many characteristics of the BM niche have been defined, the crosstalk among niche cells and stem cells, as well as the mechanisms through which the microenvironment regulates HSC fate, requires further exploration.

1.3 Stem Cell Trafficking

HSC trafficking is believed to be essential for definitive hematopoiesis during pre-natal and early post-natal periods. During development, HSCs migrate from the aorta-gonad-mesonephros (AGM) region, to the fetal liver, and finally to the BM[19]. However, HSCs continue to migrate throughout postnatal life. Some are continuously in blood circulation under homeostasis, but may migrate back to and reside in BM niches, where they hibernate, proliferate or self-renew. This two-way commute is central to hematopoietic homeostasis. It is possible that stem cell move out of the bone marrow may ferry molecules to and from the niche to other tissues and organs throughout the body.

1.3.1 Mobilization

The egression of HSCs from the BM into blood circulation is called mobilization. During mobilization, HSCs actively move close to sinusoidal vessels, pass the vascular endothelial wall, migrate into the bloodstream, and then infiltrate into other tissues (e.g. spleen)[20]. The release of HSCs from the BM into the bloodstream is believed to be a physiological phenomenon for maintaining hematopoietic homeostasis through balancing HSC numbers[21]. Egress of HPSCs into the bloodstream follows circadian rhythms. Studies showed a fluctuation of circulating HPSCs peaks 5 hours after the initiation of light and nadirs 5 hours after darkness[22-24]. After receiving photic stimulation, the circadian pacemaker in the central nervous system (CNS) down-regulates the production of SDF-1 in its niche[24]. With a compromised SDF-1 dependent HSC retention in the niche, HSPCs readily enter the circulation[24].

Furthermore, HSC migration is manifested and utilized in clinical practice using cytokine exposure. Mobilization agents such as cyclophosphamide, 5-fluorouracil, stem cell factor (SCF), stromal derived factor-1 (SDF-1), and granulocyte-colony stimulating factor (G-CSF) are used extensively in a clinical setting to obtain adequate HSPCs from the transplant donors by pushing large numbers of HSPCs into the peripheral circulation [25-29].

1.3.2 Homing

In contrast to mobilization, HSCs also continuously home back to the BM niche under homeostasis, or after BM transplantation. The homing of circulating

HSCs requires a set of molecular interactions that mediate the sequential process of endothelial adhesion, rolling and transmigration through the endothelium. Several molecules are involved in these processes, the most important ones being adhesion molecules.

1.3.3 Molecules involved in HSC migration and homing

Migration and homing are both mediated by adhesion molecules and their ligands (Table1.1). Both HSCs and endothelial cells in the niche express adhesion molecules. In the tethering process, P- and E-selectin on endothelial cells work co-operatively to bind to P-selectin glycoprotein ligand-1 (PSGL-1, a glycoform of CD44 in human) on stem cells and progenitors [30-33]. Once stem cell and progenitors are anchored, stromal derived factor-1 (SDF-1) activates intergrin by interacting with C-X-C chemokine receptor type-4 (CXCR4), and induces HSC transmigration through the vascular endothelial cell wall to the niche [34-36]. Very late antigen-4 (VLA-4) and VLA-5, both of which belong to intergrin family, interact with adhesion molecules, particularly vascular cell adhesion molecule-1 (VCAM-1), and provide rigorous binding [37-39]. Defective HSC homing or retention most likely indicates down-regulated expression of adhesion molecules, and results in reduced cell-to-cell or cell-to-extracellular matrix interaction.

Additional molecules like small GTPase and hormonal signals have been reported to be involved in HSPC homing and mobilization. Mice defective in R-Ras (Rac1/Rac2 activator) expression, exhibit decreased BM homing and increased responsiveness to G-CSF induced mobilization [40]. Cdc42, another

small GTPase that mediates adhesion, is activated in aged HSCs [41]. Elevated levels of cdc42 activity are associated with a decline in HSC retention and increased mobilization with advanced age[41]. Furthermore, Parathyroid hormone (PTH) can effectively induce the mobilization of HSPCs, whereas Prostaglandin E_2 (PGE_2) elevates HSC homing efficiency [42-44].

1.4 Ionizing radiation toxicity

Maintaining a stable supply of mature blood cells is essential for nutrient supply, pathogen defense and tumor surveillance in hematopoiesis. However, this homeostasis can be perturbed by DNA-damaging agent such as ionizing radiation. Ionizing radiation is a high-frequency radiation that has very high energy and the capacity to remove an electron from an atom. When ionizing radiation passes through a cell, its high energy causes intracellular atoms and molecules to become excited, or “ionized”. This ionization can break chemical bonds, produce free radicals, and damage molecules (e.g. DNA, RNA and proteins), which are vital in biological processes[45].

The blood forming-organs, reproductive organs, digestive organs, skin, bone and teeth are primary targets of radiation. Among the tissues mentioned above, the blood system is most sensitive to radiation due to its high turnover rate. In the mouse, after exposure to irradiation, blood cell numbers increase in the first several days (overshoot stage), then drop off, and reach a nadir at 3-4 weeks (nadir stage)[46, 47](Fig. 1.3). Subsequently, the number of blood cells begins to increase and reaches a plateau at 8 weeks post irradiation (recovery stage)[46]. The recovery stage is the most important period in increasing the

survival rate after radiation injury.

1.4.1 Radiation-induced HSC apoptosis, senescence and tumorigenesis

After exposure to ionizing radiation, radiation-induced DNA damage immediately halts cell cycle progression (cell cycle arrest) (Fig. 1.4). During the period of cell cycle arrest, DNA repair machinery is triggered and begins to repair the damage. If the repair is unsuccessful, the cells are removed by a programmed cell death mechanism (apoptosis). From the studies of the response of HSCs to ionizing radiation, beginning during the World War II, it has been learned that a majority of HSCs die after radiation exposure by triggering apoptosis[45, 48]. A dose of 4 Gy radiation induced apoptosis in 65% of HSCs (Lin^- $Sca\text{-}1^+c\text{-}Kit^+$ cells), and in 50% of primitive progenitors ($Lin^-Sca\text{-}1^-c\text{-}Kit^+$ cells)[49, 50].

In some cells, the cell cycle arrest becomes permanent. These cells lose their proliferation capacity and become senescent[49]. A study on human HSCs ($CD133^+$ cells) demonstrated that, even though these cells were successfully repaired, their ability to self-renew was permanently damaged[49]. An increase in $p16^{Ink4a}$ expression on HSCs also implies the induction of premature senescence in these cells[49].

In some circumstances, apoptosis and senescence do not functionally remove all of the damaged cells. A small number of cells survive radiation stress with chromosome aberrations (Fig.1.4). These cells are dangerous due to their genomic instability, and have potential to result in tumorigenesis in the future. It has been previously reported that DNA repair machinery reaches its maximal effectiveness after a dose of 0.4~0.5 Gy radiation[51, 52]. Therefore, high doses of

radiation or continuous low doses of radiation can readily induce tumorigenesis.

In general, a balance between cell proliferation, senescence and apoptosis is critical for tissue homeostasis. In this dissertation, I will focus on Latexin deficiency induced radio-resistance and its role in regulating apoptosis in irradiated HSCs.

1.5 Identification and quantitation of hematopoietic progenitor and stem cells

Various assays have been established to measure the number and functionality of HSCs and their progeny. These assays include in vitro phenotyping assays, in vitro clonogenic assays, and in vivo transplantation assays, all of which are used to help enhance our understanding of hematopoietic progenitor and stem cell biology.

1.5.1 Flow cytometric phenotyping

Advances in flow cytometry over the past decades have revealed important information on the phenotypes of different hematopoietic cell subsets. Combining fluorescently labeled antibodies against cell surface receptors with flow cytometric analysis allows for the identification and isolation of progenitor and stem cells[53, 54]. Although multiple approaches have been developed over the years, a common consensus is that HSCs lack lineage markers (antigens that expressed on mature granulocytes, macrophages, B and T lymphocytes and red blood cells), and express stem cell receptors (such as Sca-1 and c-Kit)[54-60]. The immunophenotypically identified population (Lineage$^-$/ Sca-1$^+$/c-Kit$^+$ cells, also

known as LSK cells) is widely accepted as a partially purified HSC fraction in which approximately 1 in 20 cells exhibits long-term reconstitution ability[56, 61-63].

In the past decade, several novel HSC marking strategies have been developed. CD34 or Flt-3 expression was shown to be associated with a loss of primitiveness in the LSK population[63-65]. Antibodies against CD34 and Flt-3 further subdivide the LSK population into three populations (LSK/$CD34^+$/$Flt\text{-}3^+$ cells, LSK/$CD34^+$/$Flt\text{-}3^-$ cells and LSK/$CD34^-$/$Flt\text{-}3^-$ cells), each of which possess different engraftment and differentiation potentials[63-65]. One of the most recent additions to HSC marking strategies is the application of antibodies against the SLAM family of receptors[66]. SLAM family receptors are a group of trans-membrane proteins that regulate T lymphocyte development and function[66]. Primitive HSCs are highly enriched in the $CD150^+$/$CD48^-$ cell population with 50% HSC activity [66, 67], which to date is the highest purity of HSC described by phenotypic identification.

Another HSC isolation strategy relies on the ability of HSC to efflux chemical compounds. Hoechst 33342 is a fluorescent vital dye that binds to DNA content in cells[68]. BM cells stained with Hoechst 33342 and subsequently observed at two emission wavelengths (Hoechst Blue and Hoechst Red) revealed a small but distinct population of cells that selectively excluded the Hoechst 33342 dye. This population was termed the "side population" (SP), and is highly enriched in HSCs[68]. This methodology allows for the selection of HSCs based on cellular activity (multi-drug resistance pumps) rather than the expression of cell surface phenotypes.

Flow cytometric phenotyping of HSCs is considered an effective way of identifying stem cells from heterogeneous BM cells. However, the currently used stem cell markers are under debate due to the lack of information regarding true HSCs functional phenotype. Generally, under unperturbed conditions, there is a good correlation between the phenotype and in vivo reconstitution potential of HSCs; under stress conditions (aging, chemo/radio therapy or transplantation), phenotypic isolation strategies vary in their efficiency in selecting HSCs.

1.5.2 Colony-forming unit (CFU) assay

The CFU assay is an informative in vitro assay widely used to detect and quantify hematopoietic progenitor cells. In this assay, BM, spleen or peripheral blood cells are mixed with methylcellulose-based medium supplied with a combination of cytokines, and cultured for one or two weeks[69-75]. Progenitor cells of different lineages form colonies which have distinct morphologies. In this assay, each colony is counted and characterized by lineage according to their morphologies. Thus, it offers insight into the lineage specificity of cells, rather than assessing the functional activity of primitive, pluripotent HSCs.

1.5.3 Cobblestone-area forming cell (CAFC) assay

The CAFC assay is an in vitro limiting-dilution assay used to determine the frequency of hematopoietic cell subsets in a developmental hierarchy (Fig.1.5)[76-79]. A stromal cell layer (e.g. FBMD-1 cells) is pre-seeded and cultured in 96-well plates, and allows for in vitro long-term culturing of stem and progenitor cell. After the stromal cells reach confluency, bone marrow cells are plated on top of them.

Primitive hematopoietic cells migrate beneath the stromal monolayer and form cobblestone-areas, a small colony of 10-50 cells. The frequencies of stem and progenitor cells are determined weekly by scoring each well for the presence of cobblestone-areas over a period of 5 weeks or longer. It has been shown that the latency of appearance of a cobblestone area is positively correlated with the primitiveness of a hematopoietic cells [76, 80]. Thus, cells that form cobblestone-areas at day 7 to day 21 are considered hematopoietic progenitor cells, and cells that form cobblestones at day 28 to day 35 or later are considered more primitive stem. It should be noted that cobblestone areas only present for a week or less so they aren't counted more than once in successive weeks. A modified CAFC assay (adhesion assay) can also be used to detect the interaction between hematopoietic cells and stromal cells[81]. In this assay, hematopoietic cells are plated onto a stromal layer and the hematopoietic cells and stromal cells are allowed to interact for 2 ~ 4 hours. The non-adherent cells are then washed away, leaving the adherent cells in culture. These adherent cells will form cobblestone-areas at later time points. The adhesion assay generally measures the adhesive properties of hematopoietic cells and studies the interaction between hematopoietic cells and stromal cells.

The CAFC assay is a reliable approach for measuring the frequency of hematopoietic progenitor and stem cells. However, the in vitro culture conditions exclude the influence from the systemic cues and does not realistically mimic the in vivo microenvironment. Furthermore, the CAFC assay lacks measurement of in vivo homing activities; thus the gold standard for stem cell activity remains in

vivo repopulation experiments.

1.5.4 In vivo transplantation

The definition of HSC relies on the fact that the cell is able to reconstitute the entire hematopoietic compartment in a lethally irradiated animal for a long period. This definition makes the in vivo transplantation assay the ultimate methodology for identifying the activities of HSCs. The first rigorously quantitative assay allowing measurement of multi-lineage reconstitution potential in vivo was reported by Harrison in 1980[82, 83]. It was a competitive repopulation (CR) assay in which support cells with known HSC activity (competitor cells) and a test cell population with unknown HSC activity were co-transplanted into lethally irradiated recipients (Fig. 1.6A). The test and competitor cells were from two distinct sources, each possessing different cell surface marker isotypes (e.g. CD45.1 or CD45.2), so as to enable tracing of cell origins. In CR assays, the HSC activity of test cells is assessed by comparing the proportion of test cell-derived cells to competitor cell-derived cells in a recipient's peripheral blood. Theoretically, with equal numbers of cells, test cells and competitive cells reconstitute hematopoiesis equally. Thus, any deviation from the 50% engraftment efficiency indicates either a competitive advantage or disadvantage. CR assays provide information about HSC reconstitution potential as well as the competitive capacity. Furthermore, since the competition occurs in a common, in vivo environment, extrinsic factors such as cytokines and stroma can be ruled out.

CR is a powerful assay to measure the multi-lineage reconstitution potential of test cells, but in the long run test cells also require self-renewal to

maintain hematopoiesis over a lifespan, a function that can't be directly measured by CR. A serial transplantation assay, however, allows the measurement of the self-renewal capacity by introducing multiple reconstitution stresses[84, 85]. Serial transplantation, as the name implied, is a repetitive transplantation in which test cells are transplanted from one host to another for several times over what cumulatively amounts to a mouse lifespan or more (Fig. 1.6B). For the primary transplant, one million test cells (CD45.2 isotype) are mixed with an equal number of competitor cells (CD45.1 isotype) and are transplanted to lethally irradiated primary recipients. For the secondary transplant, ten million recipient cells (from primary recipients) are transplanted into secondary recipients. The same regimen is repeated for the tertiary and quaternary transplants. In this way, the self-renewal capacity of the cells will be reflected by the variation in engraftment efficiency in the peripheral blood in each successive transplanted recipient.

1.6 Latexin and stem cell

Latexin contains 222 amino acids, and is the only known carboxypeptidase A4 (CPA4) inhibitor in mammalian cells. CPA4 belongs to the zinc-dependent metalocarboxypeptidase (MCP) subfamily A/B. Members of this family are located in digestive tract, brain, heart, and lung. They participate in peptide hormone activities to regulate cell proliferation and differentiation. The overall structure of latexin protein consist of two subdomains, each of which bears an alpha-helix and a four-strand beta-sheet running anti-parallel[86]. The two subdomains are linked by a third alpha-helix. The hydrophobic contacts

established by the two subdomains embrace the enzyme and perform the inhibition. Latexin shares no structural or sequence similarity with carboxypeptidase inhibitors in other species. However, latexin has a paralogue called Tig1 that has up to 30% sequence similarity with latexin. The two genes are located adjacently on chromosome 3. TIG1 has been thought as an ancestor gene of *Lxn*, and is a putative tumor suppressor gene. Its expression is epigeneticly modified in numerous cancers, including prostate, breast and some hematopoietic malignancy[87]. The *Lxn* expression is also suppressed in some hematopoietic malignancy such as chronic and acute myeloid leukemia, thus suggesting a possible role for it in tumorgenesis.

Latexin was first discovered in rat brain as a region specific marker of the lateral neocortex[88, 89]. In peripheral nervous system, latexin has been reported to be involved in pain transmission by studying constitutive *Lxn* knockout mice. Animals that have no latexin in the nervous system showed a retard sensitivity to pain[90]. *Lxn* is also highly expressed in rat peritoneal mast cells, as well as mouse macrophages[87, 91], and its expression is further regulated by several pro-inflammatory stimuli.

Though latexin has not been reported in neural stem cell compartments, our lab recently discovered that latexin is a homeostatic regulator of HSC population size in mice[92, 93]. We used a forward genetic approach, comparing two mouse strains, and indentified *Lxn* as the quantitative trait gene that regulates HSC pool size in mice. The HSC number in mice bone marrow is inversely related to quantitative *Lxn* expression level and is regulated through a concert of

proliferation, self-renewal and apoptosis. High *Lxn* expression induces an increased apoptosis as well as decreased proliferation and self-renew. Latexin acts as a break not only on HSCs, but also in multi-lineage progenitors and mature cells in circulation.

1.7 Experimental goals and significance

The experimental goal of this dissertation was to study the function of the *Lxn* gene in regulating hematopoietic stem and progenitor cell biology using a *Lxn* deficient mouse as model. Four specific aims were proposed and tested to accomplish this goal:1) to study the phenotypes of *Lxn* deficient mice in peripheral blood, spleen and bone marrow and identify the mechanisms underlying these phenotypes; 2) to explore *Lxn* function under genotoxic stress using ionizing radiation; 3) to demonstrate the effect of *Lxn* on HSC migration activities and identify the potential target gene(s) of *Lxn* that regulate HSPC mobilization; 4) to overexpress *Lxn* in B cell lymphoma cells and study the potential tumor suppressor role of *Lxn* in hematological malignancies.

The *Lxn* gene has recently been identified as a novel, homeostatic regulator of hematopoietic stem and progenitor cells through concerted mechanisms of self-renewal and apoptosis, which increase and decrease along with *Lxn* expression levels, respectively. Generally, *Lxn* acts as an autonomous brake on the expansion of the hematopoietic stem and progenitor cell populations. Unrestrained cell expansion brings the risk of genomic instability; however, finely controlled expansion aids in hematopoietic recovery after genotoxic insults such ionizing radiation. To my knowledge, the roles of *Lxn* in the

development of cancer and in response to ionizing radiation have not yet been elucidated. Therefore, examining a lymphoma cell line overexpressing *Lxn* and a *Lxn* deficient mouse models may help to establish novel strategies for treating hematologic malignancies, as well as promoting HSPC recovery in patients undergoing radiotherapy or following accidental radiation exposure.

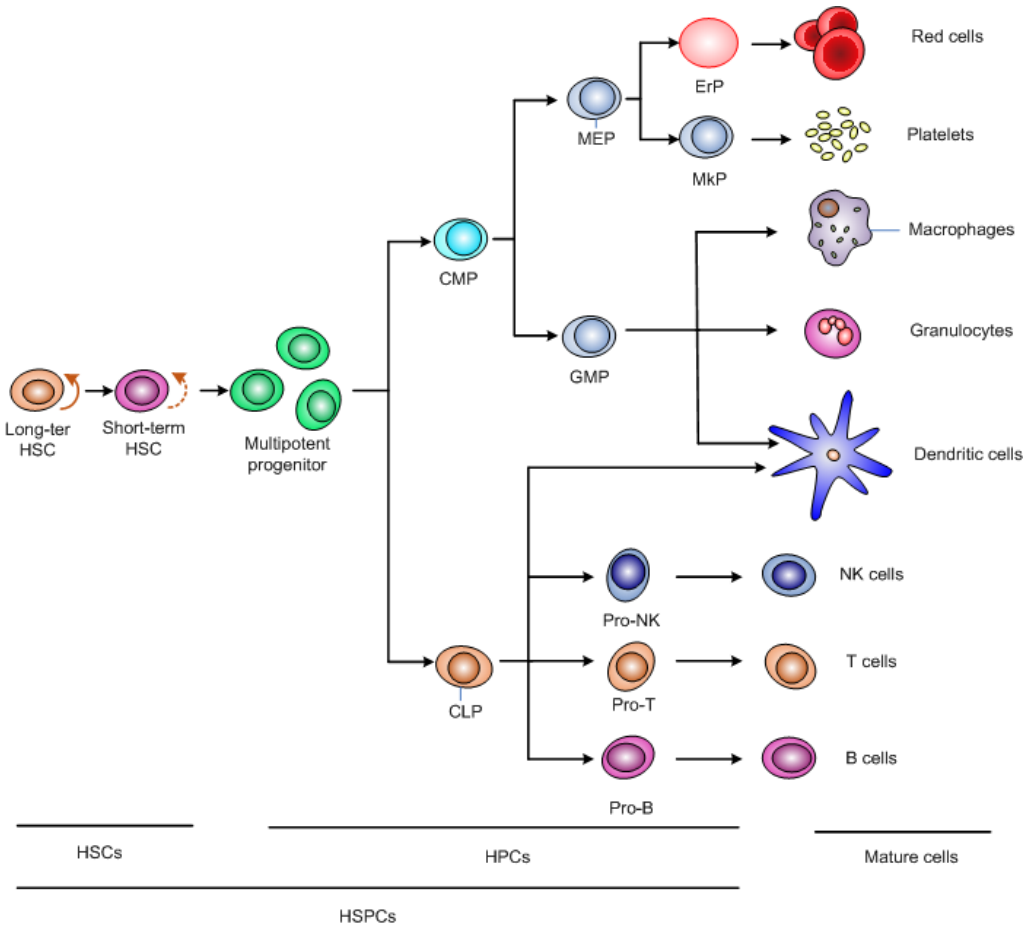

Figure 1.1 Developmental hierarchy of the hematopoietic system.

Long-term HSCs, which are pluri-potent, generate short-term HSCs and multi-potent progenitor (MPP) cells, which are multi-potent. MPP cells differentiate into committed progenitor cells (CLP and CMP), which give rise to 8 types of mature blood cells in the peripheral blood. This hierarchy pyramid is positively correlated with cell population size, but negatively correlated with self-renewal and differentiation capacities.

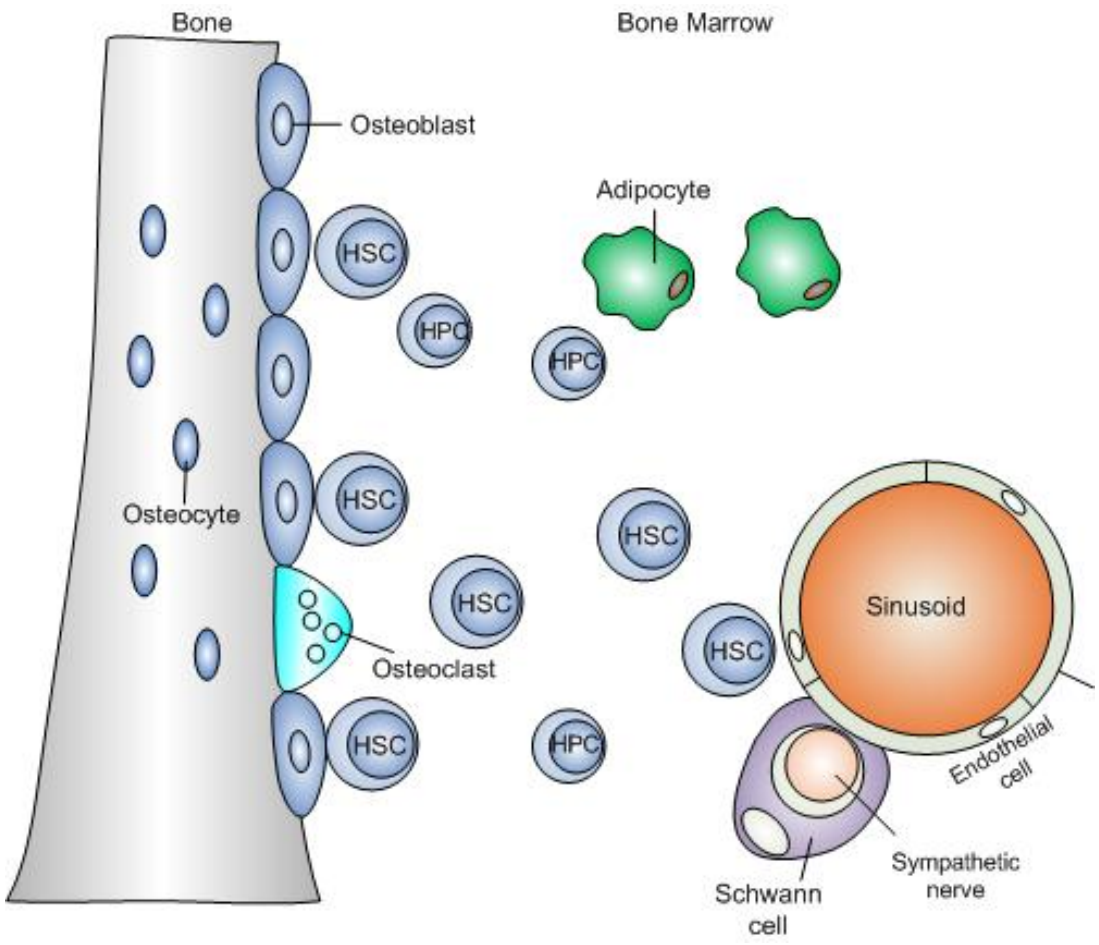

Figure 1.2 The endosteal and vascular niches.

HSCs reside in both endosteal and vascular niches. A variety of cells, including endothelial cells, adipocytes, neuronal cells, and osteoblasts, comprise of stem cell niche. HSCs localized near osteoblasts in the endosteal niche tend to be quiescent, whereas HSCs that mobilize to the vascular niche are active in proliferation and differentiation. Schwann cells wrapping the sympathetic nerve promote HSC dormancy. Adipocytes negatively regulate HSC pool size.

Table 1.1 Molecules involved in HSC migration and homing.

Molecules	Function	Reference
CXCR4/SDF-1	HSC homing and mobilization	34-36, 94
CXCR2/GROβ	HSC mobilization	95
PSGL-1/P-selectin or E-selectin	HSC homing and adhesion	33, 96
VLA-4 (CD49d/α4 integrin)/VCAM-1	HSC adhesion, homing, mobilization and HSC quiescent	38, 81
VLA-5 (CD49e/α4 integrin)/ VLA-5 receptor	HSC adhesion and homing	97
PTH/PPR	Induce HSC proliferation, homing and mobilization	43, 44, 98
PGE_2/ PGE_2R	Proliferation, homing and HSC survival	42
CD44/Osteopontin	HSC adhesion and homing	17, 32, 99
Rho GTPase (Cdc42)	HSC homing and HSC retention	40-42
CD26	HSC homing and mobilization (negative regulation)	100, 101

Adhesive molecules and their ligands, small GTPases, and hormones that are involved in HSC migration and homing.

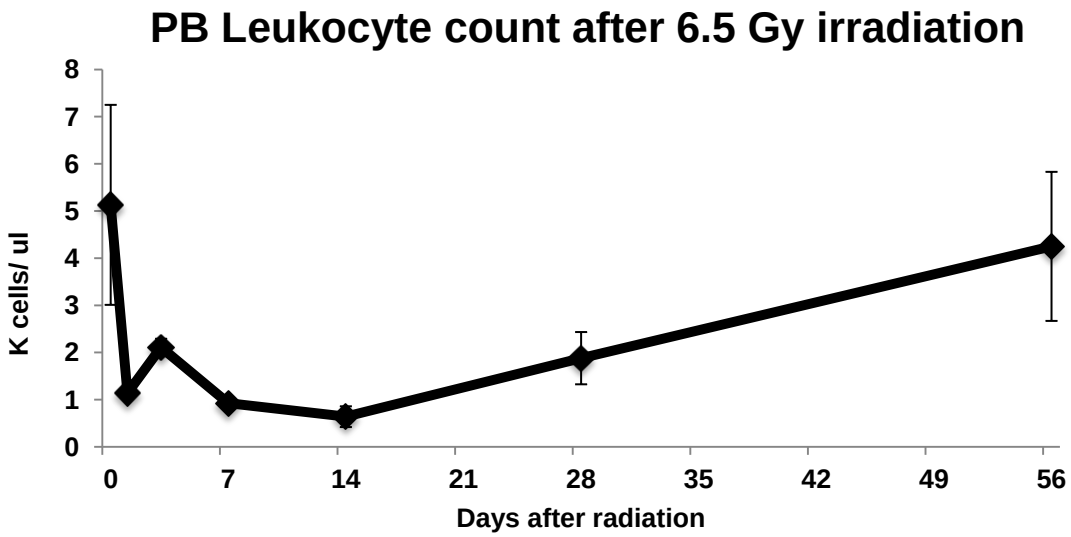

Figure 1.3 Mouse peripheral blood leukocyte dynamics after 6.5 Gy irradiation.

After exposed to 6.5 Gy gamma irradiation, blood leukocytes increase in the first several days (overshot stage), then drop off, and nadir at 3-4 weeks (nadir stage). Subsequently, the number of blood cells begins to increase and reaches a plateau at 8 weeks post irradiation (recovery stage).

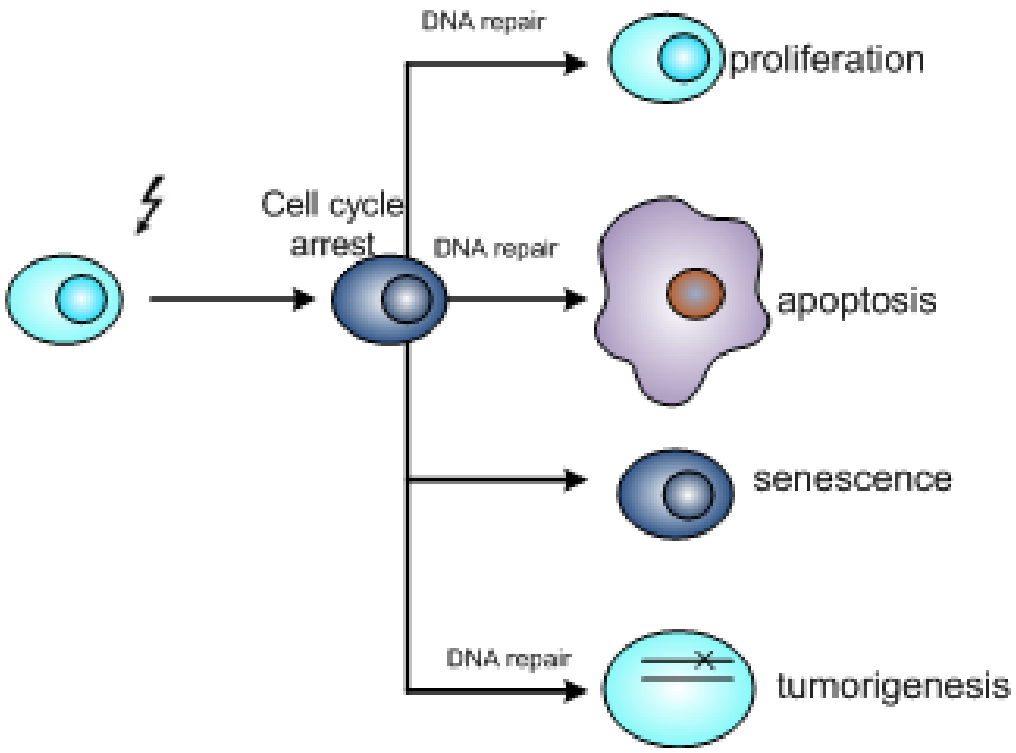

Figure 1.4 Radiation-induced apoptosis, senescence and tumorigenesis.

After exposure to ionizing radiation, radiation-induced DNA damage stops cell cycle progression. The DNA repair machinery is then triggered to repair the damage. Successfully repaired cells proliferate to repopulate hematopoiesis. However, when the repair is unsuccessful, the cells are removed by apoptosis or senescence. A small number of cells can survives radiation stress with chromosome aberrations, and may cause tumorigenesis in the future.

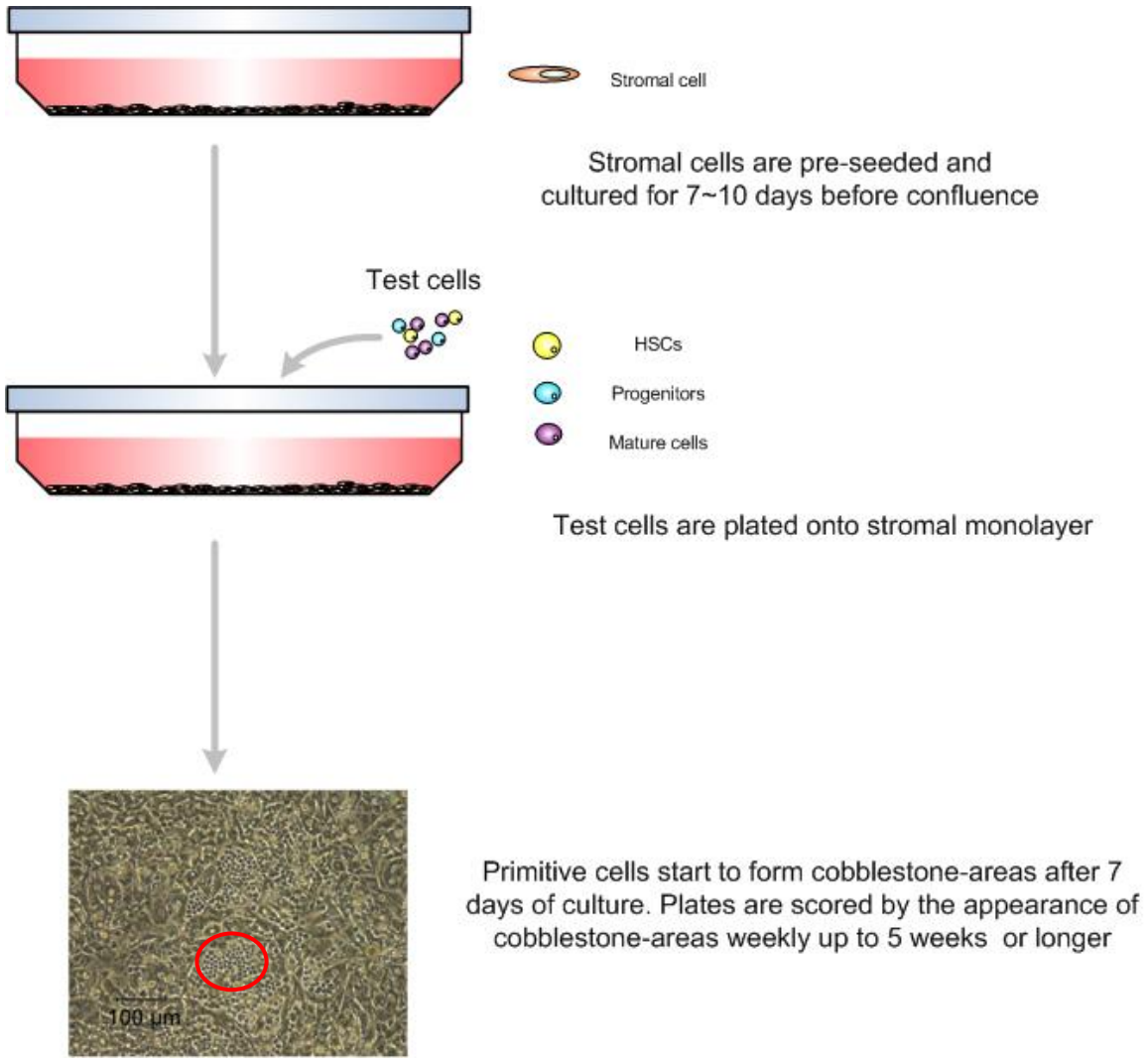

Figure 1.5 Cobblestone-forming cell (CAFC) assay.

The stromal layer (e.g. FBMD-1 cells) is pre-seeded and cultured in 96-well plates. After the stromal cells reach confluency, test cells are plated on top of the stromal monolayer in a limiting dilutions. Primitive hematopoietic cells (HSCs or progenitors) migrate beneath the stromal monolayer and form cobblestone-areas. The frequencies of stem and progenitor cells are determined by scoring each well weekly for the presence of cobblestone-areas.

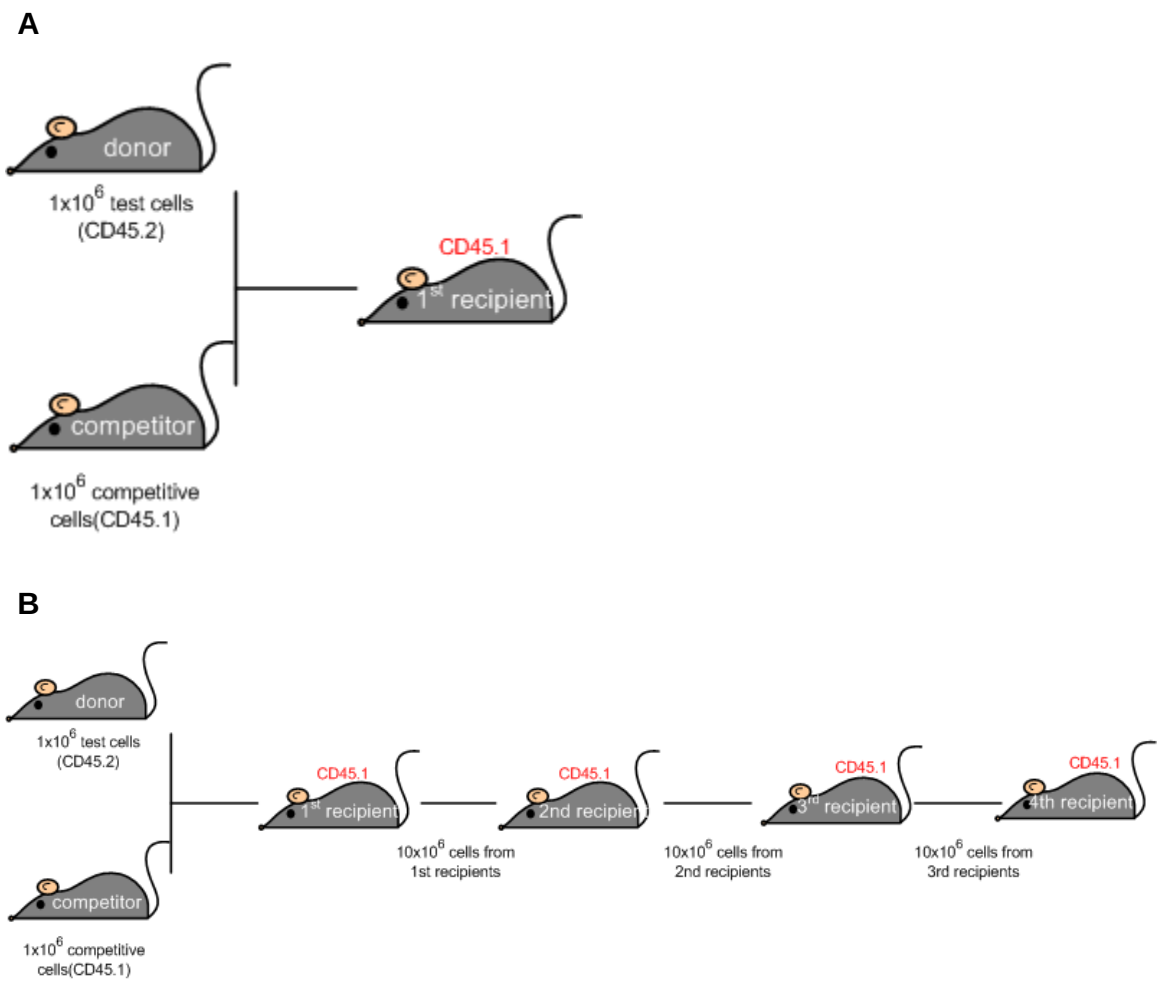

Figure 1.6 In vivo transplantation.

(A) In competitive repopulation (CR) assays, $1x10^6$ WBM test cells (CD45.2) are mixed with an equal number of competitor cells (CD45.1), and retro-obitally injected into lethally irradiated (9 Gy) CD45.1 recipient mice. (B) In serial transplantation assays, $1x10^6$ WBM test cells (CD45.2) are mixed with an equal number of competitor cells (CD45.1), and retro-obitally injected into CD45.1 primary recipients. For secondary transplants, $10x10^6$ unfractionated bone marrow cells were harvested from primary recipients (CR recipients) 15 or 16 weeks post transplantation and transplanted into lethally irradiated secondary recipients. The same regimen is repeated for tertiary and quaternary transplants.

CHAPTER 2: Loss of Latexin Confers a Hyperproliferative Hematopoiesis and Altered Self-renewal Capacity in Murine Hematopoiesis

2.1 Abstract

Previous studies in our lab have identified that a novel gene, latexin (*Lxn*), acts endogenously in murine hematopoietic stem cells (HSCs) to negatively regulate population size by enhancing apoptosis and decreasing self-renewal and proliferation. To further investigate the functionality of *Lxn* in hematopoiesis, we generated a constitutive knock-out mouse model (*Lxn-/-* mouse). We determined that this mouse model exhibited hyperproliferative hematopoiesis including bone marrow hypercellularity, splenomegaly with myeloid cell infiltration, and peripheral blood leukocytosis. The bone marrow compartment of these animals also displays expansion of early progenitor populations. In accord with our original findings, both a repopulation advantage and elevated self-renewal capacity were observed in competitive repopulation and serial transplantation assays in this mouse model**.** Reciprocal transplantation using lethally irradiated *Lxn-/-* or B6 mice as recipients showed that the repopulation advantage is intrinsic to the hematopoietic cells, and not to the microenvironment. Furthermore, we found that there is a reduction in apoptotic frequency in hematopoietic progenitors, which may account for an enlarged progenitor compartment in the bone marrow. These data indicate that loss of *Lxn* results in hyperproliferative hematopoiesis, a competitive growth advantage, and enhanced self-renewal capacity, all of which are hematopoietic cell-intrinsic. Microarray studies

performed on a purified stem cell population (HSCs) identified Thrombospondin-1 (*Thbs-1*) as a potential target of *Lxn*, and its expression level is down-regulated in *Lxn-/-* stem cells. In future studies, we plan to study downstream signaling pathways of *Lxn*, focusing on *Thbs-1*.

2.2 Introduction

Latexin was first discovered in rat brain as a region specific marker of the lateral neocortex[88, 89, 102, 103]. In the peripheral nervous system, latexin has been reported to be involved in pain transmission[90]. Animals that have no latexin in the nervous system showed a delayed sensitivity to pain. *Lxn* is also highly expressed in rat peritoneal mast cells, and mouse macrophages, and is differentially expressed along the hematopoietic hierarchy with the highest levels in the most primitive stem cells[91-93]. Our lab used a forward genetic approach, comparing two mouse strains, to indentify *Lxn* as the quantitative trait gene that regulates variation in HSC pool size in the mice[92, 93]. The HSC number in mice bone marrow is inversely correlated to quantitative *Lxn* expression level and is regulated through concerted effects on proliferation, self-renewal and apoptosis[92, 93]. High *Lxn* expression induces increased apoptosis as well as decreased proliferation and self-renewal, and vice versa.

The Latexin protein contains 222 amino acids, and is the only known zinc-finger metallocarboxypeptidase inhibitor in mammalian cells[86, 104, 105]. However, it shares no structural or sequence similarity with carboxypeptidase inhibitors in other species. *Lxn* has a paralogue called tazarotene-induced gene1 (*Tig-1*), which is a putative tumor suppressor gene[87, 106]. To test the hypothesis that *Lxn*

is a putative tumor suppressor gene like *Tig-1*, we studied *Lxn* function in hematopoietic malignancy. We found that *Lxn* expression is highly down-regulated in a extensive list of leukemia and lymphoma cancers through the mechanism of promoter hypermethylation[107] (As seen in Chapter 5). Restoring the expression of *Lxn* inhibits tumor growth in vitro and in vivo by enhancing apoptosis in tumor cells.

For these studies, we generated a *Lxn* constitutive knock-out mouse to study the its function in hematopoieisis. We found that *Lxn-/-* mice exhibited hyperproliferative hematopoiesis, a cell-autonomous repopulation advantage and elevated self-renewal. A reduced apoptotic frequency in progenitors was found in *Lxn-/-* BM cells, which may account for the enlarged progenitor population. *Thbs-1*, which expression was down-regulated in *Lxn-/-* stem and progenitor cells, was identified as a potential target of *Lxn*.

2.3 Methods

2.3.1 Animals

C57BL/6 mice (B6) (8-16 weeks) and B6.SJL/BoyJ (CD45.1) recipient mice (8-16 weeks) were purchased from The Jackson Laboratory (Bar Harbor, ME). Latexin constitutive knockout mice were generated by Taconic/Artemis (Germantown, NY) and used at a young age (8-16 weeks). All animals were housed in the animal facilities of the University of Kentucky under pathogen-free conditions according to NIH-mandated guidelines for animal welfare. They were fed with food and water *ad libitum*.

2.3.2 Generation of Lxn deficient mouse

Latexin constitutive knockout mice were commercially generated under contract to Taconic/Artemis (Germantown, NY) and used at young age (8-16 weeks). The knock-out strategy is described in Results.

2.3.3 Peripheral blood cell count

Animals were anesthetized with isoflurane from Butler Animal Health Supply (Dublin, OH). Peripheral blood was collected from retro-orbital venous plexus into EDTA-coated microtainer from Becton, Dickinson and Company (Franklin lakes, NJ). Circulating leukocytes, erythrocytes and platelets were counted by analyzing 20 ul of blood using a Hemavet 950 from Drew Scientific (Dallas, TX).

2.3.4 Hematopoietic cell identification and isolation

Bone marrow (BM) cells were flushed from the femora and tibiae into Hanks balanced salt solution (HBSS) with 2% fetal bovine serum (FBS)(both from Life Technologies, Carlsbad, CA). Progenitor cells were discriminated from stem cells by the lack of cell surface antigens characteristic of cells committed to individual lineages. Antibodies against these antigens included CD5 and CD8a, B220, Mac-1, Gr-1, and Ter119 were biotinylated. Strepavidin secondary antibody was used to detect lineage negative cells. To further purify primitive stem cells, stem cell markers Sca-1 and c-Kit, as well as CD34 and Flt3 were incorporated into the staining procedure. Phenotypes of purified stem cells are lineage^{-}, c-Kit^{+},

Sca-1^{+}, CD34^{-}, and Flt3^{-}. Lineage-committed progenitor cells, including common myeloid progenitor (CMP), granulocyte/monocyte progenitor (GMP), megakaryocyte/erythroid progenitor (MEP) and Common lymphoid progenitor (CLP), were identified by the markers FcgR, IL7R, CD34 and Flt3. The isolation strategy is shown in Fig. 2.2A. Dead cells were excluded by propidium iodide (PI) selection that stains exposed double-strand DNA. All monoclonal antibodies were purchased from eBioscience (San Diego, CA), Biolegend (San Diego, CA), or BD pharmingen (San Jose, CA).

2.3.5 Cell Analysis and Sorting

BM cells were analyzed and sorted on a FacsAria II flow cytometer (Becton Dickinson, Franklin Lakes, NJ). Cells were sorted into phosphate buffered saline (PBS) containing 0.5% FBS for further use. Each experimental group was sorted independently. Flow cytometry and FACS data were analyzed using FlowJo software (Tree star, Ashland, OR).

2.3.6 Cell cycle and proliferation analysis

Cell cycle analysis was performed using Ki-67 and 7AAD. BM cells were harvested and stained as described above, and then fixed and permeabIlized using the Fix and Perm kit from Invitrogen (Camarillo, CA). Nuclear staining of Ki-67 was performed using the fluorochrome-conjugated anti-mouse Ki-67 antibody from BD pharmingen (San Jose, CA).

In vivo 5-bromo-2-deoxyuridine (BrdU) incorporation was used to enumerate proliferative cells. For immediate incorporation, mice were injected

intraperitoneally with BrdU (1 mg/kg of body weight) and bone marrow was harvested 1 hr later for measurement of BrdU incorporation into recently synthesized DNA. For long-term incorporation, BrdU (BD Pharmingen, San Jose, CA) was administered at a concentration of 0.5 mg/mL in drinking water that was changed every 3 days. BM cells were harvested at 1hr (short term), 3 days and 5 days (long term) after incorporation, then labeled with a cocktail of HSC cell markers (CD5, CD8a, B220, Mac-1, Gr-1, Ter119, c-Kit^{+}, Sca-1^{+}, CD34^{-}, and Flt3^{-}). Subsequent co-labeling with BrdU and HSC cell markers enabled the determination of cell proliferative status in different progenitor and stem cell populations.

2.3.7 Apoptosis analysis

BM cells were prepared and immuno-fluorescently stained as described above. The fluorochrome-conjugated apoptotic marker, Annexin V, along with DNA dye, 7-AAD, (both from BD Pharmingen, San Jose, CA) was used to identify apoptotic and necrotic cells. Stained cells from *Lxn*-/- animals and B6 animals were analyzed by flow cytometer.

2.3.8 Colony forming cell (CFC) assay

Methylcellulose-based culture media was pre-made with Complete MethoCult Media (Stem Cell Technologies, Vancouver, Canada) containing cytokines including stem cell factor (SCF), IL-3 and IL-6. For this assay, 1 x 10^4 whole BM cells in 100 µL HBSS were thoroughly admixed with 1 mL complete MethoCult media, plated into 6-well petri-dish and incubated at 37°C. Individual

well of triplicates were scanned on day 7 and 14 to identify relative distribution and formation of lineage specified colonies.

2.3.9 Cobblestone Area Forming Cell (CAFC) Assay

A monolayer of FBMD-1 stromal feeder cells was seeded in 96-well tissue culture-treated plates. After 7 to 10 days (when feeder cells grew confluent), wells were seeded at doses of 333, 1000, 3000, 9000, 27000 or 81000 whole BM (erythrocyte depleted; see below) cells from *Lxn*-/- or B6 mice. Individual wells were screened at days 7, 14, 21, 28, 35, 42, and 49 for the presence of cobblestone areas. The CAFC media (IMDM, supplemented with 20% of horse serum and 1 x 10^{-5} M hydrocortisone) was changed weekly.

2.3.10 BM transplantation

In competitive repopulation (CR) assays, 1x10^{6} WBM cells from *Lxn*-/- mice or B6 test cells (both CD45.2) were mixed with an equal number of competitor cells (CD45.1) and retro-obitally injected into lethally irradiated (9 Gy) B6.SJL/BoyJ CD45.1 recipient mice. Recipients were bled from the retro-orbital sinus at 5, 10 and 15 or 16 weeks post transplantation to test engraftment efficiency. Erythrocytes were depleted by hypotonic lysis using NH_4Cl. The leukocytes were stained in triplicate with fluorescent-conjugated monoclonal anti-CD45.2 and anti-CD45.1 antibodies, as well as B220, Thy1, Mac-1 and Gr-1 lineage markers (BD pharmingen, San Jose, CA). Samples were analyzed using a FACScan instrument (Becton-Dickinson Immunocytometry Systems,).

For serial transplantation, in primary transplants, one million test cells

(CD45.2 isotype) are mixed with an equal number of competitor cells (CD45.1 isotype) and then transplanted into lethally irradiated primary recipients. In secondary transplants, $10x10^6$ unfractionated bone marrow cells were harvested from primary recipients (15 or 16 weeks post transplantation) and transplanted cells into lethally irradiated secondary recipients. The same regimen was repeated for tertiary transplantation. At each transplant, PB and BM cells were analyzed as described above. The competitive advantage and self-renewal capacity of HSCs was analyzed by comparing the percentage of *Lxn*-/--derived or B6-derived cells at each round of transplantation.

In reciprocal transplantation, $5x10^6$ unfractionated bone marrow cells (B6.SJL/BoyJ, CD45.1) were transplanted into either B6 or *Lxn-/-* recipients (both are CD45.2). At the 5, 10 and 15 weeks post transplantation, PB and BM cells were analyzed as described above. The microenvironmental effects were analyzed by assessing how well the recipient genotype facilitated engraftment efficiency.

2.3.11 Western blot

For detecting Lxn and Gfm-1 proteins, total protein was extracted from BM, spleen, liver and brain using protein lysis buffer containing a protease inhibitor cocktail. Samples were subjected to denaturing PAGE (Novex, 10% Bis-Tris gel), and electrotransferred to Immunobilon-P membranes (Millipore), which were subsequently blocked and probed with anti-Gfm-1 (Abcam, Cambridge, MA) or anti-latexin primary antibody. Primary antibodies were detected with phosphatase–conjugated secondary antibodies (Santa Cruz Biotechnology) and

electrochemifluorescent (ECF) reagent (Pharmacia Biotech) according to the manufacturer's instructions. The membrane was scanned and bands were detected and analyzed using a Molecular Dynamics STORM 860 system and Imagequant Software. The polyclonal IgG rabbit antibody against latexin was generated from the *Lxn*-specific amino acid sequence CKHNSRLPKEGQAE at the C terminus and was produced by Bethyl Laboratories (Montgomery, TX).

After the detection of Gfm-1/Lxn antibodies, membranes were stripped in 40% methanol and a buffer containing 100 mM β-mercaptoethanol, 2% SDS and 62.4 mM Tris-HCl. The stripped membranes was reprobed with antibody to β-actin (Santa Cruz Biotechnology) and detected as described above.

2.3.12 RNA isolation and quantification

RNA for qRT-PCR was purified using RNeasy Mini Kit (Qiagen, Germantown, MD). Total RNA was reverse transcribed with High Capacity cDNA Reverse Transcription Kit (Applied Biosystems, Foster City, CA). Predesigned Taqman real-time primer/probes sets for *Thbs-1* (Applied Biosystems, Foster City, CA) were obtained and PCR was performed using TaqMan Universal Master Mix (Applied Biosystems, Foster City, CA) on a ABI7500 Real-Time PCR system (Applied Biosystems, Foster City, CA). Expression levels were normalized to *Gapdh* and compared with the ΔΔ threshold cycle method.

2.3.13 Microarray analysis

Microarray experiments were performed on fresh BM Multipotent progenitor cells (LSK/CD34^{+}/Flt-3^{+}) obtained from three wild type and three *Lxn*-/-

biological samples (each of which was pooled from more than 10 individual animals) using Affymetrix Gene Chip MoGene-1_0-st-v1 Arrays (Santa Clara, CA). Microarray data were normalized based on the RMA method. To identify differentially expressed genes comparing B6 versus *Lxn*-/- mice, we used the limma package in R/Bioconductor and a p-value<0.01 was used as the cutoff to select a list of candidate genes.

2.3.14 Statistics

Statistical significance between means was determined by a two-way Student *t* test.

2.4 Results

2.4.1 Generation of Lxn deficient mouse model

From previous studies, we learned that *Lxn* acts as negative regulator of HSC population size through balancing proliferation, apoptosis and self-renewal. To further explore the in vivo roles of *Lxn*, we generated *Lxn* deficient (*Lxn*-/-) mice using a gene targeting method (Fig. 2.1A). The mouse *Lxn* gene contains six exons. A gene targeting construct to flank a region of exon 2-4 by LoxP sites. Exons 2-4 were removed after in vivo Cre-mediated deletion in targeted allele. *Lxn*-/- mice appear normal, are produced at the normal Mendelian ratio, and show no obvious abnormalities in development with either males or females.

The *Lxn* gene is embedded in the intron of another gene, G-elongation factor, mitochondrial 1(*Gfm1*), in the opposite orientation. The deletion of *Lxn*

exons 2-4 resulted in the deletion of a portion of *Gfm-1* intron 13. To test the absence of latexin protein and the integrity of Gfm-1 protein, we used western blot and antibodies against Lxn and Gfm-1 protein. The results revealed that latexin protein is not expressed in the BM, spleen, liver and brain of *Lxn*−/− mice, and *Gfm-1* expression is intact in *Lxn-/-* mice, as in B6 wild type mice (Fig. 2.1B).

2.4.2 Loss of *Lxn* leads to hyperproliferative hematopoiesis in *Lxn-/-* mice

To investigate the function of *Lxn* and its effect on hematopoiesis, we examined the spleen, peripheral blood and bone marrow in *Lxn*-/- mice. *Lxn*-/- mice showed splenomegaly (Fig. 2.2A) with a significant increase in spleen weight due to the expansion of red pulp. We also found an increase in Mac-1/Gr-1 positive monocytes and granulocytes in the spleen, suggesting monocyte and granulocyte infiltration into *Lxn*-/- spleens (Fig. 2.2B). In the peripheral blood of *Lxn*-/- mice, we found a significant increase in white blood cells (WBCs) and platelets (Fig. 2.2C) compared to wild type animals. Amongst WBC subtypes, absolute numbers of neutrophils and lymphocytes were increased by approximately 50% in *Lxn*-/- mice, whereas monocytes were increased almost 100%. (Fig. 2.2C). However, despite the observation of increased absolute numbers of granulocytes, lymphocytes and platelets, analysis of lineage contributions in PB indicated a lineage skewing that favored lymphoid-lineage cells, especially B lymphocytes (Fig. 2.8). Furthermore, the bone marrow of *Lxn*-/- mice was hypercellular with a 20% increase in the numbers of mononucleated cells (Fig. 2.3B) in femurs. Together, these findings, which include splenomegaly, leukocytosis and hypercellular bone marrow, demonstrate that *Lxn*-/- mice

develop hyperproliferative hematopoiesis in both PB and BM.

2.4.3 Loss of *Lxn* induces hyperproliferative hematopoiesis phenotype through dysregulating progenitor and stem cells

Next we examined the progenitor and stem cell compartments in the BM using both flow cytometry and functional assays. We found that the absolute numbers of common lymphoid progenitors (CLPs), common myeloid progenitors (CMPs) and granulocyte-monocyte progenitors (GMPs) were significantly increased (up to 50 %) in *Lxn*-/- mice compared to their wild type counterparts (Fig. 2.3D)(Phenotypic isolation strategy shown in Fig. 2.3A). The megakaryocyte-erythrocyte progenitors (MEP) were increased in *Lxn-/-* mice, but did not reach statistical level of significance (Fig. 2.3D). Further, we observed 50% expansion of lineage$^-$cKit$^+$Sca-1$^+$ (LSK) cells in *Lxn-/-* mice. This expansion was due to an increase (~100%) in the multipotent progenitor (MPP) population. The absolute numbers of phenotypic short-term HSCs (ST-HSCs) and Long-term HSCs (LT-HSCs) remained static (Fig. 2.3E). The colony-forming cell unit (CFU) and cobblestone-area forming cell (CAFC) assays are two classical in vitro experiments to measure the functional capacity of progenitor and stem cells. Here we used both to determine the effect of *Lxn* on hematopoietic cell functional capacity. An increased number of day 14 colony-forming cells per 10^4 BM cells was observed in *Lxn*-/- mice compare to B6 mice (Fig. 2.4A). These data demonstrated that there were increased numbers of progenitors in the BM of *Lxn-/-*, consistent with our flow cytometric data. CAFC assays revealed significantly more day 35 cobblestones in *Lxn*-/- animals (Fig. 2.4B). The cells

formed day 35 cobblestones in CAFC assays are commonly considered as stem cells. In our results, the increased day 35 cobblestones indicated up-regulated HSC numbers in *Lxn-/-* animals. However, the competitive repopulation unit (CRU) assay, the gold standard in numerating the HSC number, found no difference between the HSC numbers in *Lxn*-/- and B6 mice (data not shown). Therefore, we considered that there were increased numbers of cells only in the progenitor population, not but in the most primitive stem cell population.

2.4.4 Loss of *Lxn* confers a significant competitive advantage and self-renewal capacity to HSCs.

To further investigate the effect of *Lxn* knockout, we performed BM competitive repopulation assay and serial transplantation experiments. For the competitive repopulation experiments, one million BM cells from either wild type B6 mice (CD45.2 isotype) or *Lxn-/-* mice (CD45.2 isotype), along with same number of competitor B6.SJL cells (CD45.1 isotype), were transplanted into lethally-irradiated recipients (Fig. 2.9A). Fifteen weeks after transplantation, granulocytes (Mac-1+/Gr-1+ cells) and B lymphocytes (B220+ cells) were enriched in the PB of *Lxn-/-* mice compared to the ratio used for transplantation (1:1) (Fig. 2.4F). Over time, the proportion of *Lxn-/-* donor-derived cells gradually increased in PB, BM and BM LSK cells (Fig. 2.4C, D and E), suggesting a competitive advantage of *Lxn-/-* cells.

We then tested the self-renewal capacity of *Lxn-/-* HSCs in serial transplant experiments in which they, along with B6.SJL (CD45.1 isotype) BM cells, competed for engraftment in lethally irradiated B6.SJL recipients. For the

primary transplant, one million test cells (CD45.2 isotype) were mixed with an equal number of competitor cells (CD45.1 isotype) and were transplanted into lethally irradiated primary recipients. For the secondary transplant, ten million recipient cells (from primary recipients) were transplanted into secondary recipients. The same regimen was repeated for the tertiary transplants (Fig. 2.9B). At each transplant, PB, BM and BM LSK cells were analyzed. The percentages of *Lxn-/-* and B6 cells in each compartment were compared. *Lxn-/-* stem cells showed a sustained competitive advantage in each population (BM and BM LSK cells) at primary, secondary and tertiary transplants (Fig. 2.5B and C), demonstrating that they retained self-renewal capacity under replicative stresses. At the tertiary transplant, the number of *Lxn-/-* donor-derived BM and LSK cells remained high (Fig. 2.5C), whereas the number of their progeny (PB cells) dropped to the same level as that of the wild type. This observation may be explained by replicative senescence.

The BM microenvironment influences HSC lineage fate decisions and HSC function. The proliferative hematopoiesis can arise from hematopoietic cells themselves. It also can be induced by cues from the microenvironment endogenously. In previous studies, we observed that hyperproliferative hematopoiesis in *Lxn-/-* mice is transplantable, indicating this phenotype is at least partially cell intrinsic. To investigate the extrinsic effects, we performed reciprocal transplants (Fig. 2.9C). Congenic wild-type cells (CD45.1 isotype) were transplanted into lethally irradiated *Lxn-/-* or B6 recipient mice. By 5, 10 and 15 weeks post transplantation, there was no difference in donor-derived

leukocytes in PB between the two groups (Fig. 2.5D). Thus, the proliferative hematopoiesis observed in *Lxn-/-* mice is cell-autonomous, and was not induced by the *Lxn* deficient microenvironment. However, the donor-derived myeloid cells were significantly suppressed in *Lxn-/-* recipients, indicating *Lxn-/-* microenvironment has an influence on lineage preference (Fig. 2.5E). Skewing toward the myeloid lineage conceals the myelo-proliferation in *Lxn-/-* mice, explaining the significantly increased myeloid cells in transplants of *Lxn-/-* BM cells (Fig. 2.4F), but not in *Lxn-/-* mice (Fig. 2.8).

Ultimately, CR, serial transplantation and reciprocal transplantation experiments showed that loss of *Lxn* confers a competitive advantage and increased self-renewal capacity to hematopoietic cells at the level of the HSC (cell intrinsic).

2.4.5 Decreased apoptosis frequency in *Lxn-/-* HSPCs may account for enlarged progenitor and stem cell compartments.

As previously reported, *Lxn* expression positively regulates apoptosis but negatively influences proliferation and self-renewal (and vice versa)[92, 93]. In this study, we found a proliferative hematopoiesis caused by dysregulation at the level of the MPP. To explore the mechanism underlying the phenotype, we studied cell cycle, proliferation, and apoptosis in *Lxn-/-* hematopoietic cells. BrdU labeling and Ki-67 staining of hematopoietic cells showed no significant difference in cell cycle and proliferation status between *Lxn-/-* and B6 animals (Fig. 2.10A, B and C). We found decreased numbers of PI-/Annexin V+ cells in MPP, ST-HSC and LT-HSC populations in *Lxn-/-* mice compared to B6 mice (Fig.

2.6A and B), suggesting that *Lxn* positively regulates apoptosis in stem and progenitor cells. The apoptotic frequency of *Lxn-/-* cells was reduced the most in the MPP population (50% increase). Thus, the observed MPP expansion may be caused by a decreased rate of apoptosis.

2.4.6 Functional categories enriched in the differentially expressed genes in *Lxn-/-* MPP cells.

To gain insight into the molecular mechanisms by which loss of *Lxn* induced the various hematopoietic phenotypes, we examined the gene expression profiles. Microarray experiments were performed in LSK/CD34^{+}/Flt-3^{+} BM cells obtained from B6 and *Lxn-/-* mice using Affymetrix Gene Chip MoGene-1_0-st-v1 arrays. Using a significance threshold of 0.01, we identified 650 genes that were differentially expressed between *Lxn-/-* and B6 LSK/CD34^{+}/Flt-3^{+} cells. Some of the most highly under-expressed or expressed genes were identified (Tab. 2.1). *Thbs-1* is one of most highly down-regulated genes, Its expression level was decreased 4-fold in *Lxn-/-* hematopoietic multi-potent progenitor populations (data not shown). To study *Thbs-1* as the target gene regulated *by Lxn,* we tested *Thbs-1* expression at the level of transcript (using quantitative real-time PCR) in hematopoietic cells. Consistent with microarray results, the Q-PCR analysis revealed that *thbs-1* expression gradually decreased along hematopoietic differentiation hierarchy, in parallel with *Lxn* expression (Fig. 2.7). We also examined the *Thbs-1* expression level in FDC-P1 cells (a hematopoietic stem and progenitor cell line) overexpressing *Lxn*. The results showed that ectopic *Lxn* up-regulated *Thbs-1* expression in vitro, indicating that *Lxn* is an up-

stream regulator of *Thbs-1* (data not shown). However, the mechanism underlying *Lxn* regulation of *Thbs-1* expression has not been elucidated in these studies. The next logic step for this research will be study *Lxn* signaling pathway focusing on *Thbs-1*.

2.5 Discussion

In these studies, we found that *Lxn-/-* mice exhibited hyperproliferative hematopoiesis, including bone marrow hypercellularity, splenomegaly with myeloid cell infiltration, and peripheral blood leukocytosis, which may caused by decreased apoptosis. We also showed a cell-autonomous repopulation advantage and elevated self-renewal capacity in *Lxn-/-* mice, indicating that loss of *Lxn* leads to enhanced stem cell function. *Lxn* has been identified as a novel regulator of hematopoietic stem cell population size through balancing apoptosis, proliferation and self-renewal[93]. Congenic mice expressing low expression levels of *Lxn* exhibited decreased apoptosis activities, but increased self-renewal capacity and HSC frequency in BM cells. In our studies, loss of *Lxn* induced decreased apoptotic activities, increased self-renewal capacity, and increased day 35 cobblestones in CAFC assay, which is consistent with previous findings. However, competitive repopulation unit (CRU) experiments do not show any alteration in functional HSC frequencies in *Lxn-/-* mice compared to B6 mice (data not shown), supported by the results that the numbers of phenotypically identified long-term and short-term HSCs in *Lxn-/-* mice were not altered compared to B6 mice. This may be due to the fact that the effective window of *Lxn* activities is limited and/or its effect in regulating HSC population size is dose-

dependent. Relative high or low levels of *Lxn* expression may regulate the HSC population size, however, the absence of *Lxn* during hematopoiesis may not influence the number, but the other functional properties of HSCs. The inconsistency between the CRU and CAFC results may be explained by the controversy of the correlation between the days of appearance of a cobblestone area and the primitiveness of the stem cell. The phenotypic HSCs ($Lin^-Sca\text{-}1^+c\text{-}Kit^+CD34^-Flt\text{-}3^-CD150^+$) can form cobblestones continuously from day 28 to day 64 after plating (unpublished data). Therefore, the frequency of day 35 cobblestones does not represent the accurate numbers of HSC, and leaves the gold standard in enumerating HSCs with the CRU assay.

The hematopoietic stem cell niche is an anatomic location in the BM where HSCs remain quiescent, self-regenerate, proliferate or differentiate in response to various extrinsic cues. Direct interactions between stromal cells and stem cells, or indirect interactions through cytokines secreted by stromal cells are critical for stem cell fate decisions. Proliferative hematopoiesis is generally considered to be intrinsic to hematopoietic cells. However, recent studies have provided support for the role of the microenvironment in coordinating many aspects of hematopoietic biology. Studies utilizing transgenic mice such as RAR gamma and Nf1 have demonstrated that microenvironmental cues may influence stem cell self-renewal capacity, alter lineage distribution, and induce proliferative hematopoiesis[108, 109]. Given that the microenvironment is known to be an important regulator of stem cell fate, it is reasonable to speculate that the niche cells could induce the phenotypes observed in *Lxn-/-* mice model. In this study,

we demonstrated a proliferative hematopoiesis, which is transplantable and therefore cell-intrinsic. Under homeostasis, *Lxn-/-* mice showed increased leukocytes and platelets in PB as well as increased cellularity and an expanded HSPC population in the BM. After transplanting *Lxn-/-* or B6 BM cells with an equal number of competitor cells, *Lxn-/-* cells showed better engraftment efficiency compared to B6 cells (60% recipient engraftment for *Lxn-/-* cells vs. 40% engraftment in recipient receiving B6 cells). Further, hematopoiesis in *Lxn-/-* mice showed lineage skewing toward the B cell lymphoid lineage. We also observed this phenotype in recipients transplanted with *Lxn-/-* BM cells. Although the transplantation studies show that the proliferative hematopoiesis and lineage skewing are cell-autonomous, these data cannot rule out the effects of extrinsic factors. We performed reciprocal transplants to clarify this issue. Results from reciprocal transplants showed no significant difference of engraftment efficiency was induced by the loss of *Lxn* in the microenvironment. However, there was a modification in lineage distribution. Myeloid lineage cells were significantly decreased in the *Lxn-/-* microenvironment, whereas *Lxn-/-* cell showed a slight increase in the numbers in the background microenvironment. These observations indicate that loss of *Lxn* in the stem cell niche does not influence the competitive advantage, but may modify the lineage distribution to favor lymphoid cells.

The positive correlation between *Lxn* expression and apoptotic activity in hematopoietic cells has been previously reported[93, 107]. Mutations in other pro-apoptotic genes such as *p53* are found in hematopoietic malignancies and, in

many cases, are thought to be the initiating mutations that generate pre-leukemic cell at HSC level. Apoptosis is an intrinsic mechanism which scavenges pre-leukemic cells and protects chromosome integrity. The mutations that generate pre-leukemic cells are thought to escape apoptosis. Overexpression of *Lxn* in tumor cells suppressed tumor growth both in vitro and in vivo, demonstrating a pro-apoptotic role of *Lxn* (as seen in Chapter 5). Further, we found decreased apoptotic frequency in *Lxn-/-* cells, which may underlie the proliferative hematopoiesis we observed in the BM of *Lxn-/-* mice. Will this proliferative hematopoiesis lead to hematological malignancies? To answer this question, we examined the cells after a series of transplantation. In primary transplants, *Lxn-/-* derived BM and LSK cells were approximately 100% more than B6 derived BM and LSK cells. These advantages persisted in secondary and tertiary transplants, indicating an advanced self-renewal capacity in Lxn-/- HSCs. On the other hand, *Lxn-/-* derived PB cells in recipients were 50% more than B6 derived PB cells. However, this trend did not persist upon tertiary transplants. Instead of taking over the entire hematopoiesis in tertiary transplant recipients, the *Lxn-/-* derived PB cells showed no significant difference compared to B6 derived PB cells, indicating a reduction in differentiation from BM cell to PB cell that may due to replicative senescence, or a physiological optimum in which Lxn-/- transplanted cells maintained a maximal occupation in donor's hematopoiesis through self-(apoptosis) or systemic regulation (phagocytosis)[110]. In another series of experiments (Chapter 3), we treated *Lxn-/-* and B6 mice with 6.5 Gy sub-lethal doses of radiation and monitored their hematopoietic recovery up to 90 days post

radiation. No significant difference has been identified in PB leukocyte counts and BM cellularity in irradiated *Lxn-/-* mice compared to B6 mice. These observations imply that the loss of *Lxn* will not induce tumorigenesis in hematopoietic cells. However, this hypothesis is not definitive because no pathological examination has been performed on *Lxn-/-* BM. A hyperproliferative hematopoiesis can be induced by increased proliferation as well. In previous studies performed on congenic mice, we found that proliferative activities are negatively correlated with *Lxn* expression level[93]. However, we did not observe any changes in proliferation and cell cycling in *Lxn* knockout mice, or in tumor cells overexpressing *Lxn*. The consensus congenic interval on chromosome 3 contains approximately 30 Mb and is composed of a large number of genes. It is possible that the proliferation trait linked to this congenic interval may be accounted for by genes other than *Lxn*.

In these studies we have shown that the proliferative hematopoiesis in *Lxn-/-* cells is accounted by the increase in MPP populations, in which the cell population expanded the most. So we performed microarray experiments on purified MPP populations from *Lxn-/-* and B6 mice. We identified *Thbs-1*, as a putative target for *Lxn* using microarray analysis; Loss of *Lxn* significantly down-regulated the expression of *Thbs-1*. Thbs-1 is a glycoprotein that mediates the cell-to-cell and cell-to-ECM interactions. It plays a very important role in the niche in binding to various extracellular matrix ligands such as fibrinogen, fibronectin, collagens, TGF-β, some matrix metalloproteinases, and to cell surface receptors including CD36 and CD47[111, 112]. Loss of *Thbs-1* in mouse model showed a radio

resistance and regulated radiation-induced apoptosis through CD47 mediated signaling pathway[112, 113]. It also has been reported that *Thbs-1* is involved in tumorigenesis as a tumor suppressor gene, similar to *Lxn*[107, 114]. Its expression is either down-regulated or absent due to hypermethylation in cancer cells. *Thbs-1* deficient mice developed tumor earlier in a *p53* null background, supporting its role as a putative tumor suppressor gene[115]. Further, *Thbs-1* positively regulates apoptosis[116]. It regulates radiation-induced apoptosis through CD47 signaling pathway[112, 117].To test the hypothesis that *Thbs-1* expression correlate with Lxn expression, we overexpressed *Lxn* in FDC-P1 cells. Using Q-PCR we found that in FDC-P1 cells overexpressing *Lxn*, the expression level of *Thbs-1* was up-regulated with *Lxn* overexpression. The studies mentioned above indicate *Thbs-1* may be a potential target of *Lxn*.

In conclusion, I found that loss of *Lxn* induced hyperproliferative hematopoiesis resulting from decreased apoptosis. Loss of *Lxn* also confered a cell-autonomous repopulation advantage and elevated self-renewal capacity, indicating enhanced stem cell functions in *Lxn-/-* animals.

2.6 Acknowledgements

I gratefully acknowledge Gary Van Zant and Ying Liang for their contributions to this chapter. I thank the technical assistance of Barry Grimes and Carol Swiderski in flow cytometry and animal handling. I also thank Chi Wang's help in statistical analysis for Microarray data.

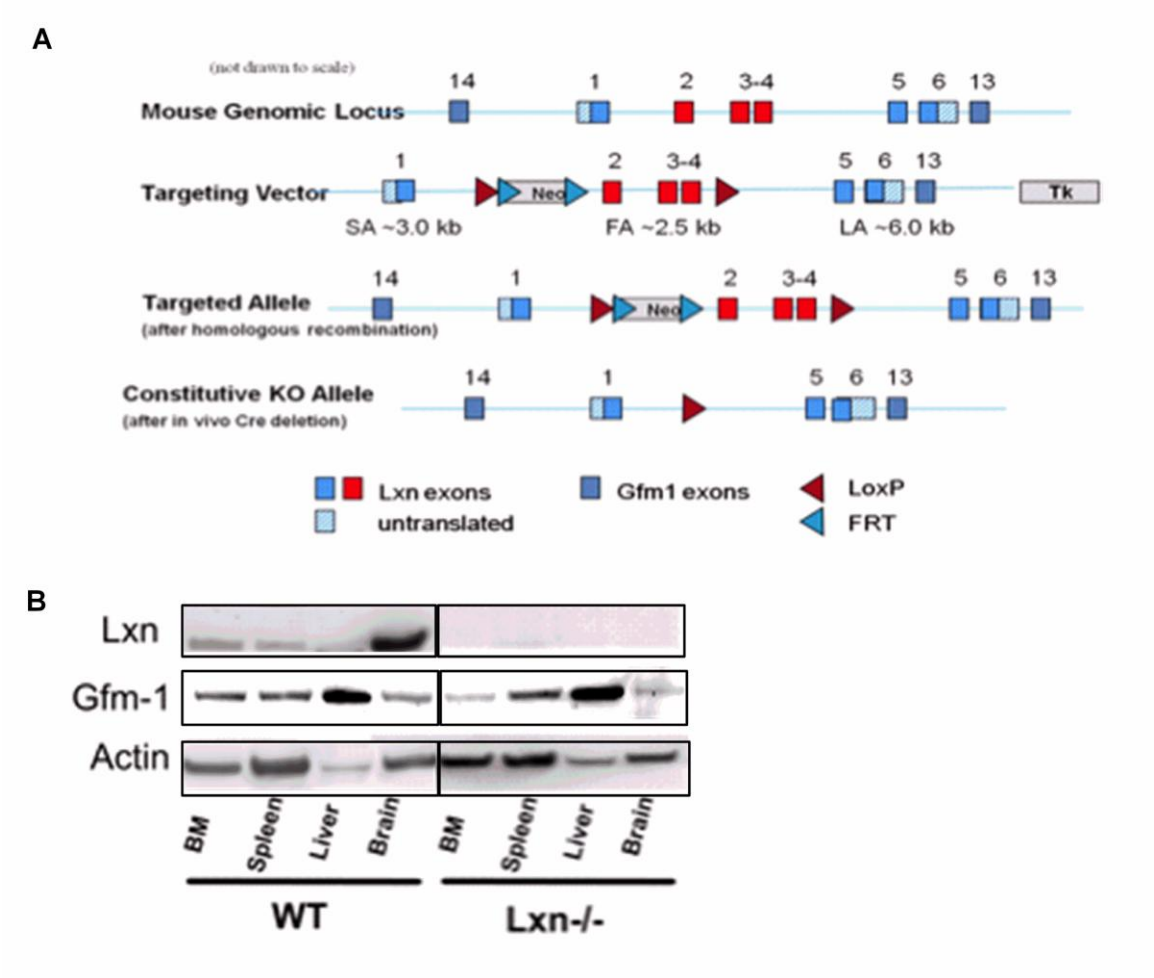

Figure 2.1 Generation of *Lxn* deficient (*Lxn*-/-) mice.

(A) The *Lxn* wild-type locus, the targeting vector, and the *Lxn* targeted allele with the *Lxn* constitutive knock out allele. (top to bottom). Coding regions are shown as filled squares labeled with exon numbers. The targeting vector introduced a functional excision sequence flanking exons 2 to 4 of the *Lxn* gene that resulted in the excision of exons 2-4 after in vivo Cre deletion. (B) Western blots of *Lxn* expression in various tissues of wild type B6 and *Lxn*-/- mice. Total protein from BM, spleen, liver and brain were probed with anti-Lxn or anti-Gfm-1 antibody, respectively.

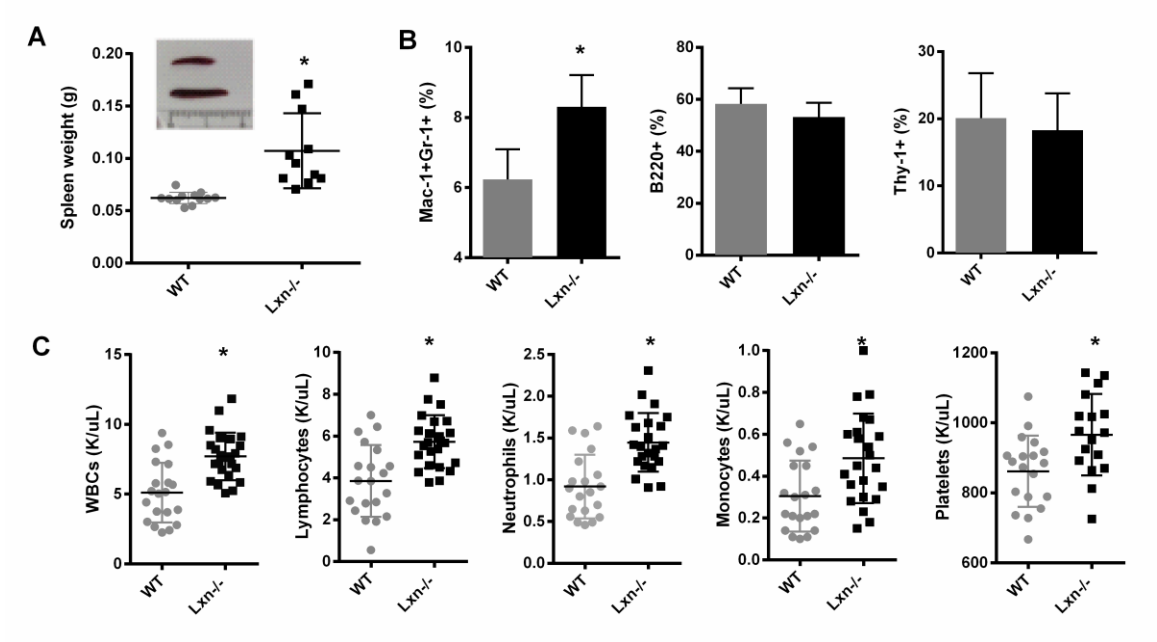

Figure 2.2 Proliferative hematopoiesis in *Lxn-/-* mouse.

(A) Enlarged spleens and expanded red pulp in *Lxn*-/- mice (n=11) compared with wild type B6 mice (n=12). (B) Flow cytometry analysis using lineage-specific markers, Gr-1/Mac-1 (myeloid), B220 (B cell) and Thy-1 (T cell), comparing the proportion of each cell types in the spleens of *Lxn*-/- and B6 mice (n>10 in each experiment). (C) Peripheral blood cells were quantified by using the Hemavet cell counter. The numbers of total white blood cell, lymphocyte, neutrophil, monocyte and platelet were compared between *Lxn*-/- and B6 mice (n>20 in each experiment). * indicated a P<0.05 hereafter. Error bar represented standard deviation (SD) hereafter if not indicated.

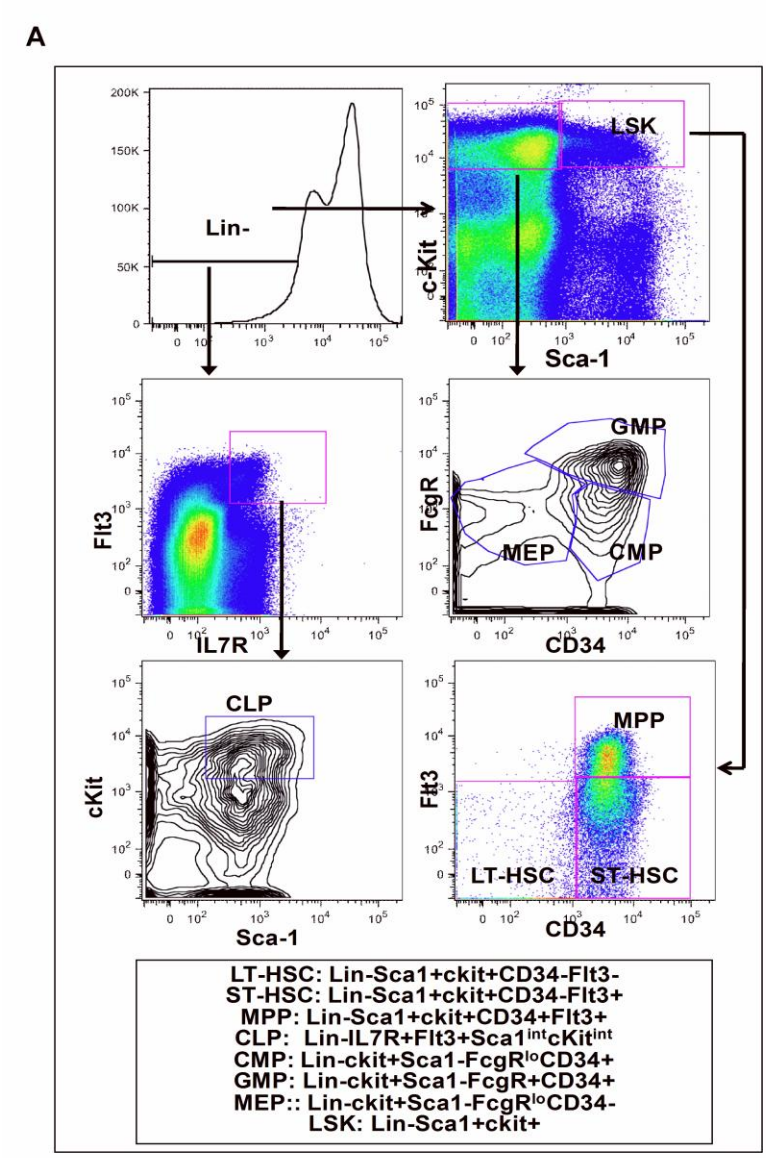

Figure 2.3 Stem cell and progenitor quantification by using phenotypic marker and flow cytometry.

(A) Flow cytometric analysis of immunological cell surface makers were used in identifying the frequency of progenitor and stem cells. Serial gating and marker panels for each subpopulation (LT-HSC, ST-HSC, MPP, CLP, CMP, GMP, MEP and LSK) are listed above.

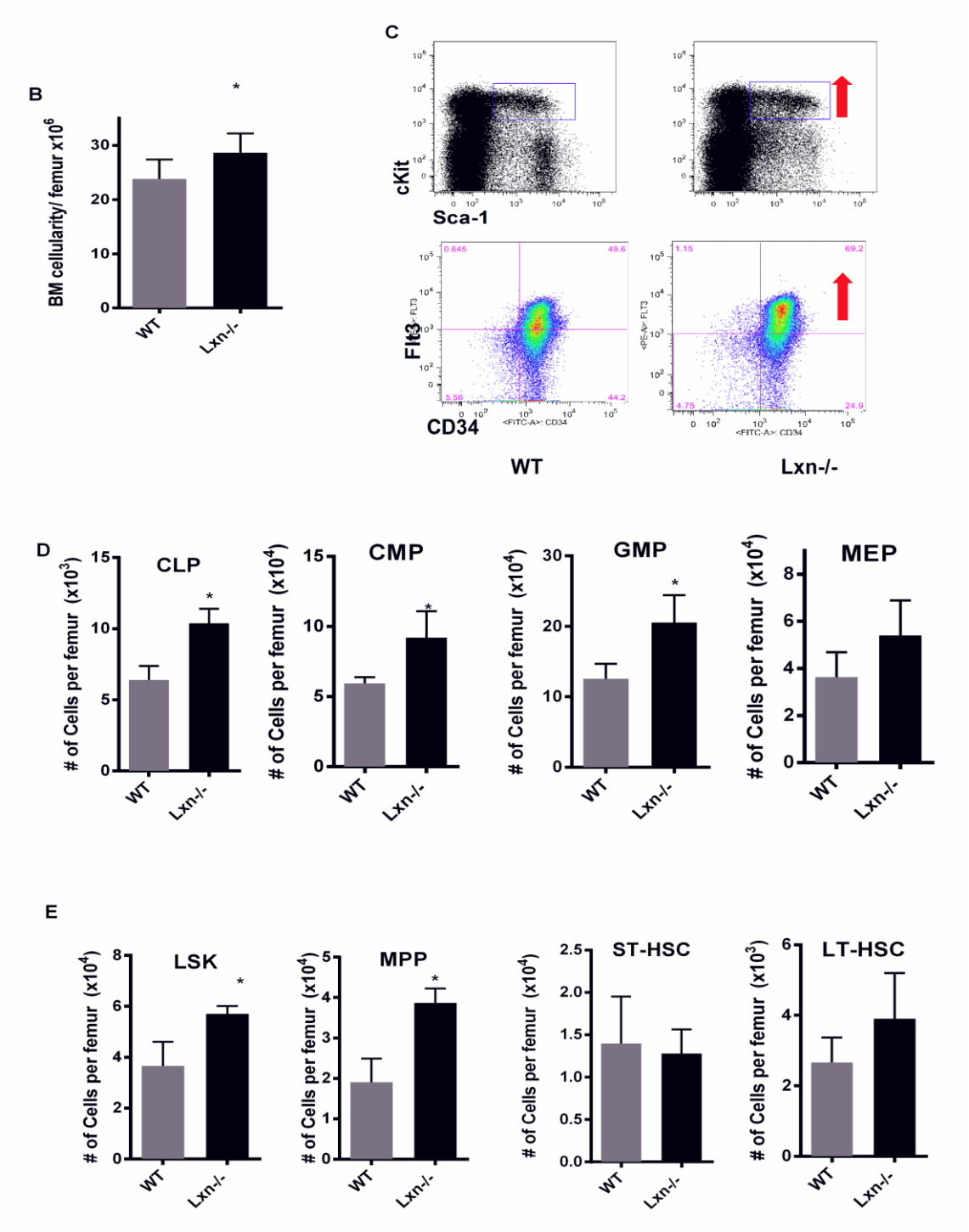

Figure 2.3 continues (B) BM cellularity (cell number/femur) in *Lxn*-/- mice (n=26) compared with wild type B6 mice (n=8). (C) Flow cytometric analysis showed an increased LSK population in *Lxn*-/- BM cells that due to an expanded MPP

population. (D) and (E) Flow cytometric studies revealed that LSK cells, multi-potent progenitors (MPPs) and lineage committed progenitors (CLPs, CMPs, and GMPs) were relatively increased in *Lxn-/-* BM cells. In (C), (D) and (E), each experiment was repeated 3 times, and at least 3 animals were pooled in each group.

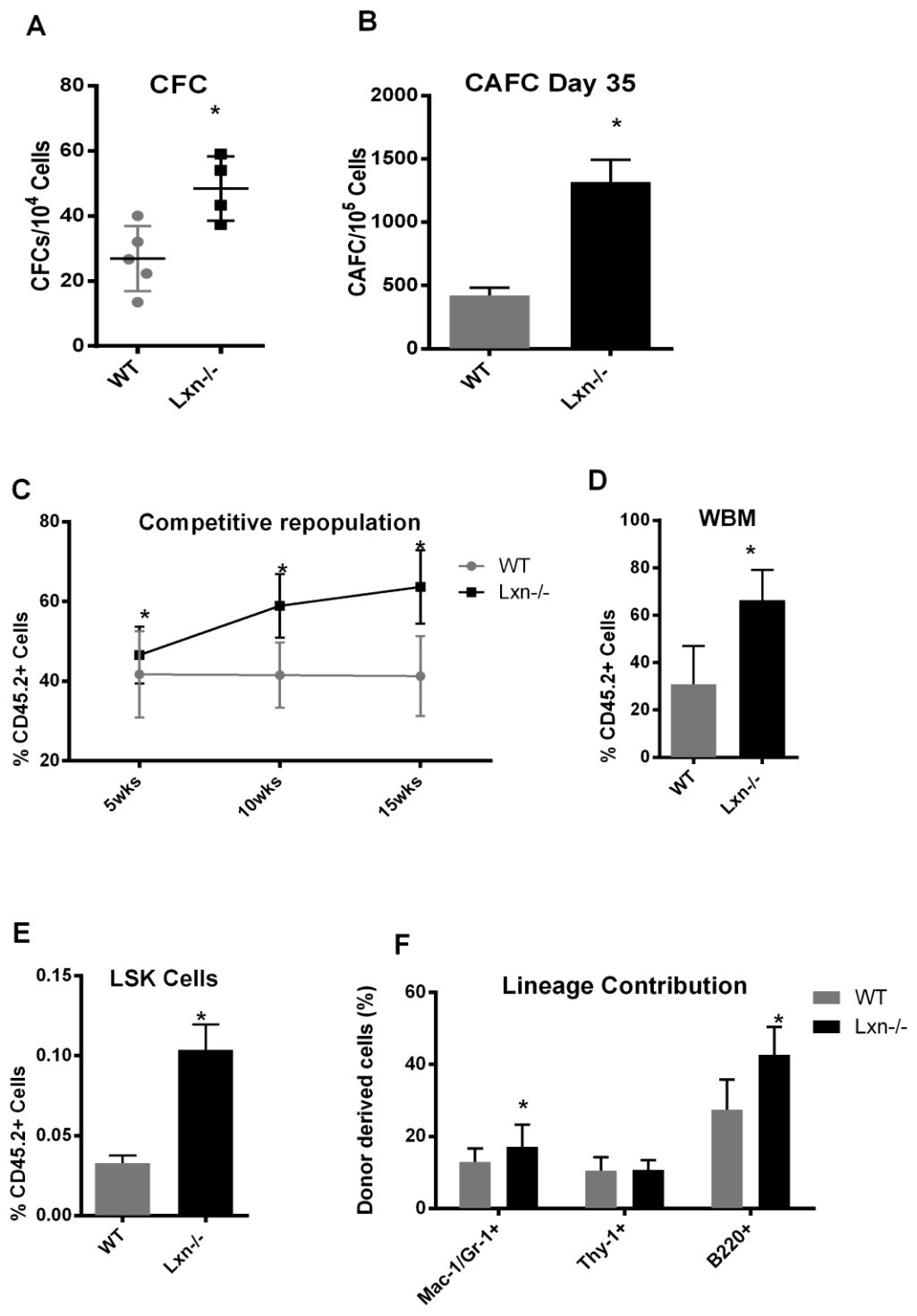

Figure 2.4 Functional analysis of *Lxn-/-* mice.

(A) Day 14 colony-forming cells formed per 10^4 cells in *Lxn*-/- mice (n=5) and B6

mice (n=4). (B) The frequency of CAFCs formed at day 35 in *Lxn*-/- (n=4) and B6 (n=3) animals. Panels C, D, E and F are flow cytometric analysis of competitive repopulation experiments with *Lxn*-/- and B6 mice (n=10 in each experimental group). (C) Flow cytometric analysis of engraftment efficiency of donor derived cells in PB of recipients at 5, 10 and 15 weeks post competitive transplantation. (D) Flow cytometric analysis of the percentage of donor-derived cells in BM of recipients at 15 weeks after competitive transplantation. (E) Flow cytometric analysis of the percentage of donor derived LSK cells in PB of recipients at 15 weeks post competitive transplantation. (F) Determination of the lineage distribution of myeloid, T and B cells in the PB of donor animals in transplanted recipients at 15 weeks post transplantation. Error bar represented standard error of the mean (SEM) in Fig. 2.4B.

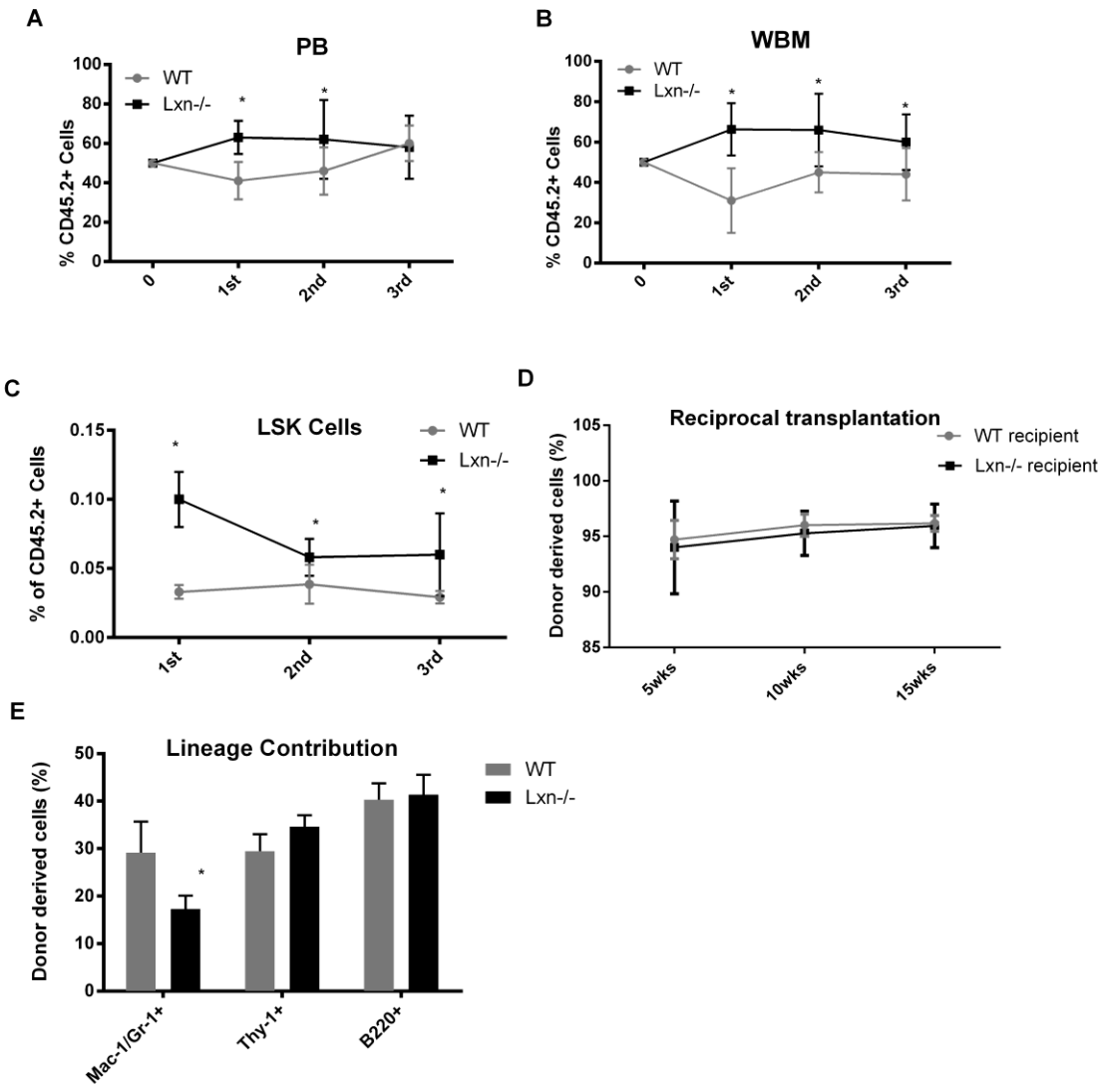

Figure 2.5 Serial transplantation and reciprocal transplantation with *Lxn-/-* mice and B6 mice.

(A, B and C) Self-renewal analysis of HSCs using serial transplantation. *Lxn-/-* (two independent experiments; n=10) or B6 (two independent experiments; n=10) derived peripheral blood leukocytes (A), BM nucleated (B) and BM LSK cells (C) were analyzed 15 weeks post transplantation in primary, secondary and tertiary recipients. (D and E) $5x10^6$ unfractionated BM cells were transplanted into either B6 (n=5) or *Lxn-/-* recipients (n=5). (D) Donor-derived PB leukocytes were analyzed At the 5, 10

and 15 weeks post transplantation. (E) Lineage distribution of donor-derived myeloid, T and B cells in PB cells 15 weeks post transplantation.

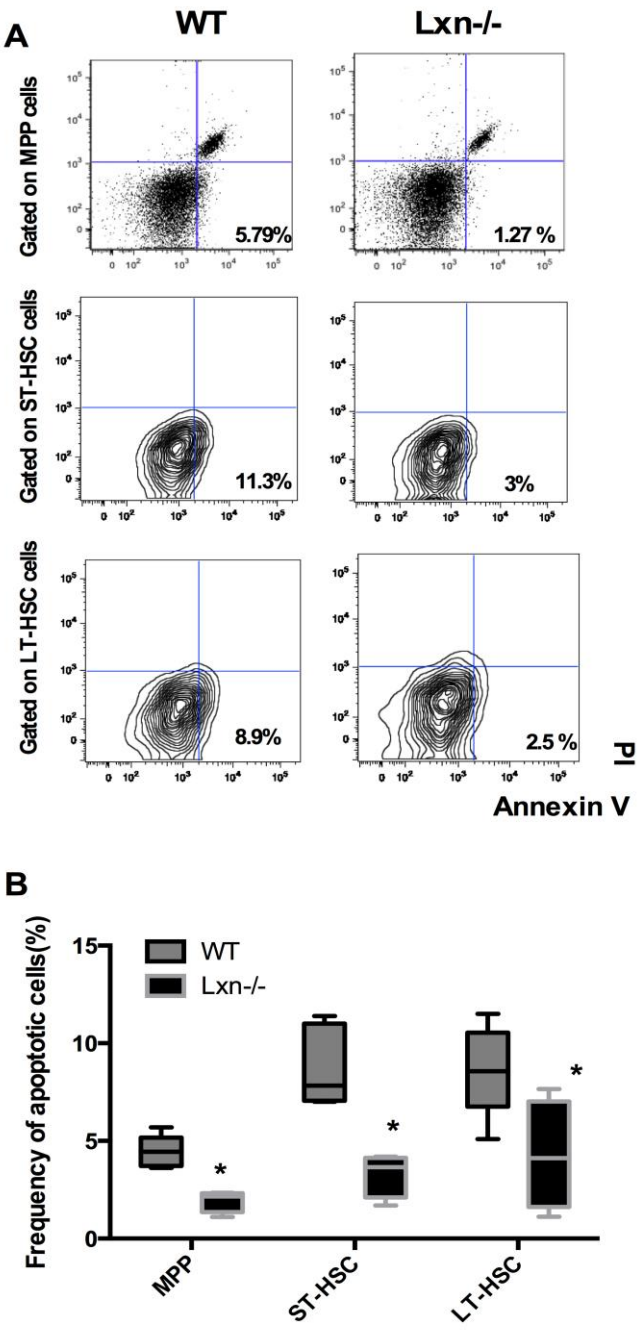

Figure 2.6 Alteration in apoptosis in *Lxn-/-* hematopoiesis.

(A) Flow cytometric analysis of BM cells stained with Annexin V (plus PI) distinguished cell subsets that are apoptotic (PI^- /Annexin V^+) in multiple cell sub-populations.(B) Decreased frequency of apoptotic cells in *Lxn-/-* mice compared to B6 mice in MPP, ST-HSC and LT-HSC populations.

Table 2.1 Genes differentially expressed in *Lxn-/-* MPP cells

Gene	Contrast
HSPA1A	+3.6
RNASE3	+2.0
TSEN15	+1.9
GAS5	+1.9
HSPS1	+1.8
KIR3DL2	-1.76
GFI1B	-1.77
SLC18A	-1.83
TRPC6	-2.3
THBS-1	-3.49

Microarray experiments were performed in LSK/CD34^{+}/Flt-3^{+} MPP BM cells obtained from B6 and *Lxn-/-* mice using Affymetrix Gene Chip MoGene-1_0-st-v1 arrays. Table 2.1shows top five of the most highly under-expressed or expressed genes with a significance threshold of 0.01.

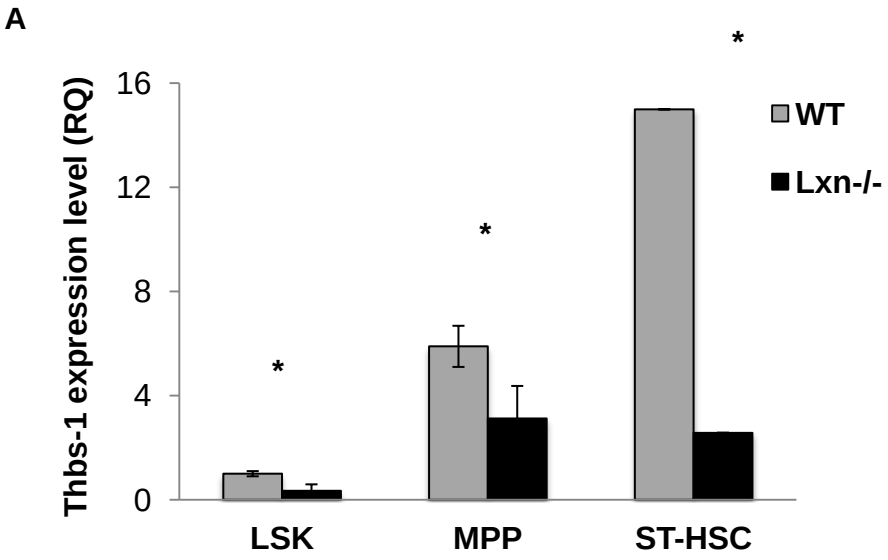

Figure. 2.7 *Thbs-1* expression level in *Lxn-/-* HSPCs.

Thbs-1 expression levels along hematopoietic differentiation hierarchy were identified by Q-PCR.

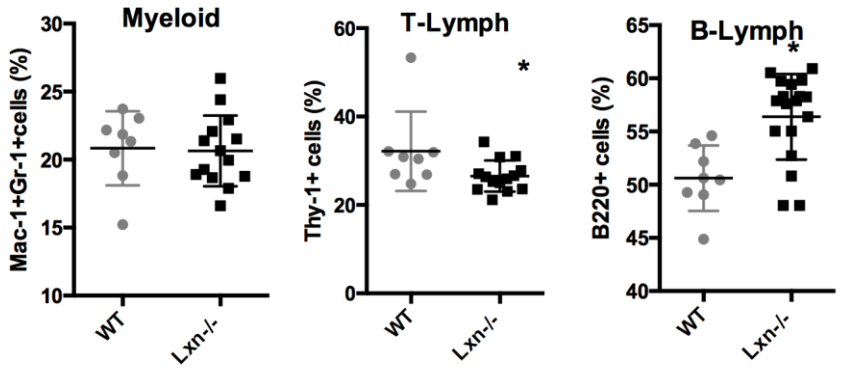

Figure. 2.8 Flow cytometric analysis of lineage distribution in PB.

Flow cytometry using lineage-specific markers, Gr-1and Mac-1 (myeloid cells), Thy-1 (T cells), and B220 (B cells), showed an altered lineage distribution in PB in *Lxn-/-* mice (n=13) compared to B6 mice (n=8).

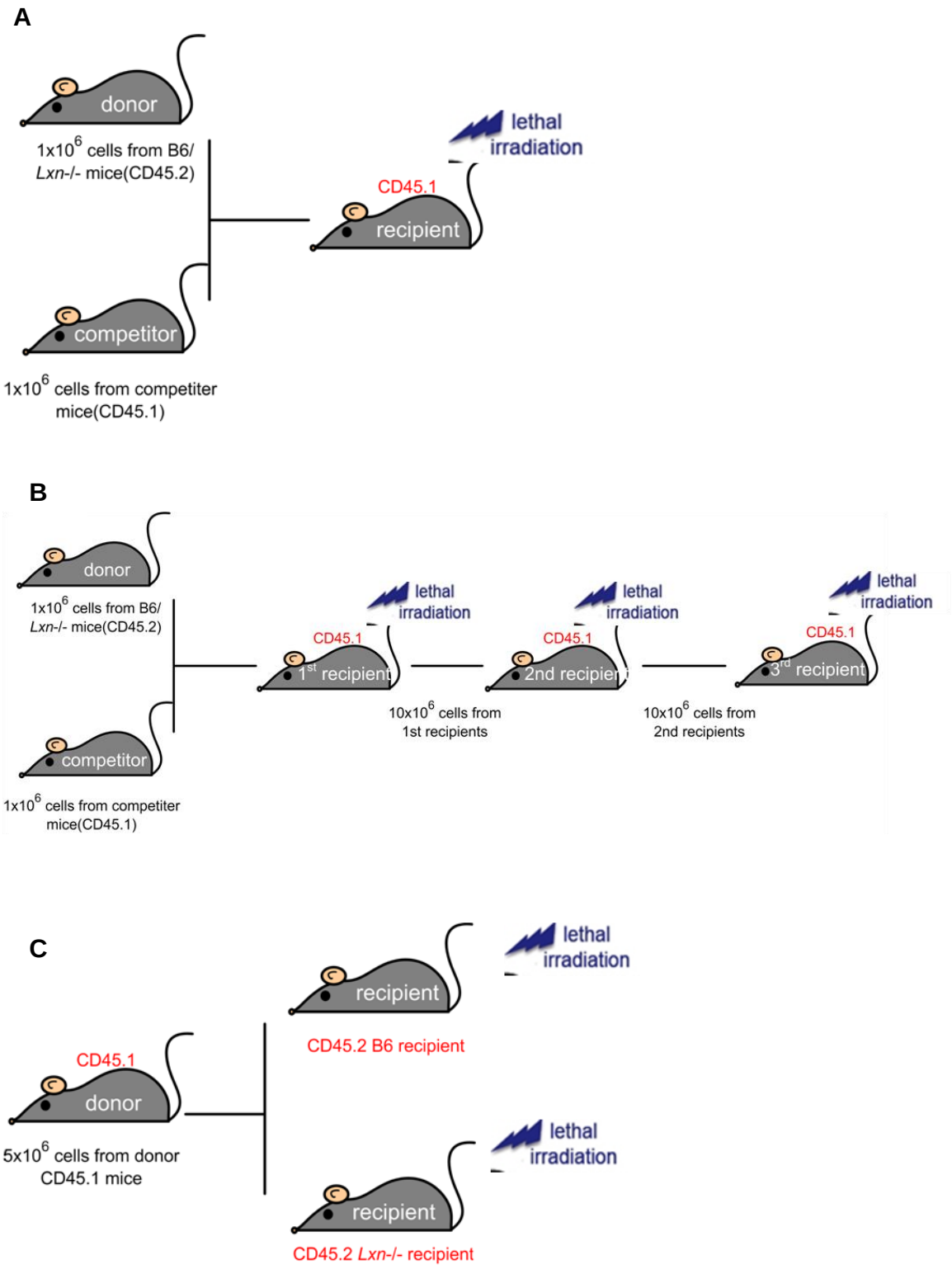

Figure 2.9 Transplantation strategy.

(A) In competitive repopulation (CR) assays, $1x10^6$ WBM cells from *Lxn*-/- mice or B6 test cells (both CD45.2) were mixed with an equal number of competitor cells

(CD45.1), and retro-obitally injected into lethally irradiated (9 Gy) CD45.1 recipient mice (B6.SJL/BoyJ). (B) In serial transplantation, one million test cells (CD45.2 isotype) are mixed with an equal number of competitor cells (CD45.1 isotype) and are transplanted to lethally irradiated primary recipients. At 15 or 16 weeks post transplantation, $10x10^6$ unfractionated bone marrow cells were harvested from primary recipients and transplanted cells into lethally irradiated secondary recipients. The same regimen was repeated for tertiary transplantation. (C) In reciprocal transplantation, $5x10^6$ unfractionated bone marrow cells (CD45.1) were transplanted into either B6 or *Lxn-/-* recipients (both CD45.2). Engraftment efficiency was measured at 5, 10 and 15 weeks transplantation.

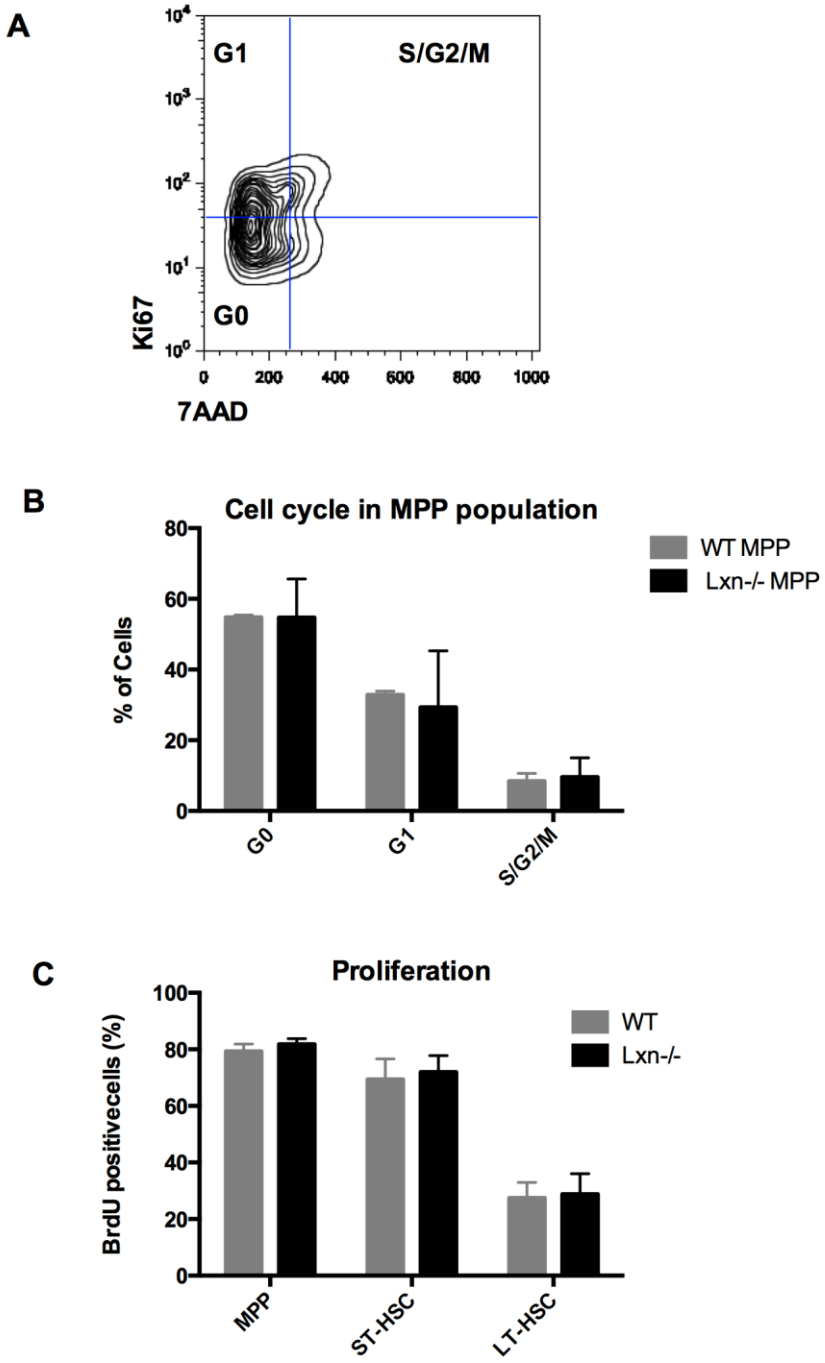

Figure 2.10 Lacking of alteration in cell cycle status and proliferation in *Lxn-/-* HSPCs.

(A) a representative scatter plot for Ki67 cell cycle analysis. Flow cytometric analysis of BM cells stained with Ki-67 (combined with DNA dye 7-AAD) distinguishes cell

subsets that in G0 (Ki-67$^-$ 7-AAD$^-$), G1 (Ki-67$^+$ 7-AAD$^-$), and S/G2/M (Ki-67$^+$ 7-AAD$^+$) phase. (B) Cell cycle status in *Lxn-/-* and B6 MPP populations. (C) Proliferative profile of HSPC subsets. Mice were exposed to BrdU for three days prior to analysis. MPPs, ST-HSCs and LT-HSCs were analyzed for BrdU incorporation (BrdU$^+$).

CHAPTER 3: Loss of Latexin in Murine Hematopoietic Stem and Progenitor Cells Mitigates Ionizing Radiation Toxicity

3.1 Abstract

Bone marrow injury is one of the major adverse side effects of radiation and chemotherapy; however, treatments that can mitigate such injury are very limited. To manage radiation or chemotherapy induced bone marrow injury, we need a better understanding of how radiation harms bone marrow cells and their environment, as well as how bone marrow cells react to such stress. In this study, we discovered a role for Latexin (*Lxn*) in the radio-sensitivity of hematopoietic stem and progenitor cells. We found that loss of *Lxn* in mice confers resistance to lethal and sub-lethal radiation. *Lxn* deletion protected 3 out 5 mice (60%) from 8 Gy irradiation, while no mouse survived in the wild type group. After exposure to sub-lethal irradiation, the LSK cell population expanded ~5-fold two weeks post irradiation in *Lxn*-/- animals, suggesting a rapid recovery to radio-resistance at the HSC/HPC level. Further, *Lxn*-/- mice displayed an enhanced hematologic and immune recovery 3 - 14 days after irradiation, with elevated numbers of total leukocytes, lymphocytes, granulocytes and platelets. We then studied the underlying mechanism that accelerates regeneration of hematopoiesis in bone marrow after irradiation, and found that ablation of *Lxn* suppressed apoptosis in primitive progenitor cells (LSK). In conclusion, our data indicate that *Lxn* promotes irradiation-induced apoptosis and loss of *Lxn* conferred a radiation resistance through regulating hematopoietic recovery. These findings provide a novel potential therapeutic target for protecting HSPCs in patients undergoing

radiotherapy or exposed to environmental radiation.

3.2 Introduction

Maintaining a stable supply of mature blood cells is essential for nutrient supply, pathogen defense, and tumor surveillance in hematopoiesis. However, this homeostasis can be perturbed by DNA-damaging agents such as ionizing radiation. Ionizing radiation is high-frequency radiation that has the capacity to remove an electron from an atom. When ionizing radiation pass through a cell, its high energy causes intracellular atoms and molecules to become excited, or "ionized". This ionization can break chemical bonds, produce free radicals, and damage molecules[45]. At low doses of ionizing radiation, hematopoietic cells trigger a rapid recovery response and amend certain levels of damage[46, 47]. However, DNA mutation may still occur that could lead to tumorigenesis in the future. When exposed to high doses of ionizing radiation, hematopoietic cells fail to repair themselves and undergo programmed cell death (apoptosis) [45, 48]. Therefore, ionizing radiation induced-apoptosis is necessary to balance tumorigenesis prevention and organismal survival. We propose that low levels of apoptotic activity are beneficial to tissue regeneration and may promote the restoration of hematopoiesis when cells are exposed to high doses of ionizing radiation.

We previously discovered a role for *Lxn* in inhibiting tumor growth through promoting apoptosis in cancer cells[107] (Chapter 5). Ectopic overexpression of *Lxn* in murine lymphoma cells (A20 cell line) slowed their growth rate in vitro and inhibited tumor formation in vivo by significantly increasing apoptosis through the

down-regulation of two anti-apoptotic genes: *Bcl-2* and *Pim-2*[107]. Furthermore, in mice lacking *Lxn* expression (*Lxn-/-*) we observed expanded hematopoiesis due to decreased apoptosis activity in progenitor and stem cells (Chapter 2). These phenomena are consistent with what we previously observed in a study with congenic animals in which *Lxn* expression was positively correlated with apoptotic frequency in hematopoietic cells[93]. These findings implicate *Lxn* as a pro-apoptotic factor, and prompted us to explore *Lxn* function under genotoxic stress, such as radiation, where apoptosis is critical to tissue regeneration.

In the present study, we demonstrated that deletion of *Lxn* allows mice to withstand lethal and sub-lethal doses of radiation. Remarkably, loss of *Lxn* protected hematopoietic progenitor and stem cells from ionizing radiation, and accelerated both hematopoietic and immunologic recovery. Further, *Lxn* deficiency significantly suppressed radiation-induced apoptosis in hematopoietic progenitor and stem cells. In conclusion, our findings provide evidence that deletion of *Lxn* may be a novel strategy for promoting HSPC recovery in patients undergoing radiotherapy or following accidental radiation.

3.3 Methods

3.3.1 Animals

Young C57BL/6 (B6) mice (8-16 weeks) were purchased from The Jackson Laboratories (Bar Harbor, ME). Latexin constitutive knockout mice were generated by Taconic/Artemis (Germantown, NY) and used at a young age (8-16 weeks). Male animals were used in this study. All animals were housed in the

animal facilities of the University of Kentucky under pathogen-free conditions according to NIH-mandated guidelines for animal welfare and were given food and water *ad libitum*.

3.3.2 Ionizing radiation

The mice and cells were exposed to various doses of radiation (6.5 Gy, 8 Gy, 9 Gy and split doses of 12 Gy) in a 137 Cs gamma irradiatior (J.L. Shepherd and Associates, Glendale, GA) at a dose rate of 153 rad/min.

3.3.3 Peripheral blood cell counts.

Animals were anesthetized with isoflurane (Butler Animal Health Supply, Dublin, OH). Peripheral blood was collected from retro-orbital venous plexus into EDTA-coated microtainer tubes (Becton, Dickinson and Company, Franklin lakes, NJ). Circulating leukocytes, erythrocytes and platelets were counted by analyzing 20 ul of blood using a Hemavet 950 (Drew Scientific, Dallas, TX).

3.3.4 Hematopoietic cell identification and isolation

Bone marrow cells were flushed from the femora and tibiae using a 1 ml syringe and 22G needle into Hanks balanced salt solution (HBSS) with 2% fetal bovine serum (FBS) (Gibco, Grand Island, NY). Progenitor cells were discriminated from stem cells by the lack of cell surface antigens characteristic of cells committed to individual lineages. Antibodies against these antigens included CD5 and CD8a, B220, Mac-1, Gr-1, and Ter119 were biotinylated. Strepavidin secondary antibody was used to detect lineage negative cells. To

further purify primitive stem cells, the stem cell markers Sca-1 and c-Kit were incorporated into the staining procedure. Dead cells were excluded by propidium iodide (PI) that stains exposed double-strand DNA. All monoclonal antibodies were purchased from eBioscience (San Diego, CA), Biolegend (San Diego, CA), or BD Pharmingen (San Jose, CA).

3.3.5 Cell analysis and sorting

Bone marrow cells were analyzed and sorted on a BD FacsAria II flow cytometer (Becton Dickinson, Franklin Lakes, NJ). Cells were sorted into phosphate buffered saline (PBS) with 0.5% FBS for further use. Flow cytometry data was analyzed using FlowJo software (Tree star, Ashland, OR).

3.3.6 Apoptosis analysis

Bone marrow cells were prepared and stained as described above. The fluorochrome-conjugated apoptotic marker Annexin V along with Propidium Iodide (PI) (both from BD Pharmingen) were used to identify apoptotic cells (PI^- /Annexin V^+). Stained cells from *Lxn*-/- animals and B6 animals were analyzed by flow cytometer.

3.3.7 Colony forming cell (CFC) assay

Methylcellulose-based culture media (MethoCult) was purchased from Stem Cell Technologies, Vancouver, Canada and contained the following cytokines: stem cell factor (SCF), IL-3 and IL-6. For this assay, 5×10^4 whole BM cells in 100 µL HBSS were thoroughly admixed with 1 mL complete MethoCult

media, plated into petri-dishes, and incubated at 37°C. Individual wells of duplicates were counted on day 10 to quantify lineage specific colonies.

3.3.9 Statistics

Statistical significance between means was determined by a two-way Student *t* test.

3.4 Results

3.4.1 Loss of *Lxn* mitigates lethal and sub-lethal irradiation with various doses

From previous studies, a pro-apoptotic role of *Lxn* has been observed[93, 107]. In order to further study *Lxn* function in response to hematopoietic stress induced-apoptosis, we used Lxn constitutive knock-out mice as a model and treated the mice with ionizing radiation. The *Lxn* deficient mouse model was generated by Taconic/armetis with a deletion of exons 2-4 in the *Lxn* gene which results in the disruption of the protein (Chapter 2). We first studied the effects of loss of *Lxn* in BM cell radiation resistance. Total body irradiation (TBI) was administrated to both *Lxn*-/- mice and B6 control mice. We tested various dosages of gamma radiation including lethal doses of 8 Gy and 9 Gy, as well as clinically relevant split doses totaling 12 Gy. We then studied the survival rate for each treatment. As expected, all of the lethally irradiated B6 animals died within 20 days after receiving a single 8 or 9 Gy dose (Fig. 3.1A). Surprisingly, the survival rate of *Lxn-/-* mice was significantly greater. As shown in Fig 3.1A, 60% of the *Lxn-/-* mice survived the 8 Gy dose of irradiation and 20% of *Lxn-/-* mice

survived the 9 Gy dose. To further characterize the radio-protective effect and study its implication in medical treatment, we irradiated two experimental groups with 12 Gy TBI using a fractionated schedule of 2 Gy every 12 hours. Consistent with our previous results, all of the knockout animals survived, whereas only 4 out of 5 wild type mice survived (Fig. 3.1B).

3.4.2 Loss of *Lxn* promotes the recovery of hematopoietic stem/ progenitor cells post radiation exposure

HSCs and HPCs are vital to long-term and short-term recovery after ionizing radiation. To elucidate the underlying mechanism of radio-resistance in *Lxn-/-* mice, we studied the recovery of HSCs and HPCs after radiation exposure. A single dose of 6.5 Gy TBI (sub-lethal dose) was administrated to both experimental groups (*Lxn-/-* mice and wild-type B6 mice). The recovery of HSPC post irradiation was determined by both flow cytometer (which counts phenotypic HSPC) and in vitro colony-forming unit (CFU) assay (which measures functional HSPC) in a time dependent manner. At each time point, we harvested BM cells, analyzed BM cellularity, and measured the size of the surviving LSK cell population in both groups. The number of phenotypic HSPCs (LSK cells) in *Lxn-/-* mice was significant greater than B6 mice before irradiation and 3 days after exposure to irradiation (Fig 3.2A). LSK cell counts dropped dramatically at day 7 in both experiment groups. However, the HSC recovery rate was accelerated in *Lxn-/-* mice. The number of LSK cells compartment increased approximately 6-fold at day 14 and 3-fold at day 21 in *Lxn-/-* mice (Fig 3.2A and B). The numbers of LK ($Lin^-/c\text{-}Kit^+/Sca\text{-}1^-$) and LS ($Lin^-/c\text{-}Kit^-/Sca\text{-}1^+$) cells were also increased at

day 14, though not to the same extent of LSK cells. These data indicate that deletion of Lxn selectively protects primitive cells more so than differentiated cells (Fig 3.2B).

In flow cytometric analysis, we used phenotypic markers to quantify HSPC numbers. To further identify the numbers of functional HSPCs, we performed CFU assays with $5x10^4$ whole BM cells from 6.5 Gy sub-lethally irradiated animals. The pattern of HSPC recovery in *Lxn*-/- mice is similar to what we observed using phenotypic markers. *Lxn*-/- whole BM cells from mice at day 0, 1, 3,14 and 28 post irradiation formed significantly more colonies, which indicated an accelerated recovery rate compared to B6 cells (Fig. 3.2C). This observation supported previous LSK cell population frequency results.

We also observed a similar trend in BM cell recovery. The numbers of surviving whole BM cells were significantly diminished (24~28 million cells per femur to less than 3 million cells per femur) shortly after irradiation (day 3), and subsequently stable returned back to normal levels by day 28 in *Lxn-/-* mice (Fig. 3.2D). *Lxn-/-* BM cells showed an accelerated recovery rate over B6 BM cells at day 7, 14 and 28 (Fig. 3.2D), in accordance with increased tempo in recovery of HSPCs (Fig. 3.2A). Collectively, our results showed that deletion of *Lxn* up-regulates radio-resistance by promoting HSPC recovery and speeding the regeneration of BM hematopoiesis after irradiation.

3.4.3 Loss of *Lxn* facilitates hematologic and immunologic recovery post radiation exposure

Radiation-induced hematological failure and immune failure are the

primary causes of low survival after high dose radiation exposure. To further address the question of how *Lxn* deletion results in radiation resistance, we examined the hematologic and immune recovery in a time dependent manner following radiation exposure. Wild type B6 and *Lxn*-/- animals were exposed to a sub-lethal (6.5 Gy) dose of radiation to trigger reversible hematopoietic injury. We then monitored the rate of recovery of blood cells. As demonstrated in Fig. 3.3A, loss of *Lxn* significantly accelerated the recovery of total leukocytes in blood. Untreated *Lxn*-/- mice have ~ 30% more leukocytes than their wild type counterparts (Fig. 3.3A). Leukocytes in both strains dropped to approximately 1,000 cells/ul in peripheral blood one day after irradiation. The number of *Lxn*-/- leukocytes rapidly recovered at day 7 and remained significantly greater than B6 (approximately 100% more) up to day 14. The counts of neutrophils (Fig. 3.3B) and lymphocytes (Fig. 3.3B and C) had similar recovery patterns as the total leukocytes. *Lxn*-/- mice showed a faster recovery over the period from day 7 to 28 compared to B6 animals. The level of neutrophil counts in both groups overshot normal levels, whereas lymphocytes never fully recovered. Platelet (Fig. 3.3D) counts in both groups recovered to normal by day 28. The number of *Lxn*-/- platelets was significantly greater than B6 platelets 3 ~ 7 after irradiation. Collectively, a recovery advantage was observed at multiple time points in both hematologic and immune systems in PB, possibly resulting from accelerated recovery in HSPCs in BM.

We also studied the lineage distribution of mature blood cells between granulocyte, monocyte, T-cell and B-cell lymphocytes using various lineage

markers. The gamma irradiation caused immediate lympho- and myelo-ablation at day 1 and an altered lineage distribution that favored the myeloid lineage (Fig. 3.3E). The lymphoid lineage started to gradually recover 3 days after radiation. The distribution of B lymphocytes in *Lxn-/-* mice recovered to near normal (50%), but B6 B lymphocytes never fully recovered (30%) (Fig. 3.3E). This result is consistent with what we observed in animals transplanted with *Lxn-/-* BM cells. *Lxn-/-* cells showed a preference for B-cell production in reconstituted hematopoiesis. In sum, our results indicate that the recoveries of total leukocyte, platelet, granulocyte and lymphocyte subsets were accelerated in *Lxn*-/- mice following ionizing radiation. Further, *Lxn-/-* cells favor B cell lineage production in long-term reconstitution.

3.4.5 *Lxn* ablation diminished radiation-induced apoptosis in hematopoietic stem/ progenitor cells

We previously reported that Lxn regulates cell populations through its role in apoptosis. Here we hypothesized that loss of *Lxn* renders HSCs and HPCs more resistant to apoptosis after exposure to ionizing irradiation. To test this theory, we directly examined the apoptotic frequency using Annexin V staining, and found the percentage of apoptotic LSK cells was significantly lower in *Lxn*-/- mice after 6.5 Gy sub-lethal irradiation (Fig. 3.4A). During homeostasis, apoptotic cell frequency is inherently significantly lower in *Lxn-/-* LSK cells (day 0 in Fig. 3.4A). This low apoptotic frequency was sustained from day 7 to day 28 after irradiation. On day 14 the percentage of apoptotic LSK cells was 5-fold lower in *Lxn*-/- mice compared to B6 mice (Fig. 3.4A, B and C). Notably, the percentage of

apoptotic cells in Lin-, LK and LS subpopulations diminished along with *Lxn* ablation on day 14, but did not reach statistical significance (Fig. 3.4C). The apoptotic frequency was significantly reduced only in LSK cells, indicating that loss of Lxn selectively affected the apoptotic rate in primitive BM cells.

3.5 Discussion

Exposure to moderate or high doses of total body irradiation leads to long-term irreversible hematopoietic injury. This injury has been attributed to quantitative and qualitative damages to hematopoietic cells. Radiation-induced apoptosis and senescence are the major cellular mechanisms which induce quantitative or qualitative radiation-induced damage to stem cells, respectively[48, 50]. From previous studies we learned that a majority of HSCs die after radiation exposure by triggering apoptosis[49, 118]. The apoptotic activity of the cells is critical for regulating the radiation-resistance and survival rate after exposure to high doses of radiation.

In vivo proapoptotic functions of *Lxn* were previously demonstrated in B lymphoma cells[107]. Furthermore, in mice lacking *Lxn* expression (*Lxn-/-*) we observed expanded hematopoiesis due to decreased apoptotic activity in progenitor and short-term HSCs (Chapter 2). These results suggest that *Lxn* regulates apoptotic activities of hematopoietic cells. In this chapter, we studied the function of *Lxn* in response to ionizing radiation, under which apoptotic activities are key factors in post radiation recovery, using *Lxn* deficient mouse as a model.

We first examined the radio-protective activities of *Lxn* in murine

hematopoiesis by studying the survival rates of *Lxn-/-* and B6 mice after lethal doses of radiation exposure. When exposed to lethal doses of total body irradiation (above 7.5 Gy, single dose), death is usually caused by hematological failure[119-121]. Three days after radiation, BM cell counts (both leukocytes and platelets) drop dramatically. Another target organ of irradiation-induced injury potentially leading to mortality is the small intestine[122]. However, previous reports demonstrated a rapid recovery of the small intestine injured at the level when exposed to 7.5~9 Gy, suggesting that gut injury is not the primary cause of death at these doses of radiation. In this study, we performed 8, 9, and 12 Gy split doses of radiation to study *Lxn* function on the survival rate of *Lxn-/-* mice. Administrating 12 Gy TBI using a fractionated schedule of 2 Gy every 12 hours is a clinically relevant and is roughly equal to a single dose of 7 Gy irradiation[123]. We employed this radiation dose in order to demonstrate the potential radio-protective function of *Lxn* deficiency which may benefit patients undergoing radiotherapy. The results showed that loss of *Lxn* leads to the long-term survival of more than 60% of the *Lxn-/-* mice irradiated with 8 Gy, whereas all wild type B6 mice succumbed. However, *Lxn-/-* mice showed only a 20% increases in the survival rate after 9 Gy as well as split doses of 12 Gy radiation. These results suggested that the effective window of *Lxn* deficiency is quite limited and its effect in mitigating radiation-induced mortalities is dose-dependent.

When given a sub-lethal dose of radiation, leukocyte and platelet counts drop off shortly after radiation exposure. However, unlike after a lethal dose of irradiation, HSPCs that survive a sub-lethal dose reconstitute hematopoiesis

within 8 weeks after radiation exposure[50]. To further characterize the function of *Lxn* in mitigating radiation-induced BM failure, mice were exposed to a 6.5 Gy sub-lethal dose of total body irradiation. The hematopoietic recovery was closely monitored and our results show that the loss of *Lxn* significantly accelerates the recovery of both leukocytes and platelets. Measurements of CFCs in the BM at day 10 post radiation conclusively demonstrate the hematopoietic progenitor cell numbers are increased in *Lxn-/-* mice. Increased frequencies of BM LSK cells (stem cells) and LK cells (progenitor cells) indicate that loss of *Lxn* promotes the recovery of hematopoiesis at the level of stem cell/progenitor cells. *Lxn-/-* mice exhibit an endogenous, proliferative hematopoiesis, including higher levels of leukocytes, increased BM cellularity, and increased HSC numbers (LSK cells) under homeostasis (which continuously stay higher during hematologic recovery). However, this advantage diminishes after hematopoiesis is reconstituted. A possible explanation for this observation is replicative exhaustion in which stem cells lose their functional capacity after periods of active proliferation and differentiation.

How does the loss of *Lxn* facilitate hematopoietic stem/progenitor recovery post irradiation? Ionizing radiation produces free radicals that damage DNA content and induces apoptotic and mitotic death[49]. As we hypothesized, *Lxn* deficiency may protect HSPCs from apoptosis. Our data shown in Fig.3.4 indicates that loss of *Lxn* decreases apoptosis in irradiated hematopoietic stem and progenitor cells, especially stem cells (LSK cells). Another possibility that could induce a rapid recovery after radiation is an advantage in cell proliferation.

Increased cell proliferation activity will expand the cell population and accelerate hematologic recovery. In previous studies, we found that the loss of *Lxn* does not affect proliferation and cell cycling activities in stem and progenitor cells under homeostasis. Therefore, in this paper, we did not examine the proliferative activities during hematologic recovery. However, it is possible that the loss of *Lxn* may influence cell cycling status and proliferation after radiation exposure. In the future we will test the proliferative activities of HSPCs after sub-lethal doses radiation using BrdU incorporation, which labels newly synthesized DNA in proliferating cells.

From studies on B lymphoma cells, we found that *Lxn* overexpression decreased the expression of the anti-apoptotic gene *Bcl-2* and inhibited tumor cell growth through promoting apoptosis[107]. Apoptosis is controlled by a balance of positive (pro-apoptotic) and negative (anti-apoptotic) signals. Decreased levels of Bcl-2 allow other pro-apoptotic proteins to aggregate and induce apoptosis [124]. Tumor suppressor p53 is a regulator of Bcl-2[125, 126]. Induction of p53 resulted in a decreased expression level of *Bcl-2*[125]*.* The p53 signaling pathway is central in ionizing radiation-induced apoptosis[127-129]. It is possible that the mechanisms underlying *Lxn* -/-induced radio-resistance are involved in p53 and *Bcl-2* mediated apoptosis pathways. In future studies, we will test the expression level of the key players in p53 mediated signaling pathway such as *MDM2/X, phospho-p53, p53, Bcl-2, Bax* and *Bad* using immuno-blots.

Another potential candidate gene involved in *Lxn* induced-apoptosis is *Thbs-1*. We have demonstrated a significantly decreased level of *Thbs-1* in *Lxn-/-*

multipotent progenitor cell population, compared to wild-type animals. *Thbs-1* null mice showed a radio-resistance[130], similar to what we observed in *Lxn-/-* mice. It has been reported that *Thbs-1* is involved in regulating radiation-induced apoptosis through CD47-mediated signaling pathway[112, 117]. In future experiments, we will study *Thbs-1* as a potential target gene of *Lxn* by overexpressing *Thbs-1* in *Lxn-/-* BM cells and transplant the transduced cells. Radio sensitivities will be tested in recipients transplanted with transduced or control *Lxn-/-* cells.

Premature senescence and tumorigenesis are two possible outcomes of radiation exposure other than apoptosis. It was previously reported that a small portion of surviving HSCs lose their expansion and self-renewal capacities after radiation exposure[50]. In Fig. 3.2 A and B, we showed that HSC numbers (LSK cells) in *Lxn-/-* mice were significantly increased compared to B6 mice. But do these phenotypically defined HSCs function normally? To explore the answer to this question, CAFC assays or in vivo transplantation assays will be used to measure the functional activities of HSCs. Also, a small number of cells survive radiation stress with chromosome aberrations which can result in tumorigenesis. To address this scenario, we monitored the surviving mice after split doses of 12 Gy radiation for 8 months. Their hematologic and immune parameters remained within the normal range (data not shown), and no tumorigenesis occurred in irradiated *Lxn-/-* mice. These observations suggest that the loss of *Lxn* confers little genetic instability while preventing apoptosis after radiation exposure. The loss of *Lxn* is unlikely to promote cancer growth in the irradiated mice.

In conclusion, the loss of *Lxn* protects HSPCs against lethal and sub-lethal

radiation and promotes hematopoietic and immune recovery post radiation exposure by regulating apoptotic activities in HSPCs. Studying the mechanisms underlying *Lxn* radio-sensitive function provides a novel potential therapeutic target for protecting HSPCs in patients undergoing radiotherapy and mitigating toxicity from environmental radiation.

3.6 Acknowledgements

I gratefully acknowledge Gary Van Zant and Ying Liang for their contributions to this chapter. I also thank the technical assistance of Barry Grimes and Carol Swiderski in flow cytometry and animal handling.

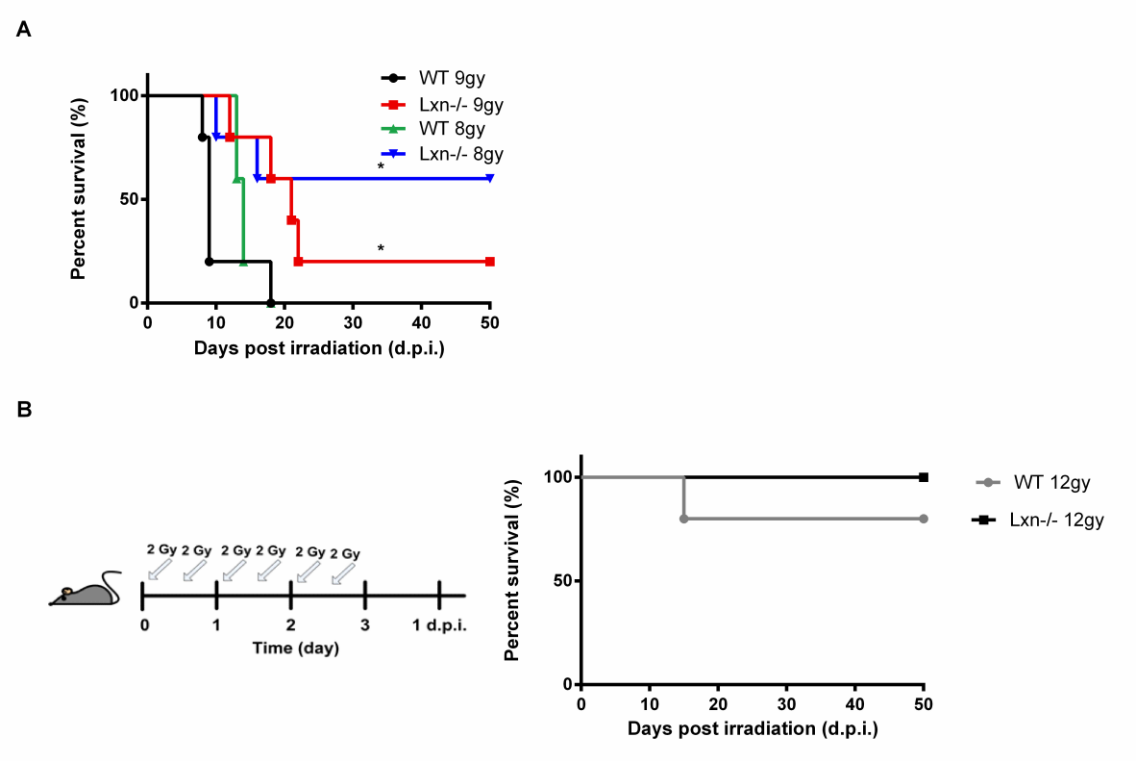

Figure 3.1 Kaplan-Meier curves demonstrate survival rate.

(A) Kaplan-Meier survival curves of mice exposed to lethal total body irradiation. B6 and *Lxn-/-* mice (n=5 for each experimental group) were given a single dose of 8 or 9 Gy irradiation, and monitored for their survival. (B) Kaplan-Meier survival curves of mice exposed to clinically relevant total body irradiation. Mice (n=5 for each experimental group) were given a total of 12 Gy (2 Gy administrated 6 times). * indicated a $P<0.05$ hereafter.

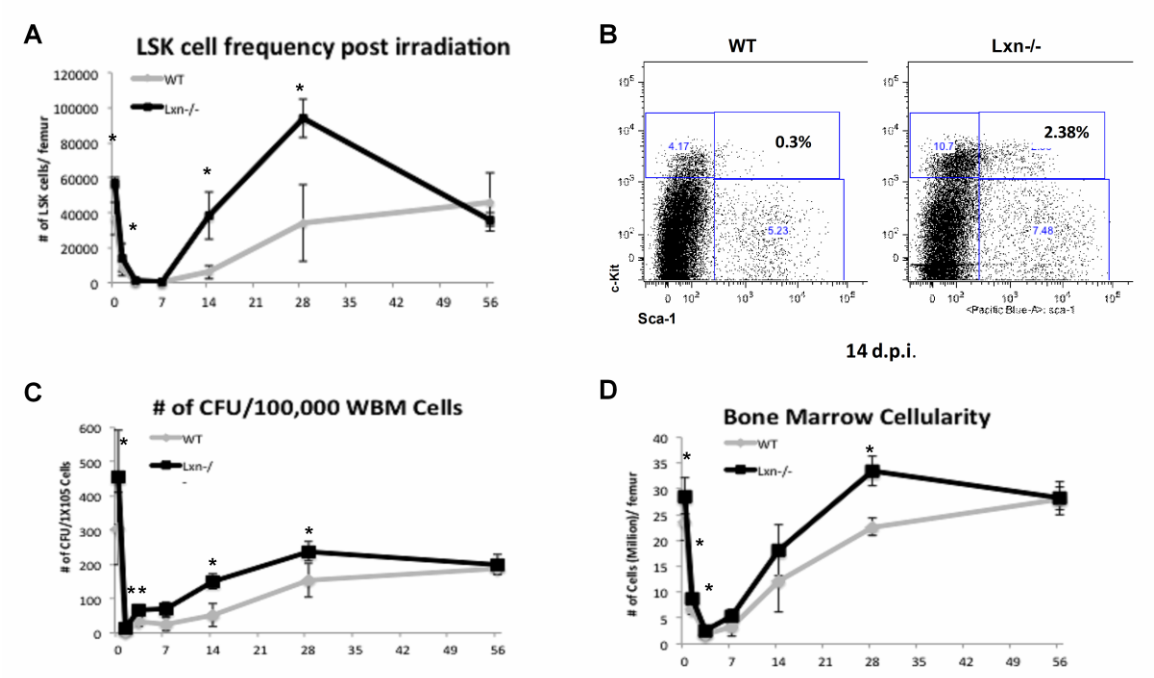

Figure 3.2 Ablation of *Lxn* confers protection of HSPCs against gamma-irradiation and speeds recovery.

B6 and *Lxn-/-* mice (n=3 for each experimental group) were irradiated with a sub-lethal 6.5 Gy dose of irradiation. We then monitored bone marrow progenitor and stem cell kinetics for 56 days post radiation. (A) The numbers of surviving LSK cell in one femur were compared between the two groups. (B) Flow cytometric analysis showed the expanded LSK, LK, and LS cell populations at day 14 post irradiation for both *Lxn-/-* and B6 mice. (C) The frequencies of hematopoietic stem and progenitor cells were determined by in vitro colony forming cell assay. (D) The numbers of surviving bone marrow cells in one femur were compared between two groups.

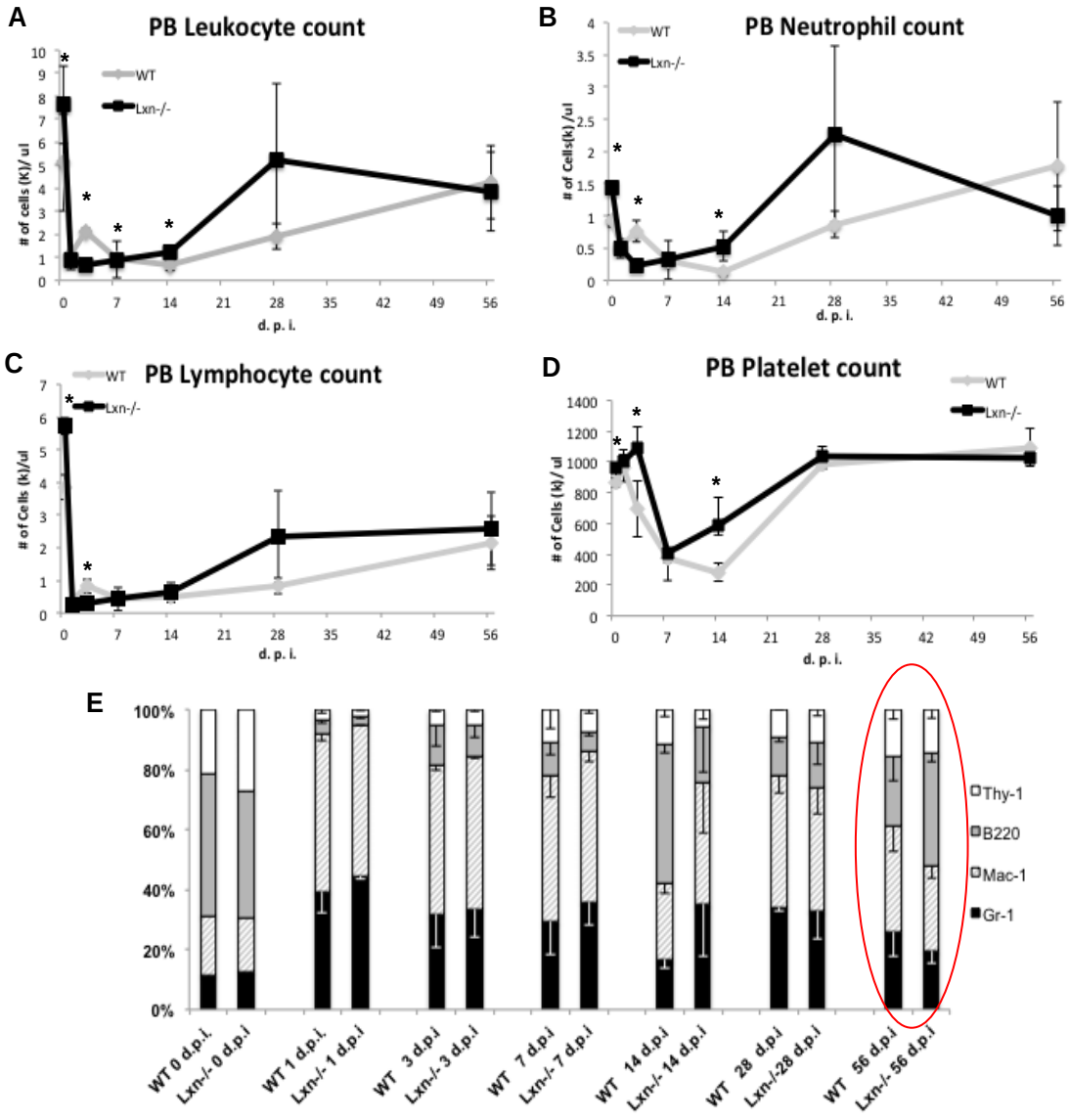

Figure 3.3 Ablation of *Lxn* promote hematological recovery at HSPC level.

B6 and *Lxn-/-* mice (n=3 for each experimental group) were irradiated with a sub-lethal 6.5 Gy dose and their hematologic and immunologic recovery was monitored in peripheral blood over 56 days. The counts of total leukocytes (A), neutrophils (B), lymphocytes (C) and platelets (D) were determined by using a Hemavet cell counter. (E) Differentiated lineage cells were measured by flow cytometer using lineage-specific antibodies (Gr-1, Mac-1, B220 and Thy-1).

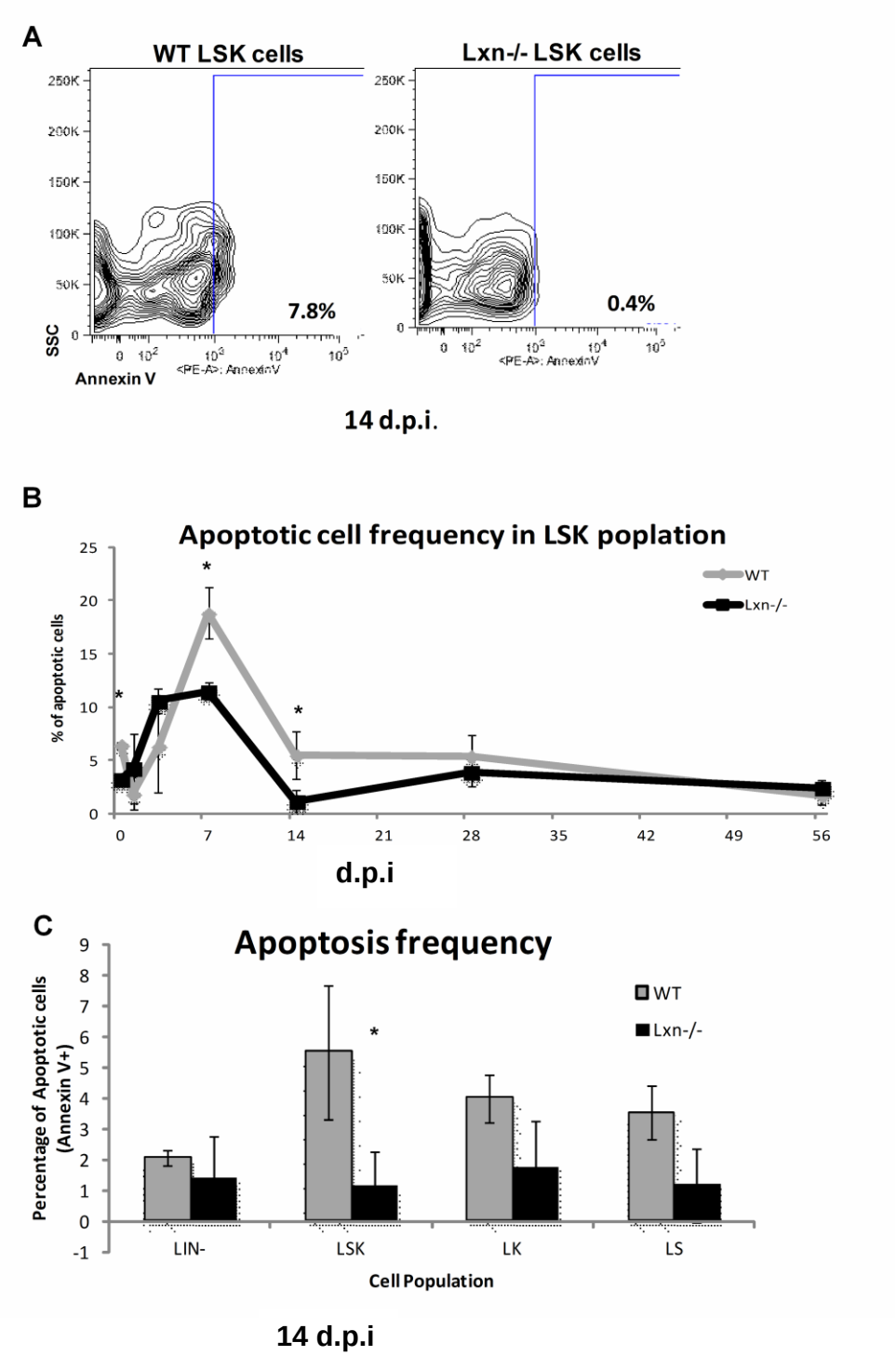

Figure 3.4 *Lxn* ablation in mice diminished radiation-induced apoptosis in progenitor and stem cells.

B6 and *Lxn-/-* mice (n=3 for each experimental group) were irradiated with a sub-lethal 6.5 Gy dose of radiation. Apoptotic activities in HSPCs were measured

using the apoptotic marker Annexin V and flow cytometry. (A) The flow cytometric analysis of apoptotic cells on day 14 post irradiation using Annexin-V and DNA dye staining. (B) Analysis of apoptotic rate dynamics (over 56 days post 6.5 Gy irradiation) in the LSK population. (C) The apoptotic frequency of LSK, LK, LS and LIN- sub-populations in *Lxn-/-* animals in day 14 post radiation.

CHAPTER 4: Loss of Latexin Compromises Progenitor and Stem Cell Retention and Results in An Enhanced Mobilization in Murine Hematopoiesis

4.1 Abstract

Engraftment and maintenance of hematopoietic stem and progenitor cells (HSPC) depends on their interaction with a specific bone marrow (BM) microenvironment, commonly known as the niche. Mobilization of HSPCs from niche into peripheral blood in response to granulocyte colony-stimulating factor (G-CSF) involves detachment of HSPCs from stromal cells, which make up a large portion of the niche. The influence of latexin (*Lxn*) on stem/progenitor cell-stroma interactions has not yet been studied. Using G-CSF-induced mobilization in *Lxn* deficient (*Lxn*-/-) mice, we found that the number of phenotypically identified HSPC ($Lin^-c\text{-}Kit^+$ cells) mobilized into the bloodstream is about 2-fold greater in *Lxn*-/- mice. In vitro adhesion assays showed that the adhesive properties of hematopoietic cells are compromised in *Lxn*-/- animals, perhaps allowing them to spill into the bloodstream more easily. Microarray experiments on multipotent progenitor cells identified several pathways that were altered upon *Lxn* deletion. The signaling pathways of cell-to-cell and cell-to-ECM interaction were significantly reduced, implying an enhanced mobilization efficiency in primitive hematopoietic cells from *Lxn*-/- mice. These findings may explain the reduced adhesion of hematopoietic progenitor cells to stroma in *Lxn*-/- mice. Amongst the genes that were significantly under-expressed, thrombospondin-1

(*thbs-1*) expression level stood out as the most down-regulated in *Lxn-/-* progenitor and stem cells.

4.2 Introduction

Hematopoietic progenitor and stem cells (HSPCs) reside in a cavity with stromal cells in the bone marrow, and this area is commonly referred to as the HSC niche. In their niche, HSCs remain quiescent, self-regenerate, proliferate, differentiate and/or migrate into the peripheral blood in response to various extrinsic cues. The release of HSPCs from the niche into the bloodstream is termed " mobilization", during which, HSPCs actively move close to sinusoidal vessels, pass through the vascular endothelial wall, migrate into bloodstream, and then infiltrate other tissues (e.g. spleen), or return to the marrow[20]. HSPC mobilization is believed to be a physiological phenomenon for maintaining hematopoietic homeostasis[21]. Redundant HSPCs in the BM niche egress into the bloodstream in order to balance HSPC numbers in both systems. This phenomenon is utilized in clinical practice to obtain adequate HSPCs from a transplant donor; such that mobilization cytokines are used to push large amounts of HSPCs into the peripheral circulation for harvesting[25-29].

HSPCs are anchored in the niche through direct cell-to-cell and cell-to-ECM interactions. The adhesive molecules, including members from the intergrin, cadherin and selectin families, is essential for HSPCs retention[34-36]. Any dysregulation in adhesive molecules may affect mobilization of HSPCs.

Previous studies show that *Lxn* deficient mice displayed a hyperproliferative hematopoiesis in BM, and there are increased numbers of LSK

cells in *Lxn-/-* PB. Two hypothesis may explain these findings: 1) The HSPC population expands due to increased proliferation and/or decreased apoptotic activity. Excessive HSPCs egress into the blood circulation to maintain the homeostasis. 2) A compromised HSPC retention capacity induces increased mobilization. Thus, weak interactions between HSPCs and stromal cells enable HPSCs to readily egress into the blood circulation under homeostasis, or after the administration of mobilization cytokines. As mentioned previously, *Lxn-/-* mice exhibit a hyperproliferative hematopoiesis in the BM, implying that the up-regulation of LSK population in PB is induced by homeostatic machinery. However, these findings are not conclusive because they do not rule out the influence from the microenvironmental niche cells.

To further explore the effects of *Lxn* on HSPC retention capacity in the BM, we used G-CSF induced mobilization. We found that *Lxn-/-* mice show not only increased mobilization proficiency, but also decreased cell retention capacities of *Lxn* -/- HSPCs. Microarray experimental results indicate that the enhanced mobilization proficiency of *Lxn-/-* primitive hematopoietic cells is correlated with reduced adhesion of hematopoietic progenitor cells to stroma. *Thbs-1* has been identified as a potential target of *Lxn* in regulating enhanced mobilization in *Lxn-/-* mice. The expression level of *Thbs-1* gradually decreases along the hematopoietic differentiation hierarchy in parallel with *Lxn* expression. I am currently ectopically overexpressing *Thbs-1* in primitive hematopoietic cells. The next logical step for this project is to study the mobilization proficiency and retention capacity of HSPCs overexpressing *Thbs-1* both in vivo and in vitro.

4.3 Methods

4.3.1 Animals

C57BL/6 mice (B6) (8-16 weeks) were purchased from The Jackson Laboratory (Bar Harbor, ME). *Lxn* constitutive knockout mice were generated by Taconic/Artemis (Germantown, NY) and used at a young age (8-16 weeks). All animals were housed in the animal facilities of the University of Kentucky under pathogen-free conditions according to NIH-mandated guidelines for animal welfare. They were fed with food and water *ad libitum*.

4.3.2 Hematopoietic cell identification and isolation

Bone marrow cells were flushed from the femora and tibiae using a 1 ml syringe and 22G needle into Hanks balanced salt solution (HBSS) with 2% fetal bovine serum (FBS). Progenitor cells were discriminated from stem cells by the lack of cell surface antigens characteristic of cells committed to individual lineages. Antibodies against these antigens include CD5 and CD8a, B220, Mac-1, Gr-1, and Ter119 are biotinylated. Strepavidin secondary antibody was used to detect lineage negative cells. To further purify primitive cells, the stem cell markers Sca-1 and c-Kit were incorporated into the staining procedure. The multi-potent progenitor (MPP) cells are identified by immunophenotyping as cells negative for Lineage markers, but positive for Sca-1, c-Kit, Flt-3 and CD34. Dead cells were excluded by propidium iodide (PI) that stains exposed double-strand DNA. All monoclonal antibodies were purchased from eBioscience (San Diego, CA), Biolegend (San Diego, CA), or DB pharmingen (San Jose, CA).

4.3.3 Cell analysis and sorting

BM cells were analyzed and sorted on a FacsAria II flow cytometer (Becton Dickinson, Franklin Lakes, NJ). Cells were sorted into phosphate buffered saline (PBS) with 0.5% FBS for further use. Each experimental group was sorted independently. Flow cytometry and FACS data were analyzed using FlowJo software (Tree star, Ashland, OR).

4.3.4 Mobilization assay

To mobilize HSPCs to blood circulation, recombinant human G-CSF (rhuG-CSF) (Amgen Biologicals, Thousand Oaks, CA) was intra-peritoneally (i. p.) injected at 100 ug/kg daily for 5 days at a concentration of 12.5 ug/mL in PBS/0.1% BSA. HSPC frequency in PB, BM and spleen was measured by CFC assay and flow cytometry.

4.3.5 Colony forming cell (CFC) assay

Methylcellulose-based culture media was obtained with Complete MethoCult Media (Stem Cell Technologies, Vancouver, Canada) containing cytokines including stem cell factor (SCF), IL-3 and IL-6 cytokines. For this assay, 10 ul PB or 1 x 10^5 spleen cells in 100 µL HBSS were thoroughly admixed with 1 mL complete MethoCult media, plated into 6-well petri-dish and incubated at 37°C. Wells of triplicate cultures were counted on day 7 for PB and on day 8 or 14 for spleen to quantify lineage-specific colonies.

4.3.6 HPC adhesion assay

As in the CAFC assay, FBMD-1 stromal cells were pre-seeded in 96-well tissue culture-treated plates. After FBMD-1 cell monolayers reached confluence (7-10 days post plating), whole BM cells were plated at doses of 400, 800, 1600, 3200, 6400, 12800, 25600 and 51200 per well with CAFC medium. To assess the progenitor cell adhesion, 2 hours later non-adherent cells were washed by gently aspirating the medium up and down with a micropipet, and the cells were then removed. Fresh medium was then added to each well. The frequency of total HPCs and adherent HPCs was assessed by the appearance of cobblestone-areas in each well on day 7. The difference between the number of the cobblestones formed in unmanipulated wells and washed wells provided an index of the strength of adhesion between the CAFCs and the FBMD-1 stromal cells. The adhesion of HPCs was calculated by normalizing the numbers of cobblestones formed in washed wells to the unmanipulated wells (%).

4.3.6 Microarray analysis

As described in Chapter 2, microarray experiments were performed on fresh BM multipotent progenitor cells obtained from three wild type and three *Lxn*-/- biological samples using Affymetrix Gene Chip MoGene-1_0-st-v1 arrays. Data were normalized based on the RMA method[131]. To study pathway changes in response to the genomic alteration, in this chapter we performed the gene set enrichment analysis (GSEA) based on the GSEA Java desktop software application, using the same microarray experiment data[132]. Genes were pre-

ranked based on the absolute values of the test statistics calculated using the LIMMA package in R/Bioconductor. We investigated all the pathways in the KEGG database. Five enriched pathways were identified with false discovery rate of less than 25%. Individual genes that were differentially expressed were identified with a p-value less than 0.01.

4.3.7 Statistics

Statistical significance between means was determined by a two-way Student *t* test.

4.4 Results

4.4.1 Mobilization of HSPCs is increased in *Lxn-/-* mice

Granulocyte colony-stimulating factor (G-CSF) is widely used in clinical practice to stimulate the movement of stem and progenitor cells from the BM into peripheral blood circulation. In this study, we used G-CSF induced mobilization to explore the effect of *Lxn* in hematopoietic cell function. *Lxn-/-* mice and B6 mice were given G-CSF daily for 5 days. Flow cytometric analysis combined with cell surface marker antibodies were used to identify phenotypic HSPCs in PB after G-CSF administration. HPCs were identified by immunophenotyping as cells negative for lineage markers and Sca-1 antigen, and positive for c-Kit receptors ($Lin^-Sca\text{-}1^-c\text{-}Kit^+$), whereas HSCs were negative for lineage markers and positive for Sca-1 and c-Kit receptors ($Lin^-Sca\text{-}1^+c\text{-}Kit^+$) (Fig. 4.1A). HSPCs were negative for lineage markers and positive c-Kit receptors ($Lin^-c\text{-}Kit^+$) (Fig. 4.1A). Using

these parameters, we demonstrated that the mobilization of HSPCs in *Lxn-/-* mice was significantly increased (2-fold) after G-CSF administration (Fig. 4.1A and B). Within the HSPC population, the number of HPCs in PB was increased 3.5-fold, whereas the number of HSCs in PB remained intact (Fig. 4.1A and B). These data showed that the mobilization of HPC from BM into PB was increased by loss of *Lxn* expression in hematopoietic cells.

Colony forming cell (CFC) assay is an in vitro assay specifically measuring the number of functional hematopoietic progenitor cells. Next we used CFC assays to determine the HPC mobilization in both *Lxn-/-* and B6 animals. Blood was collected and analyzed on day 6 and the frequency of HPCs in PB was measured by the CFC assay. Before mobilization, PB CFC frequency in *Lxn-/-* mice is 30% more than the frequency in wild type B6 mice (Fig. 4.2A). G-CSF mobilized 15 and 13-fold more HPCs to PB in *Lxn-/-* and B6 mice respectively, compared to unmobilized cells (Fig. 4.2A). After mobilization, the frequency of CFC in the PB of *Lxn-/-* mice showed an increased trend compared to the frequency of CFCs in the PB of B6 mice, however, it did not reach the statistical difference (Fig. 4.2A).

G-CSF administration not only leads to the redistribution of primitive hematopoietic cells from the BM to peripheral blood, but also induces their mobilization to spleen. Thus, we studied the frequency of CFCs in the spleens of *Lxn-/-* and B6 mice before and after G-CSF administration. Before mobilization, *Lxn-/-* mice showed a 3-fold increase in CFC frequency in spleen compared to wild type B6 mice (Fig. 4.2B). Post mobilization, *Lxn-/-* spleen CFC frequency

was increased 10-fold over pre-mobilization frequency, whereas B6 mobilization frequency was increased 25-fold (Fig. 4.2B). Mobilized *Lxn-/-* mice also showed an increased trend in CFC frequency in spleen, but which was not significant, compared to mobilized B6 animals (Fig. 4.2B).

In this set of experiments, we found more HPCs (measured by CFC) in *Lxn-/-* spleen and PB compared to B6 in untreated animals (Fig. 4.2A and B). These data indicate that loss of *Lxn* could enhance the mobilization to PB and spleen in HPCs under homeostatic conditions. However, the frequencies of CFC in the PB and spleen of *Lxn-/-* mice showed increased trends but with no significant difference when compared to B6 mice. These findings were inconsistent with increased phenotypic HSPCs in *Lxn-/-* mice identified by flow cytometry (Fig. 4.1A and B). This may due to the sample pool size used in these experiments. In the future, we will repeat the CFC assays with more *Lxn-/-* and B6 animals to elucidate the functional progenitor cell numbers in PB and spleen.

4.4.2 Loss of *Lxn* impaired HSPCs adhesion to stromal cells

We next studied the adhesive properties of *Lxn*-/- HSPCs by directly measuring the adhesion of HSPCs to a bone marrow-derived stromal cells (FBMD-1) using the adhesion assay-a modified cobblestone-area forming cell (CAFC) assay. The CAFC assay is a well-established in vitro assay to measure HSPC activity. In this assay, stromal cells (FBMD-1 cells) were plated in a 94-well plate and allowed to grow to confluency. BM cells were plated in each well in limiting dilutions, and later scored for the presence of cobblestone-areas. Unlike in a traditional CAFC assay, non-adherent HSPCs were washed off 2 hours post

plating onto the stromal cell (Fig. 4.3A). The frequency of adhesive HSPCs was subsequently determined at day 7 and normalized to the frequency of HSPC in unwashed plates. This experiment allowed us to study the ability of HSPCs to anchor and adhere to the stroma in vitro. We performed the adhesion assay with *Lxn-/-* and B6 BM cells, and found that *Lxn-/-* BM cells showed a 40% reduction in the ability to adhere to stromal cells when compared to B6 compared to B6 cells (Fig. 4.3B). This result suggests that increased mobilization of HSPC may be caused by compromised adhesive properties of BM cells in the niche.

4.4.3 Decreased levels of adhesive molecules in *Lxn-/-* mice

The adhesion and detachment of HSPCs from the stroma were tightly regulated by adhesion molecule activities. To study whether changes in adhesion/mobilization efficiency correlate with changes in adhesive molecule expression, we conducted microarray experiments on MPP cells obtained from *Lxn-/-* mice and B6 (see in Chapter 2). Gene set enrichment analysis (GSEA) identified five enriched pathways that were significantly dysregulated (Tab. 4.1). Among these five pathways, cell-to-cell communication and ECM-receptor interaction pathways are involved in regulating HSPC adhesion/mobilization. The expression levels of most adhesive molecules were down-regulated, indicating that the enhanced mobilization efficiency of hematopoietic cells from *Lxn-/-* mice may be caused by reduced adhesion properties of hematopoietic progenitor cells to stroma (Tab. 4.2 and 3). In previous studies, the *Thbs-1* gene was identified as one of the most down-regulated adhesion-related molecules in our microarray studies. Its expression level was decreased 4-fold in *Lxn-/-* hematopoietic multi-

potent progenitor populations (not shown). In previous studies, we tested *Thbs-1* expression at the levels of transcript (quantitative real-time PCR) in hematopoietic cells and found the *thbs-1* expression gradually decreased along the hematopoietic differentiation hierarchy, in parallel with *Lxn* expression (as in Chapter 2). To further study the in vivo role of *Thbs-1* in regulating increased mobilization in *Lxn-/-* mice, *Thbs-1* will be overepxressed in primitive hematopoietic cells and the retention properties of cells overexpressing *Thbs-1* will be tested

4.5 Discussion

HSCs change locations several times during embryonic development, shifting from the yolk sac and Aorta-gonad-mesonephros (AGM) region to the fetal liver, and finally to the BM[19]. In adult life, HSCs remain dynamic, trafficking between BM niches and extramedullary sites such as spleen, liver and blood in response to various stresses[20]. The periodic and diurnal release of HSCs into blood stream is an essential mechanism for regulating homeostasis, and extramedullary hematopoiesis commonly occurs in hematopoietic disorders[21].

While studying the hematopoietic system in *Lxn-/-* mice, we identified an increased HSC population in the peripheral blood system. There are two possible explanations for this observation: hyperproliferative hematopoiesis or compromised HSC retention in the BM niche. We observed hyperproliferative hematopoiesis in both the PB and BM of *Lxn-/-* mice. However, to our knowledge, no studies have been performed focusing on HSC retention capacity and mobilization in *Lxn-/-* mice. Here we identified a role for *Lxn* in regulating the

mobilization of HSPCs, as shown by the fact that loss of *Lxn* enhanced mobilization proficiency and decreased cell retention during homeostasis and after G-CSF administration. We identified that the mobilization of HSPCs (phenotypically identified) from BM to PB in *Lxn-/-* mice was significantly increased (2-fold) compared to B6 mice after G-CSF administration (Fig. 4.1A and B). However, the results from PB CFC assay found no significant difference between the number of CFCs formed by PB from *Lxn-/-* and B6 mice after G-CSF administration. This observation may be explained by the sample size. We performed CFC experiments once with 3 biological samples in each experimental group, which may not be adequate to show statistic difference. The person who will carry this project will need to repeat this experiment two more time and with more *Lxn-/-* and B6 animals. The other possible explanation for this observation is that the progenitor mobilized into PB become non-functional, therefore would not form colonies. To test the hypothesis that HSPCs lose their function in *Lxn-/-* mice after mobilization, we can perform the CFC assay with purified phenotypic *Lxn-/-* and B6 HSPCs ($Lin^{-}c\text{-}Kit^{+}$ cells). If what we hypothesized is true, there will be less colonies formed with equal numbers of HSPCs from *Lxn-/-* mice than B6 mice after mobilization. Because even though flow cytometric analysis showed more HSPCs are released to PB in *Lxn-/-* mice, most of progenitor cells are non-functional.

Many of the same adhesion molecules are expressed on both on stem cells and stromal cells. The overlapping expressions of these molecules (that bind to the same ligands or shared similar functions) provide redundancies in

expression and function[34-36]. This strategy ensures that a minor reduction in one or several adhesion molecules does not affect stem cell behavior and homeostasis. However, in our studies, microarray analysis identified an extensive list of adhesion molecules (involved in cell-to-cell and cell-to-ECM interactions) which were universally under-expressed. It is possible that small reductions in gene expression of many individual genes compromise HSPC retention and promote HSPC mobilization in *Lxn-/-* mice[133]. This hypothesis explains the observation that more HSPCs (phenotypically identified) are released into blood circulation in *Lxn-/-* PB compared to B6. In clinical practice, the interactions between stem/progenitor cells and stromal cells are disrupted by G-CSF or other cytokines, resulting in the relocalization of HSPCs to the peripheral blood[25-29]. In this study, G-CSF administration manifests the defect (a compromised HSPC retention) and induces the release of significantly more HSPCs (phenotypically identified) into blood circulation.

Among the adhesion molecules, *thbs-1* is the most down-regulated. Its expression level was decreased 4-fold in *Lxn-/-* MPP population. The thbs-1 protein is an adhesive glycoprotein that mediates cell-to-cell and cell-to-matrix interactions[133, 134]. It is a critical part of the stem cell niche, and is involved in binding to other adhesion molecules such as fibrinogen, fibronectin, intergrin and collagen[10]. To further study the in vivo role of *thbs-1* in regulating increased mobilization in *Lxn-/-* mice, we ectopically overexpressed *thbs-1* in primitive hematopoietic cells. The cells overexpressing *Thbs-1* will be tested for their retention capacity using in vitro and in vivo experiments.

In conclusion, the loss of *Lxn* in hematopoietic cells enhances their mobilization into peripheral blood system and results in a compromised retention capacity through down-regulating the adhesion molecules which involved in cell-to-cell and cell-to-ECM interactions.

4.6 Acknowledgements

I gratefully acknowledge Gary Van Zant and Ying Liang for their contributions to this chapter. I also thank the technical assistance of Barry Grimes in flow cytometry**,** and statistical helps from Chi Wang.

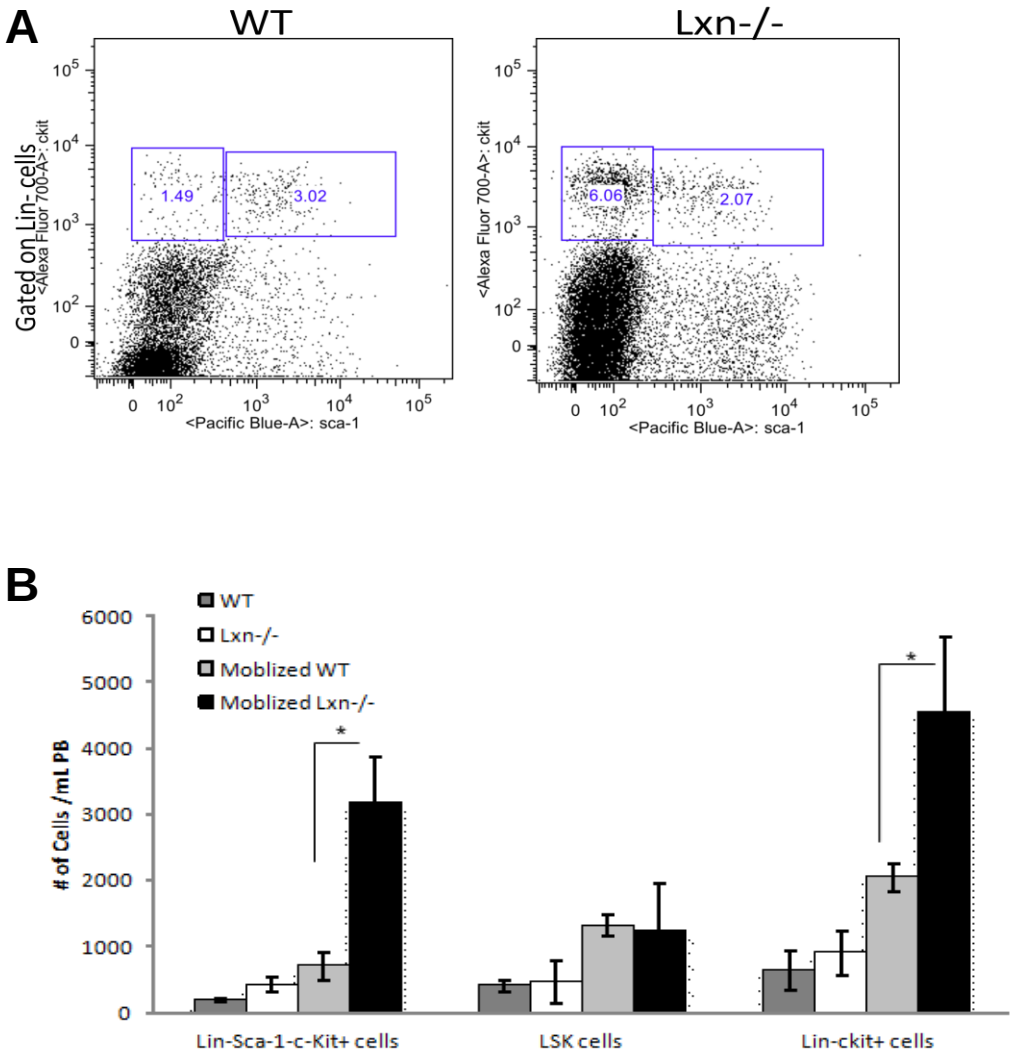

Figure 4.1 Flow cytometric analysis of mobilized HSPCs in PB of B6 and *Lxn-/-* mice.

(A) and (B) Flow cytometric analysis demonstrating the numbers of $Lin^{-}Sca\text{-}1^{+}c\text{-}Kit^{+}$ cells (HSCs), $Lin^{-}Sca\text{-}1^{-}c\text{-}Kit^{+}$ cells (HPCs) and $Lin^{-}c\text{-}Kit^{+}$ cells (HSPCs) in the PB of unmobilized or mobilized B6 and *Lxn-/-* mice (n=4 for each group). * indicated a $P<0.05$ hereafter.

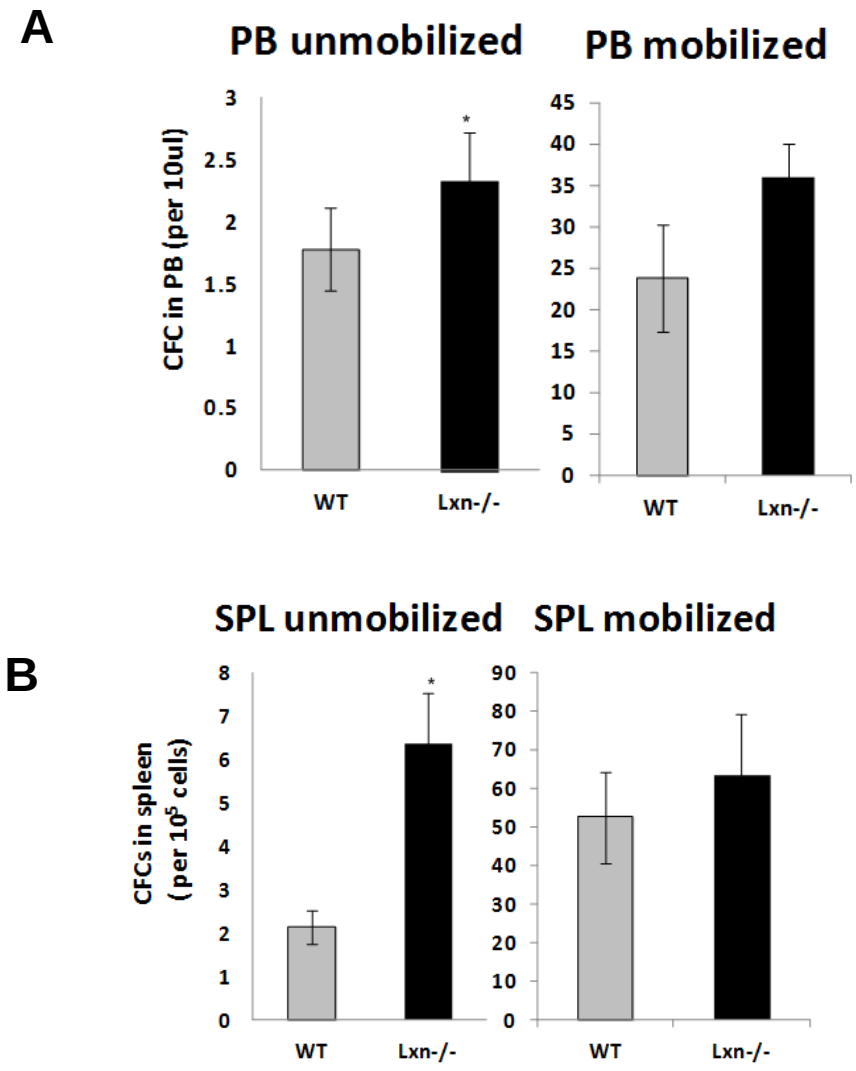

Figure 4.2 Mobilization of HSPC in B6 and *Lxn-/-* mice measured by CFU assay.

(A) The frequency of CFCs in 10 uL PB in unmobilized or mobilized B6 and *Lxn-/-* mice (n=3 for each group). (B) The frequency of CFCs in spleen in unmobilized or mobilized B6 and *Lxn-/-* mice (n=3 for each group).

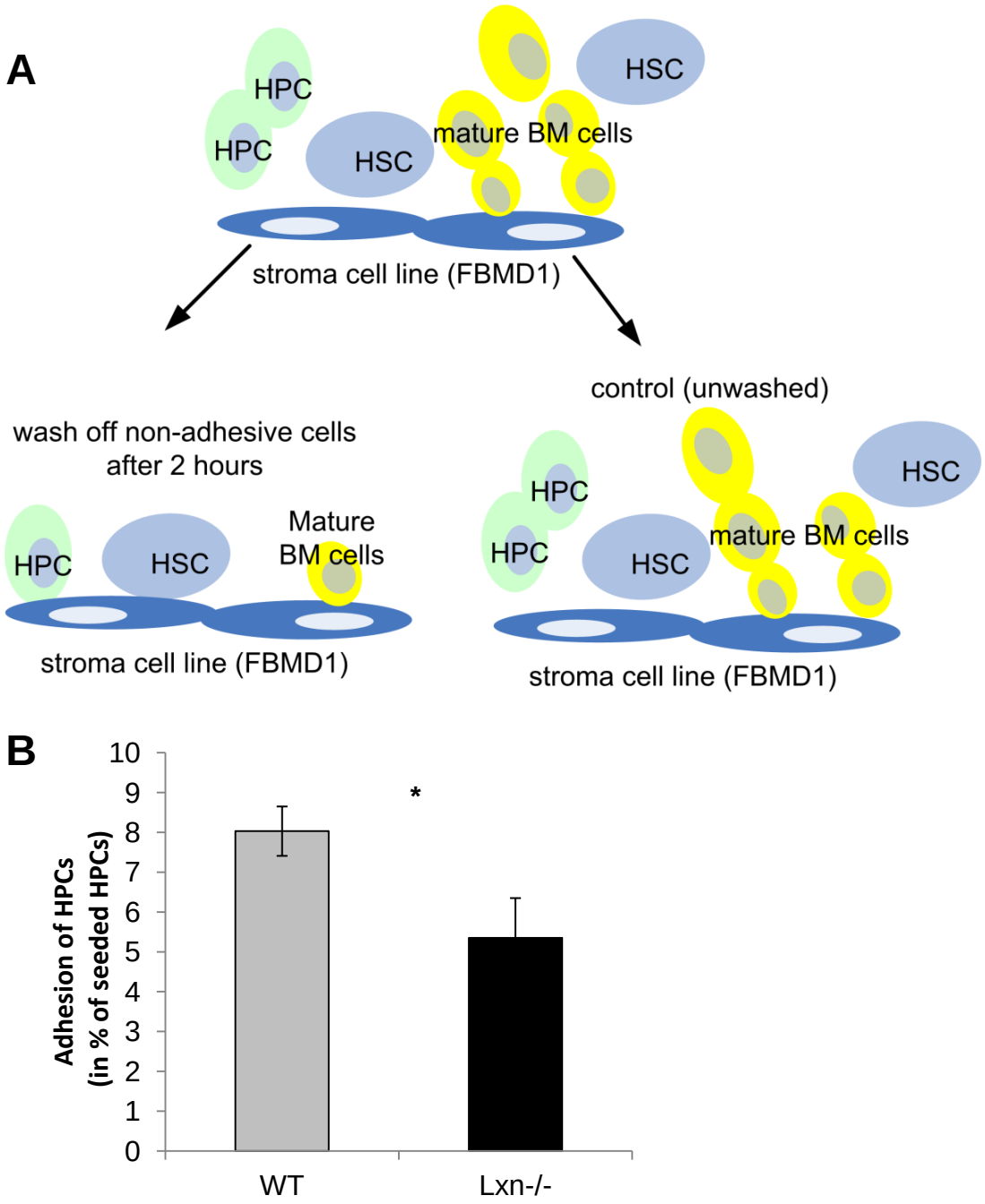

Figure 4.3 Adhesion capacities in HSPCs in B6 and *Lxn-/-* mice.

(A) Experimental design of the adhesion assay. BM cells from the unmobilized B6 and *Lxn-/-* mice were added to wells containing confluent feeder cells. Non-adhesive cells were washed away after 2 hours and plates were scored at day 7. The frequency of adherent HPCs (washed) was normalized to the initial HPC frequency

(unwashed). (B) Percentage of adherent HPCs (the frequency of adherent HPCs normalized to the initial HPC frequency) (n=3 for each group).

Table 4.1 GSEA enrichment table of pathways altered in *Lxn-/-* MPP cells

Name	Size	FDR q-value	# of genes in leading edge
Proteasome	18	0.004	14
Cell-Communication	120	0.003	88
Neuroactive-ligand-receptor	222	0.003	147
ECM-Receptor-interaction	80	0.002	44
Cell-cycle	95	0.19	79

List of 5 top differentially expressed pathways from *Lxn-/-* MPP population. The number of genes in each pathway, number of genes in the leading edge, and corresponding FDR q-value are listed as above.

Table 4.2 Gene expression profile of genes in Cell-to-ECM interaction pathways.

Gene	Contrast	Gene	Contrast	Gene	Contrast
THBS4	-1.25	*GP9*	-1.25	*ITGB7*	-1.10
COL5A2	-1.24	*LAMA3*	-1.15	*ITGA10*	1.0
COL1A2	-1.26	*ITGA2*	-1.25	*SV2B*	-1.10
COL4A6	-1.23	*COL11A2*	-1.11	*GP1BA*	-1.05
FNDC5	-1.23	*ITGB6*	-1.12	*TNR*	-1.0659
ITGA7	-1.23	*SV2C*	-1.11	*SDC1*	-1.10
THBS1	**-3.44**	*FNDC1*	-1.1	*ITGA8*	-1.106
SDC4	-1.25	*ITGB8*	-1.17	*LAMA5*	-1.04
LAMA1	-1.18	*FNDC3A*	1.12	*SPP1*	1.04
TNN	-1.22	*COL5A3*	-1.12	*THBS2*	-1.04
LAMB3	-1.18	*LAMC3*	-1.12	*LAMB2*	-1.03
COL4A4	-1.21	*CD44*	1.12	*SV2A*	-1.03
ITGA2B	-1.24	*LAMA4*	-1.10	*FNDC4*	-1.03
LAMC2	-1.17	*TNXB*	-1.13	*CD47*	1.02
COL11A1	-1.19	*ITGA6*	1.12	*ITGB3*	-1.02
LAMA2	-1.19	*TNC*	-1.13	*ITGA4*	-1.02
COL1A1	-1.20	*COL6A2*	-1.11	*AGRN*	1.02
COL2A1	-1.19	*ITGA3*	-1.12	*ITGA11*	-1.01
THBS3	-1.15	*COL4A2*	-1.10	*SDC3*	-1.02
COL6A3	-1.17	*GP5*	-1.119	*ITGB5*	-1.01
HMMR	1.25	*ITGAV*	-1.11	*DAG1*	-1.01
ITGA9	-1.31	*LAMC1*	1.1	*SDC2*	1.1
VWF	-1.15	*ITGA1*	-1.20	*FN1*	-1.0
HSPG2	-1.14	*COL4A1*	-1.10	*CD36*	-1.1

Table 4.2 continues

CHAD	-1.27	*COL6A1*	-1.10	*GP9*	-1.25
COL5A1	-1.14	*RELN*	-1.10	*VTN*	-1.16

80 genes in Cell-to-ECM interaction pathway have been listed above with their expression level altered in *Lxn-/-* MPP cells. Majority of the genes have been down-regulated.

Table 4.3 Gene expression profile of genes in Cell-to-Cell interaction pathway.

Gene	Contrast	Gene	Contrast	Gene	Contrast
THBS4	-1.25	*COL2A1*	-1.19	*GJA3*	-1.11
COL5A2	-1.24	*THBS3*	-1.15	*GJA5*	-1.14
COL1A2	-1.26	*COL6A3*	-1.17	*LAMA4*	-1.10
KRT86	-1.30	*VWF*	-1.15	*GJA10*	-1.14
COL4A6	-1.23	*KRT12*	-1.15	*TNXB*	-1.13
KRT74	-1.20	*CHAD*	-1.27	*KRT15*	-1.10
THBS1	**-3.44**	*KRT2*	-1.14	*ITGA6*	1.12
KRT75	-1.21	*COL5A1*	-1.14	*GJC1*	-1.11
KRT31	-1.18	*GJD2*	-1.13	*TNC*	-1.13
KRT28	-1.2	*VTN*	-1.16	*LMNB1*	1.1
KRT24	-1.23	*GJB6*	-1.15	*COL6A2*	-1.1
KRT84	-1.24	*KRT40*	-1.14	*KRT35*	-1.11
GJA8	-1.18	*KRT78*	-1.12	*KRT34*	-1.10
LAMA1	-1.18	*LAMA3*	-1.15	*KRT20*	-1.13
TNN	-1.22	*KRT23*	-1.20	*GJB3*	-1.13
KRT9	-1.22	*KRT33B*	-1.15	*GJD4*	-1.10
DES	-1.18	*COL11A2*	-1.11	*COL4A2*	-1.10
GJB1	-1.18	*KRT4*	-1.15	*KRT14*	-1.12
LAMB3	-1.18	*KRT77*	-1.13	*GJC2*	-1.10
COL4A4	-1.21	*KRT76*	-1.15	*KRT17*	-1.10
LAMC2	-1.17	*KRT19*	-1.15	*KRT1*	-1.10
COL11A1	-1.19	*GJD3*	-1.11	*KRT33A*	-1.10
LAMA2	-1.191	*KRT13*	-1.14	*KRT82*	-1.10
COL1A1	-1.12	*KRT18*	-1.24	*LAMC1*	1.10

table 4.3 continues

DSC2	-1.18	*COL5A3*	-1.12	*COL4A1*	10
KRT36	-1.17	*GJA4*	-1.10	*DSG4*	-1.10
GJB5	-1.10	*DSC1*	-1.10	*LMNA*	1.10
RELN	-1.10	*PRPH*	-1.10	*KRT83*	-1.04
KRT72	-1.10	*KRT39*	-1.10	*KRT6B*	1.04
GJB4	-1.10	*KRT25*	1.05	*KRT73*	-1.02
VIM	1.10	*TNR*	-1.10	*DSC3*	-1.02
KRT32	-1.10	*KRT8*	1.05	*NES*	-1.02
IBSP	-1.10	*KRT79*	-1.04	*ACTB*	1.01
DSG2	-1.12	*KRT27*	-1.04	*KRT5*	-1.01
COL3A1	-1.10	*LAMA5*	-1.04	*KRT6A*	1.003
GJA1	1.10	*SPP1*	1.04	*FN1*	-1.004
COMP	-1.10	*KRT7*	-1.04	*KRT16*	1.003
LMNB2	1.10	*THBS2*	-1.04	*KRT71*	-1.001
DSG3	-1.10	*LAMB2*	-1.03	*KRT10*	-1.00009

120 genes in Cell-to-Cell communication and interaction pathway have been listed above with their expression level altered in *Lxn-/-* MPP cells. Majority of the genes have been down-regulated.

CHAPTER 5: Latexin is Down-regulated in Hematopoietic Malignancies and Restoration of Expression Inhibits Lymphoma Growth

5.1 Abstract

Latexin is a negative regulator of hematopoietic stem cell number in mice. Its dysregulated expression in other tumors led us to hypothesize that latexin may have tumor suppressor properties in hematological malignancies. We found that latexin was down-regulated in a variety of leukemia and lymphoma cell lines as well as in CD34+ cells from the blood and marrow of patients with these malignancies. 5-aza-2'-deoxycytodine treatment and bisulfite sequencing revealed hypermethylation of latexin promoter in tumor cells. Retrovirus-mediated latexin overexpression in A20 mouse lymphoma cells inhibited their in vitro growth by 16 fold and in vivo tumor volume by 2 fold. Latexin caused growth inhibition of lymphoma cells by significantly increasing apoptosis through the down-regulation of anti-apoptotic genes Bcl-2 and Pim-2. The molecular mechanism underlying latexin-mediated tumor inhibition was not through its canonical carboxypeptidase inhibitor activity. These results are consistent with a tumor suppressor role for latexin and suggest that latexin may have clinical efficacy in the treatment of malignancies.

5.2 Introduction

Both solid and liquid tumors are now understood to originate from the malignant transformation of resident adult stem and progenitor cells[135, 136].

Nowhere is this paradigm better established than in leukemia, yet events causing neoplastic conversion remain poorly understood[137]. We identified latexin (*Lxn*) as a novel, homeostatic regulator of the size of the hematopoietic stem cell population in mice[93]. The stem cell pool size was inversely related to quantitative *Lxn* expression at both the levels of transcript and protein. We found that population size was influenced by *Lxn* in a stem cell-autonomous manner, and acting through the concerted mechanisms of self-renewal and apoptosis, which were decreased and increased, respectively, by *Lxn* abundance[93]. Thus, *Lxn* acts as a brake on the expansion of stem cell population. Unrestrained stem cell expansion carries with it the risk of mutations, genomic instability and carcinogenesis. We therefore hypothesized that *Lxn* expression patterns in stem and progenitor cells may act as a tumor suppressor by inhibiting stem and progenitor cell proliferation, influencing the crucial steps toward malignancy.

Lxn was primarily studied in the nervous system, involving the specification of cortical brain regions during development[89, 138-141], as well as the speed of nerve transmission in adult peripheral nervous systems[90]. *Lxn* was found to be involved in the inflammatory response in macrophages owing to its paired cystatin-like domains[142]. It was detected in mast cells associated with a unique type of intracellular granule distinct from histamine-containing secretory granules and lysosomes[91]. *Lxn* has about 30% sequence homology, but much greater structural homology, with tazarotene-induced gene 1 (*TIG1*) (or retinoic acid receptor responder 1, RARRES1), whose expression was down-regulated in an extensive list of tumor types in humans[106, 142-145]. *Lxn* and *TIG1* are closely

linked genetically and may represent members of a family of functionally related genes. Moreover, *Lxn* was reported to be a TNF-responsive gene in human papillovirus-infected keratinocytes, suggesting that it may contribute to TNF-mediated suppression of cervical cancer development[146]. A recent report revealed that *Lxn* was down-regulated in patients with gastric carcinomas, and overexpression or knockdown of *Lxn* inhibited or stimulated tumor growth respectively[147]. Decreased or absent *Lxn* expression was observed in several human leukemia and lymphoma cell lines[148], as well as in malignant melanoma patients[149]. However, there is still lack of direct evidence for the cause-effect relationship between *Lxn* and hematopoietic malignancy.

Gene silencing, especially of tumor suppressors, and inappropriate gene activation, especially of oncogenes, are common themes in carcinogenesis[150]. Both often occur through aberrant DNA methylation that is accentuated during aging[151-156]. A CpG-enriched region was identified in *Lxn* promoter and its hypermethylation was found in a variety of human gastric carcinoma cell lines[147]. Promoter hypermethylation of *TIG1* was also associated with its silencing in tumor cells [106, 145]. However, it is not known whether *Lxn* expression is regulated by promoter methylation in hematopoietic malignancy.

Molecular mechanisms underlying the role of *Lxn* in regulating hematopoiesis has not been determined yet. *Lxn* protein binds to carboxypeptidase A (Cpa) and inhibits its enzymatic activity, indicating that *Lxn* regulates protein degradation and metabolism[148]. *Lxn* was highly expressed in mast cells and its expression was further enhanced by LPS, indicating its

potential function in inflammation[142]. Proteomic analysis on *Lxn* knock-out hematopoietic cells revealed that *Lxn* deletion reduced the abundance of multiple cellular proteins, especially those involving cell-stroma interaction, such as N-cadherin, Tie2, and Roundabout 4[148]. Ectopic expression of *Lxn* in gastric cancer cell lines led to the differential expressions of several cancer-related genes, including Maspin, WFDC1, SLPI, S100P, and PDGEFB [147], although none of them are overlapped with previously mentioned proteomic results. A recent study revealed ATP/GTP binding protein-like 2 (AGBL2) as a novel binding partner of TIG1. The interaction between TIG1 and AGBL2 regulates the microtubule tyrosination cycle, which is implicated in tumorigenesis, stem cell differentiation and development[157]. *Lxn* thus may have the similar mechanisms as TIG1 to regulate hematopoiesis.

Here, we provide evidence obtained from a variety of lymphoma and leukemia cell lines, as well as from primary cells from patients with these diseases, that *Lxn* expression is almost universally absent or significantly reduced from that of normal stem and progenitor cells. Moreover, treatment with a de-methylating agent at least partially restores *Lxn* expression in a variety of tumor cell lines, and methylation level of the CpG island in the *Lxn* promoter region is inversely associated with its expression. Perhaps most importantly, we show that when *Lxn* expression was re-initiated ectopically in two lymphoma cell lines using a retroviral expression vector, their growth, both *in vitro* and *in vivo*, was significantly blunted. We further show that *Lxn* inhibits lymphoma cell growth by significantly increasing apoptosis through the down-regulation of anti-

apoptotic genes and that its anti-tumor activity is mediated via mechanisms unique from its canonical inhibition of carboxypeptidase A. These results demonstrate that *Lxn* plays a functional role in tumor cell growth and introduces an unexplored pathway potentially important to cancer treatment in patients.

5.3 Material and Methods

5.3.1 Animal

Young 8-to 12- week old female C57BL/6 (B6) and 7-week old female BALB/c mice were purchased from the Jackson Laboratories (Bar Harbor, ME). Mice were kept in the animal facilities of the University of Kentucky under pathogen-free conditions according to NIH-mandated guidelines for animal welfare. They were fed with acidified water and food *ad libitum*. All animal work in this study was approved by Institutional Animal Care and Use committee (IACUC) at the University of Kentucky (Identification number: 2010-0753)

5.3.2 Leukemia cell lines

Nine human leukemic cell lines (K562, Molt4, CCRF-CEM, J45.01, Jurkat, U937, HL-60, KG-1 and SupB15) and two mouse lymphoma cell lines (WEHI-231 and A20) were included in our study. Human leukemic cell lines were purchased from American Type Culture Collection (ATCC) (Manassas, VA). Mouse lymphoma cell lines are gifts from Dr. Bondada [158]. The leukemia cell lines were maintained in IMDM supplemented with either 10% (K562) or 20% (KG-1, HL-60 and Sup-B15) fetal bovine serum (FBS), or RPMI medium with 10% FBS, 10mM

Hepes (Molt4, CCRF-CEM, J45.01, Jurkat and U937), 0.05mM 2-mecaptoethanol, 80 U/mL penicillin, and 80mg/mL streptomycin. The cells were incubated in a humidified atmosphere of 5% CO2 in air at 37°C.

5.3.3 Isolation of CD34+ cells

Primary AML cells were obtained from the peripheral blood and bone marrow of patients at the Markey Cancer Center and Northwestern University. Normal bone marrow was obtained as discarded material following pathologic analysis, surgical marrow harvest, or from the National Disease Research Interchange (NDRI). CB was obtained from patients at the University of Kentucky Obstetrics Department or from the NDRI. All tissues were obtained with the approval of the respective institutional review boards and appropriate informed consent (confirmation number is 11-0315-F3R from University of Kentucky). Some samples were collected from Northwestern University and transferred to University of Illinois at Urbana-Champaign with approval of Material Transfer Agreement (MTA). We processed 9 normal and 9 leukemia and lymphoma samples, the age and disease type of each sample are described in the figure 5.5 legends. Marrow and blood cells were depleted of erythrocytes by suspending in 150 mM NH4Cl plus 10 mM NaHCO3 for 5 minutes, followed by 2 washes with phosphate-buffered saline (PBS). Blood cells were subjected to Ficoll-Paque (Pharmacia Biotech, Piscataway, NJ) density gradient separation to isolate the mononuclear white blood cell compartment. Resulting leukocytes from marrow or blood were then used for immunoaffinity selection and flow cytometric sorting. For CD34+ cell selection, the Miltenyi immunoaffinity device (VarioMACS)

was used according to the manufacturer's instructions (Miltenyi Biotech, Auburn, CA), and further purified by immune-staining with anti-CD34 antibodies (Pharmingen, San Diego, CA) and sorting in a triple-laser FACSVantage flow cytometer (Becton Dickinson Immunocytometry Systems, San Jose, CA). In some cases, leukocytes were cryopreserved at a concentration of 5 x 10^7 cells/mL in freezing medium consisting of Iscoves modified Dulbecco medium (IMDM), 40% FBS, and 10% dimethyl sulfoxide (DMSO).

5.3.4 Quantitative real-time PCR

To measure the expression of *Lxn* in leukemic cells, quantitative real-time PCR was performed. Identical numbers (200,000) of cells were used for total RNA extraction using RNeasy Mini kit (QIAGEN, Valencia, CA) according to the manufacture's instruction. Isolated total RNA was reverse transcribed into cDNA using random hexamers in a TaqMan® reverse transcription solution (PN N8080234) and stored at -20ºC. In real-time PCR reactions, primer and probe mix for LXN (human and mouse) were purchased from Applied Biosystems (Foster city, CA, USA). TaqMan® human glyceraldehyde-3-phosphate dehydrogenase (GAPDH) was served as an endogenous control to normalize LXN expression. PCR reactions were set up according to manufacturer's instructions using TaqMan® universal PCR master mix (PN 4304437). Analyses of gene expression were performed in single reporter assays in an ABI PRISM 7700 sequence detection system (PE Biosystems, Foster city, CA, USA).

RT^2 Profiler Apoptosis PCR Array (PAMM-012Z, QIAGEN) was performed according to the manufacturer's instructions. cDNAs was prepared from A20 cells

infected with empty or lxn expression vectors with RT^2 First Strand cDNA Kit (C-03, QIAGEN) and added to RT^2 qPCR master mix (PA-012). The mixture was aliquoted across the PCR array which contains 84 apoptosis-related genes. Gene expression and quantification was performed in an ABI PRISM 7700 sequence detection system, and data was analyzed with using web-based software (http://pcrdataanalysis.sabiosciences.com/pcr/arrayanalysis.php). The genes with more than 2-fold change in expression and showing statistically significant ($p<0.05$) were chosen for candidate gene.

5.3.5 Western blots

Cell samples were lysed at a concentration of $2x10^7$ cells/ml in a protein lysis buffer containing: 10mM Tris pH7.5, 50mM NaCl, 30mM sodium pyrophosphate, 50mM NaF, 5µM ZnCl2 and 1 % Triton X-100, 2.8ug/ml aprotinin (Sigma-Aldrich; St. Louis, MO), 1mM phenylmethylsulfonyl fluoride (Sigma), 1mM sodium vanadate (Na3VO4) 1ug/ml pepstatin, and 1µg/ml leupeptin (Oncogene Research, MA, USA). Lysate was incubated on ice for 30 minutes, and then centrifuged at 15,000 x g for 10 minutes to remove debris. The resulting supernatant was then aliquoted and stored at -80°C. For Western blot, protein lysates were thawed and mixed with running buffer and a reducing agent (Novex, San Diego, CA, USA, per manufacturer's instructions) and heated at 95°C for 5 minutes. Samples were then analyzed by denaturing PAGE (Novex, 10% bis-Tris gel) using the equivalent of $4x10^5$ cells per lane. Following electrophoresis, samples were electro-transferred onto immunobilon-P membranes (Millipore, Bedford, MA, USA), which were subsequently blocked and probed with

polyclonal rabbit anti-LXN Ig-G antibody at a 1:3000 dilution. This antibody was generated from the *Lxn*-specific amino acid sequence CKHNSRLPKEGQAE at the carboxyl terminus, and was produced by Bethyl Laboratories, Inc. (Montgomery, TX). The antibody for detection of human LXN was purchased from Abcam Inc. (Cambridge, MA) and used at 1:2000 dilution. The antibodies for apoptotic proteins, Bcl-2, Bcl-xl, Bax, Bad (Santa Cruz Biotechnology) were provided by Dr. Bondada. The antibody for Pim-2 was purchased from eBioscience (San Diego, CA). Primary antibodies were detected using alkaline phosphatase-conjugated secondary antibodies (Santa Cruz Biotechnology) and electro-chemifluorescent (ECF) reagent (Pharmacia Biotech) according to the manufacturer's instructions. Blots were visualized using a Molecular Dynamics STORM 860 system and Imagequant Software. Following the detection and quantification of anti-LXN antibody, immunobilon-P membrane was sequentially stripped in 40% methanol and the buffer containing 100mm ß-mercaptoethanol, 2% sodium dodecyl sulfate and 62.4mM Tris-HCl to remove ECF reaction product and antibodies, respectively. The stripped membrane was re-probed with anti-actin antibody (Sigma) at 1:500,000 dilution and detected as described previously.

5.3.6 Genomic bisulfite sequencing

To investigate the methylation pattern of *Lxn* promoter, CpG island analysis in the upstream sequence of *Lxn* open reading frame. Nucleotide sequence of *Lxn* in upstream region (–1000 bp) and the first 3 exons (+373bp) was obtained from Ensembl database (www.ensembl.org) with ID number ENSG00000079257. CpG island search using CpG island searcher website

(http://www.uscnorris.com/cpgislands2/cpg.aspx) showed a 252bp region (–208bp to +44bp) in upstream of *Lxn* sequence enriched for CpG repeats. The criteria of 5 CpG island is: GC content >50%, ratio of CpG to GpC > 0.6 and 200 bp of minimum length. Genomic DNAs were isolated using AquaPure Genomic DNA kit (Bio-Rad, Hercules, CA) and modified by sodium bisulfite using EpiTect® Bisulfite kit (QIAGEN, Valencia, CA). For the *Lxn* promoter methylation study, we designed primers that could amplify a 423bp fragment in the upstream region of *Lxn* containing CpG island. The forward primer sequence is 5' GTTGGTGTTTGATAAGTATGTGG 3', and the reverse primer sequence is 5' TTTAACCTTCTACACCTCAAACAC 3'. The annealing temperatures for primers were 52°C for 2 minutes. Hot-start PCR with a total cycle number of 30 was used in all PCR amplifications. Denaturation and extension cycles were maintained for 95 °C, 30 seconds and 72 °C, 1 minutes respectively. The amplified fragments were cloned into the pCR2.1-TOPO vector using TOPO TA Cloning Kit (Invitrogen Carlsbad, CA) and sequenced (MWG Technology) ($n \geq 3$ clones for cell line and $n \geq 8$ clones for primary cells).

5.3.7 5-aza-2'-deoxycytidine treatment

To examine the correlation of promoter hypermethylation and *Lxn* gene expression, the leukemia cell line, shown to have a lack or decrease of *Lxn* expression, was subject to 5-aza-2'-deoxycytidine treatment. Cells were plated with 2uM 5-aza-2'-deoxycytidine (Sigma-Aldrich; St. Louis, MO) and incubated for 4 days. The medium and the drug were replaced every 24 hours and cells were harvested for RNA and DNA extraction 4 days after treatment.

5.3.8 Infection of WEHI231 and A20 cells with *Lxn* expression vector

Cloning of the mouse *Lxn* gene into Sfbeta 91 retroviral vector and production of viral supernatant were performed exactly as described previously[93]. WEHI-231 and A20 cells were infected by 10ml viral supernatant at a density of $1x10^6$ cells per 10cm plate along with 4 µg/ml of polybrene for 48 hours. The infected cells (GFP+ cells) were sorted and expanded in culture medium. The expanded GFP+ population, if not used immediately, was cryopreserved at a concentration of 1 X 10^7 cells/mL in freezing medium consisting of 80% fetal bovine serum, and 20% dimethyl sulfoxide (DMSO).

5.3.9 Measurement of growth of retrovirally-transduced tumor cells

Sorted GFP+ A20 cells over expressing *Lxn* or Sfbeta 91 empty vector were counted on a hemacytometer using trypan blue dye exclusion and 500,000 cells were seeded into $25cm^2$ tissue culture flask in 4mls media. Cells were incubated in a humidified atmosphere of 5% CO2 in air at 37°C and subsequently counted on days 3, 8, 12, 16 and 20. At each time point, cells were split and maintained at a concentration of 500,000 cells per 4 ml media. The cumulative cell number was calculated from the cell counts and the dilutions made at each culture split. FACS analysis was also performed at each time-point to measure the percentage of GFP+ cells. For the in vivo measurement of tumor cell growth, various numbers (5,000; 25,000; 50,000 and 100,000) of GFP+ A20 cells over expressing *Lxn* or Sfbeta 91 empty vector were injected in a 50µl bolus subcutaneously in the shaved flank of BALB/cJ mice given 3.0 Gy of gamma

radiation 4 hrs. prior. Lymphomas were detectable by palpation 10-12 days post-injection and all three dimensions of tumors were measured blind with calipers on days 12, 14, 16, 19, and 21. The same individual made the measurements from day-to-day without knowing the treatment regimen the mice received. At day 21, host mice were euthanized, the lymphomas were excised, and single cell suspensions were made of each to determine the fraction of tumor cells expressing GFP.

5.3.10 Cell cycle and apoptotic analysis

The culture of GFP+ A20 cells was maintained as described above. At each time-point, cell cycle analysis was measured by BrdU labeling using BrdU Flow Kit (Pharmingen, San Diego, CA) according to the manufacturer's instruction. 10ul of BrdU solution (1mM) was added to $1x10^6$ cells in 1 ml culture medium and incubated for 1 hour. The cells were fixed and permeabilized by Cytofix/Cytoperm Buffer and treated with 30ug DNase for 1 hour at 37^oC. After washing with Perm/Wash buffer, cells were stained with PE-conjugated anti-BrdU antibody for 20 minutes at room temperature, washed and 20 ul of 7-AAD was added. The cells were analyzed by flow cytometry on Facscan (Becton Dickinson Immunocytometry Systems, San Jose, CA).

5.3.11 Immunohistochemstry of A20 cells treated with potato carboxypeptidase inhibitor (PCPI)

PCI was purchased from Sigma-Aldrich Co. (St. Louis, MO). FITC labeling of PCI was performed by using FLUOROTAG™ FITC CONJUGATION KIT

(Sigma-Aldrich) according to manufacturer's instruction, and was used to treat A20 cells for fluorescence internalization assays. Cells are cultured on 22x22mm microscope cover glasses (Fisher Scientific Co., Pittsburgh, PA) in media as described above. Cells were fixed onto cover glasses with 1:1 methanol:acetic acid and washed 3 times by PBS. Cells were incubated with FITC-conjugated PCI at a concentration of 30ug/ml at 37^{o}C for 30 minutes, washed and stained with phycoerythrin (PE)-conjugated B220 and DAPI. The cover glass coated with A20 cell monolayer was flipped immediately and sealed onto glass slide. The image was taken with a Zeiss Axiovert- 200 microscope using a high-resolution Zeiss digital camera (Carl Zeiss Inc., Thornwood, NY)

5.3.12 Culture of A20 cells with potato carboxypeptidase inhibitor

To determine the effects of PCPI on A20 cell growth, A20 cells were seeded at a density of 6x10^{5}/ well in 6-well plates, cultured overnight before the addition of 0, 5, 15, 30 or 60ug/ml PCI. The cells were fed every 2 days with fresh medium (as above) containing the respective concentration of PCI, and viable cells were counted on a hemacytometer using trypan blue dye exclusion. Cells were split according to cell population size to maintain a cell concentration of 2-5 x 10^{6}/ml and cultures were maintained for 12 days. The cumulative cell number was calculated from the cell counts and the dilutions made at each culture split.

5.3.13 Statistical analysis

Data were analyzed by either student *t*-test assuming unequal variance

with $P < 0.05$ (two-tail), or a one-way ANOVA.

5.4 Results

5.4.1 Loss of *Lxn* expression in malignant cells

We first determined *Lxn* mRNA abundance in tumor cell lines by quantitative real-time PCR (Fig. 5.1A). Compared with normal primitive hematopoietic cells, *Lxn* mRNA expression was completely absent in a majority of tested leukemic lines, including K562, Molt4, CRF-CEM, J45.01, Jurkat and U937, and was significantly diminished in HL-60, KG-1 and SupB15 cell lines. LXN protein expression was also tested in all samples using Western blotting and nearly identical results were obtained in tested cell lines (Fig. 5.1B). Our results are consistent with those previously reported[148] and include additional leukemia and lymphoma cell lines.

5.4.2 Aberrant promoter hypermethylation of *Lxn* in hematopoietic malignancy

To assess whether the loss or decrease of *Lxn* expression in malignant cell lines resulted from promoter hypermethylation, methylation of the 5' CpG island of *Lxn* gene surrounding its transcriptional start site was determined by genomic bisulfite sequencing. The CpG island spans from within the canonical 5' promoter (-208nt) to the transcription start site (+1nt), and extends through the entire first exon (+44nt). There are 15 CpG dinucleotides within this region (Fig. 5.2A). The CpG island identified here is not exactly same as the one reported previously, this may be due to the different criteria we used for defining this region. Figure 2B depicts the

quantitative variation in methylation for each CpG site among nine tumor cell lines. Almost complete methylation was seen in J45.01, U937, Jurkat, Molt4 and CCRF-CEM (>90%) lines, which commensurately showed an absence of *Lxn* expression. Scattered methylated CpG sites were found in K562, KG-1 and SupB15 lines, which were linked to the weak expression of *Lxn*. Surprisingly, although HL-60 had very low *Lxn* expression, we found that none of the CpG sites were methylated. This is probably due to other epigenetic mechanisms, such as histone deacetylation of latexin promoter in HL 60 cells

5.4.3 Reactivation of Lxn expression with demethylation reagent treatment

To test the hypothesis that *Lxn* promoter hypermethylation might be involved in the loss of expression in leukemia and lymphoma cell lines, we studied the effect of 5-aza-2'-deoxycytidine, a DNA demethylating reagent, on *Lxn* expression (Fig. 5.2C). After treatment with 2 uM 5-aza-2'-deoxycytidine for 4 days, *Lxn* gene expression was reactivated in cell lines completely lacking *Lxn* expression prior to treatment (K562, Molt4, CCRF-CEM, J45.01, Jurkat and U937), and was significantly up-regulated in HL-60, KG-1 and SupB15 lines. The up-regulation of *Lxn* by 5-aza-2'-deoxycytidine in HL60 cells, which shows no hypermethylation of CpG sties (Fig. 5.2B), might be because the demethylation of other DNA sequences induces chromatin remodeling, thus exposing *Lxn* promoter for the transcriptional initiation.

5.4.4 Suppression of growth of mouse lymphoma cell lines *in vitro* and *in vivo* following ectopic *Lxn* expression

To determine a correlative or causative relationship between *Lxn* expression and tumor development, we next asked whether or not the re-initiation of *Lxn* expression affected the growth rate of malignant cells *in vitro* and *in vivo*. To that end, we ectopically expressed *Lxn*, using a retroviral expression vector containing green fluorescent protein (GFP) marker, in the mouse BALB/c-derived A20 B lymphoma cell line, which lacks *Lxn* expression (Fig. 5.3C). The controls are A20 cells either un-infected or infected with empty vector. The GFP positive A20 cells were purified by flow cytometric cell sorting, and their growth was determined in vitro and in vivo.

Fig. 5.3 shows the potent effects of *Lxn* expression on inhibiting tumor growth in vitro and in vivo. Fig. 5.3A shows that cultures of A20 cells infected with the *Lxn* expression vector contained only about half the number of cells at day 3 as compared to A20 cells infected with the control (empty) vector or uninfected control cells (A20 control). The growth suppression by *Lxn* overexpression was exponentially amplified during subsequent days of culture and by day 20 nearly 16 fold less tumor cells were present in *Lxn*-overexpressing group than in control cultures (right panel). Fig. 5.3B shows that the fraction of GFP+ cells remained at 90-100% throughout the 20 days of culture in both the *Lxn* vector- or control vector-infected cells. Fig. 5.3C shows that at day 20 of culture neither uninfected A20 cells nor A20 cells infected with the control (empty) vector expressed detectable *Lxn* protein, whereas in the Western blot a strong *Lxn* band was

evident in lysate of cells infected with the *Lxn* vector (upper band). LXN protein level at day 0 of culture in these cells is nearly identical to that at day 20 (data not shown). In a separate series of experiments, we have found a similar growth reduction *in vitro* when *Lxn* was ectopically expressed in WEHI231 lymphoma cells (data not shown).

Fig. 5.3D shows a compilation of two independent experiments in which ectopic *Lxn* expression suppressed the growth of A20 cell *in vivo*. 100,000 GFP+ A20 cells infected with either the *Lxn* expression vector or the GFP only control vector, or uninfected A20 cells, were injected subcutaneously into the flanks of BALB/c mice. Beginning at day 12 when tumors were first palpable, the *Lxn*-expressing cells caused significantly smaller tumors (filled circles; $P<0.005$). By day 21 when the experiments were terminated, the tumors in the *Lxn* vector-injected group averaged only 40% of the volume of tumors in the other two control groups ($P<0.05$, n=12 in each group). At day 21, we determined the fraction of tumor cells expressing GFP and Fig. 5.3F shows that virtually all of the tumor cells in the *Lxn* and control vector groups were GFP+. More to the point, Western blots confirmed strong expression of *Lxn* as in the cells analyzed after 20 days in culture (Fig. 5.3C). Thus, the reduction in tumor growth was due to durable *Lxn* expression in the tumor cells themselves.

To explore the effects of cell dose on tumor size and latency before being palpable, we ejected graded doses of *Lxn*-expressing or control A20 cells (Fig. 5.3E) to BALB/c recipient (n=4/group). At the 5,000 and 25,000 inoculum sizes, the *Lxn*-expressing cells not only resulted in more impressive suppression of the

size of tumors than with the 100,000 cell inoculum in Fig. 5.3D, but resulted in delayed onset of measurable-sized tumors. At day 21, the reduction in tumor size caused by ectopic *Lxn* expression was 83% and 63% at the 5,000 and 25,000 cell doses, respectively. Host animals were necropsied for evidence of gross metastases to spleen, thymus and liver. No evident tumors were found in any of the treatment groups. Similarly, flow cytometry detected no GFP+ cells in these anatomical sites (data not shown).

5.4.5 *Lxn* inhibits tumor cell growth through increasing apoptosis but not via its canonical function

As we previously reported in our normal hematopoietic stem cell studies, high *Lxn* expression is associated with increased apoptosis and decreased proliferation. To determine if these mechanisms were applied to our results with tumor cells, we next measured these two parameters in vector-infected A20 cells throughout 21 days of culture. As shown in Fig. 5.4A, flow cytometric analysis of cells stained with BrdU and 7AAD allows for the discrimination of cell subsets that are apoptotic (A), necrotic (N) or reside in G0/G1, S and G2/M phase of cell cycle. By day 5 of culture, 10 fold more *Lxn*-expressing tumor cells were undergoing apoptosis than control cells (10.6% vs 1%). No significant differences in the proliferation and the numbers of necrotic cells were observed between *Lxn*-overexpressing and control cells (data not shown). These results point to apoptosis as the major cellular mechanism in *Lxn*-mediated tumor suppression. We next investigated the molecular mechanisms underlying *Lxn*-induced apoptosis. We performed apoptosis pathway-specific PCR arrays in A20 cells

infected with either empty or *Lxn*-expressing vectors. We found that 17 out of 84 apoptosis-related genes were differentially expressed in *Lxn*-overexpressing cells, and majority of them (15 genes) were down-regulated (data not shown). We specifically examined several well-known apoptotic genes, including Bcl-2, Pim-2, Bcl-xl, Bax, and Bad, and plotted their expression in Fig. 5.4B. Two anti-apoptotic genes, Bcl-2 and Pim-2, were down-regulated by at least 3-fold in *Lxn*-overexpressing cells (left panel) as compared to the control, whereas pro-apoptotic genes, including Bax and Bad, did not show any change in their mRNA levels. Western blots of these proteins observed the similar reduction in Bcl-2 and Pim-2 (all three isoforms) but not in Bcl-xl, Bax and Bad in *Lxn*-overexpressing A20 cells (right panel), which is consistent with PCR array result. Thus our data indicate that *Lxn*-induced apoptosis in A20 cells is mainly through the down-regulation of anti-apoptotic regulators, such as Bcl-2 and Pim-2.

A well-known function of *Lxn* is its role as the sole carboxypeptidase A (CPA) inhibitor in mammalian cells. There are six *Cpa* genes (1-6) in this family. In order to test whether or not the suppressive effect of ectopic *Lxn* expression on the growth of A20 and WEHI231 cells was due to its canonical inhibitory activity, we carried out the following experiments. We first determined which *Cpa* genes are enriched in hematopoietic stem/progenitor cells. By searching our gene expression profile of hematopoietic stem/progenitor cells (unpublished data), we found that *Cpa3* is the only gene highly expressed in hematopoietic cells (Tab. 5.1). Next, we tested *Cpa3* expression in A20 cells that were uninfected, or infected with empty or *Lxn* expression vectors, and found that it

was not expressed in any type of these cells (Fig. 5.6). Last, we treated A20 and WEHI cells with potato carboxypeptidase A inhibitor (PCPI), a 39 amino acid protein which strongly inhibits mammalian CPA, at a series of concentrations ranging from 5 to 60ug/ml of culture medium. As seen in Fig. 5.4C, none of the concentrations had any effect on the growth patterns of the tumor lines, despite the continuous presence of PCPI for 12 days of culture. To rule out the possibility that PCPI failed to inhibit tumor growth because it did not enter the cells, we used fluorescein isothyiocyanate (FITC) to label PCPI in cells. Fig. 5.4D shows A20 cells following a 30 min incubation with labeled PCPI (30ug/ml of culture medium). The three-color micrograph shows PCPI in green (FITC), the nucleus in blue (DAPI), and the B220 lymphoid cell surface marker in red (phycoerythrin, PE). It is apparent that PCPI is plentiful in the cytosol but is not found in the nucleus. The doses of PCPI chosen for the above experiments were taken directly from a study in which the inhibitor was shown to inhibit the growth of pancreatic adenocarcinoma cells by directly interfering with the epidermal growth factor signaling pathway[159]. Maximal growth inhibition was achieved at 30-50ug/ml. Thus, the mechanisms by which *Lxn* regulates both stem cell population size and lymphoma growth inhibition reside in a novel pathway involving apoptosis.

5.4.6 Down-regulation of *Lxn* in primary leukemia and lymphoma cells

Based on the strong evidence for the tumor suppressive function of *Lxn* in leukemia and lymphoma cell lines, we asked whether or not *Lxn* expression is altered in primary cells derived from patients with malignancies. We isolated

stem/progenitor-enriched CD34+ cells from bone marrow and blood cells in lymphoma and leukemia patients, as well as in normal donors. The patients included those with acute myeloid leukemia (AML), T cell pro-lymphocytic leukemia (T-PLL), plasma cell leukemia (PCL), acute T cell lymphoma (ATLL) and acute lymphoid leukemia (ALL, preB phenotype). The normal CD34+ cell samples were derived from cord blood (CB) and young (31 and 35 years) and old (85 and 97 years) adults. *Lxn* mRNA expression, quantified by real-time PCR, was decreased by at least two-thirds in primary malignant CD34+ cells (Fig. 5.5A). Quantification of LXN in CD34+ cells of all human normal and leukemic samples compiled to date is plotted in Fig. 5.5B. The result shows a significant decrease of LXN protein expression in malignant cells (P=0.03) even though *Lxn* expression at the protein level is more variable than that at the mRNA level. Two additional old samples in the normal control group contribute to this variation, which is consistent with the report that the number and functionality of HSCs in old individuals, perhaps stem cell regulatory gene(s), showed more dramatic variations as compared to their young counterparts[160]. In summary, these data indicate that *Lxn* dysregulation may be involved in human hematological malignancies. In the future study, it will be interesting to examine the expression of two anti-apoptotic genes, Bcl-2 and Pim-2, in patient samples to see whether or not they are up-regulated.

5.5 Discussion

Recently we found that *Lxn* is a natural regulator of hematopoietic stem cell population in mice by influencing self-renewal and apoptosis[93]. *Lxn*

expression in stem cells is inversely proportional to the size of the population in mice and thus acts as a negative regulator through cell-intrinsic mechanisms. The observation that low *Lxn* expression in hematopoietic cells was associated with increased replication led us to hypothesize that *Lxn* was down-regulated in malignancies with high proliferative rates and/or low apoptosis.

Here, we show that *Lxn* is either not expressed or is strongly down-regulated in a variety of leukemias and lymphomas. As a result of these findings and close linkage structurally and genetically with TIG1, we proposed that *Lxn* may similarly act as a tumor suppressor. Along with this proposal, there is expectation that manipulation of *Lxn* levels in malignant cells would alter their growth characteristics. Accordingly, two lymphoma cell lines in which *Lxn* expression was absent were infected with a *Lxn* expression vector. In one of the most significant findings of this study, we found that re-initiation of *Lxn* expression dramatically reduced their growth *in vitro* and *in vivo*. These results demonstrate that the level of *Lxn* expression is functionally related to both normal and malignant cell growth and, if the findings are true for human tumors, may provide an avenue for therapeutic intervention. Surprisingly, *Lxn* knock-out mice did not development leukemia nor lymphoma even though their hematopoietic stem cell pool was over-expanded and blast cells were detected in the peripheral blood[148]. These results suggest that *Lxn* may influence the crucial step in carcinogenesis[161]. It thus will be of great interest to introduce additional carcinogenetic “hits”, such as oncogenes or alkylating agents, to *Lxn* knockout stem cells to determine whether *Lxn* deletion will accelerate tumor development.

In addition, we observed that re-initiation of *Lxn* expression did not completely suppress tumor cell growth, suggesting that it would at best be a part of a multi-drug regimen.

We investigated the possible mechanisms by which ectopic *Lxn* expression may suppress growth of lymphoma cells and found increased apoptosis to be the major mechanism causing inhibition. Consistent with our study of normal hematopoietic cells, our recent findings indicate that high *Lxn* content is associated with more apoptotic cells, thus fewer stem cells [93]. Apoptosis is controlled by the balance of both positive (pro-apoptotic) and negative (anti-apoptotic) signals. We found that *Lxn*-induced apoptosis is mainly through the down-regulation of anti-apoptotic genes, such as Bcl-2 and Pim-2. Decreased level of Bcl-2 allows other pro-apoptotic proteins such as BAX and BAK to aggregate, inducing cytochrome C release and caspase activation, and apoptosis. Dysregulation of Bcl-2 is implicated in a variety of hematopoietic malignancies. [124] Three Pim-2 protein isoforms are active kinases which phosphorylate pro-apoptotic protein BAD and dissociate its binding from Bcl-xL, resulting in the inhibition of Bad-induced cell death.[162, 163] Enhanced expression of Pim-2 was detected in multiple B-cell lymphoma types[164], T-cell lymphoblastic leukemia/lymphoma[165], and acute myeloid leukemia[166]. Thus our studies identify *Lxn* as a novel regulator of the apoptotic pathway, in which it suppresses tumor survival through the down-regulation of Bcl-2 and Pim-2 anti-apoptotic factors.

The well- known function of *Lxn* is the sole carboxypeptidase A inhibitor in mammals.[91] Therefore, it was plausible that other carboxypeptidase A inhibitors

might mimic *Lxn*'s anti-tumor effects. A CPA inhibitor from potato tubers has been shown to be an effective inhibitor of mammalian CPA and was therefore chosen to test its anti-tumor properties. We found that it freely entered A20 lymphoma cells but did not have suppressive growth effects via apoptosis, irrespective of dose. Since CPAs are not expressed in A20 cells, we conclude that non-canonical functions of *Lxn* were responsible, yet unknown intracellular functions of *Lxn* account for its anti-tumor effects. In addition, it is unlikely that tumor suppressive effect of *Lxn* is through the regulation of ABGL2-mediated microtubule tyrosination cycle, like TIG1, because we did not detect the expression of ABGL2 in hematopoietic cells (data not shown). These results are in line with findings of other investigations in which gene expression or protein abundance regulated by *Lxn* were not related to carboxypeptidase inhibition [147, 148]. Thus, the action of mode of *Lxn* in regulating normal and malignant hematopoiesis is not through its canonical CPA inhibitor activity. Future studies aimed at identifying direct targets, or downstream signaling pathways, of *Lxn* will be critical for our understanding of its function in normal and malignant hematopoiesis.

Addressing the issue of why and how *Lxn* expression is down-regulated in tumor cells, we found that CpG dinucleotides in regulatory regions of the *Lxn* gene were methylated. Most human leukemia and lymphoma cell lines tested showed strong patterns of methylation involving most of the 15 CpG dinucleotides in *Lxn* promoter. This, in turn, led to a loss of gene expression that was at least partially reversible. When cell lines were treated with de-methylating

reagent, 5-aza-2'-deoxycytidine, *Lxn* expression was re-initiated or up-regulated. Thus, hypermethylation of the CpG island in the *Lxn* promoter may contribute to silencing or down-regulation of *Lxn* expression in leukemia and lymphoma cells. Ongoing studies will focus on the genetic and epigenetic regulation of *Lxn* transcription in cancer stem cells, with promise for improved targeted approaches for cancer prevention, diagnosis, and therapy.

5.6 Acknowledgements

I gratefully acknowledge Gary Van Zant, Dianna Howard, Kyle Rector, Carol Swiderski, Jason Brandon, Lawrence Schook, Jayesh Mehta, J. Scott Bryson, Subbarao Bondada, and Ying Liang for their contributions to this manuscript. I thank the technical assistance of Xian Gao in image capturing of immunocytochemstry staining, Barry Grimes in flow cytometry**,** and Hope Johnson and Paula Thomason for editing manuscript.

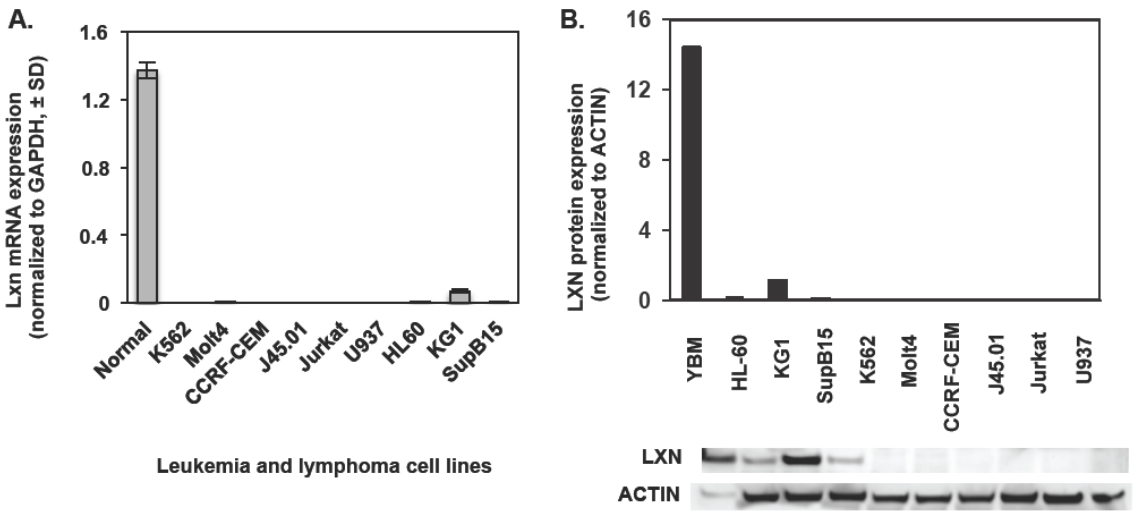

Figure 5.1. Decrease or loss of *Lxn* expression in leukemic and lymphoma cell lines.

(A) *Lxn* mRNA expression in leukemia cell lines. *Lxn* mRNA level was measured by quantitative real-time PCR and shown as mean (± 1 SD) (n=12). Control is normal bone marrow (BM). (B) *Lxn* protein expression in leukemic cell lines measured by western blot. The blot (bottom) and their quantification (top) profiles demonstrate the absent or weak expression of LXN protein in leukemic and lymphoma cell lines. Actin was used as the internal control.

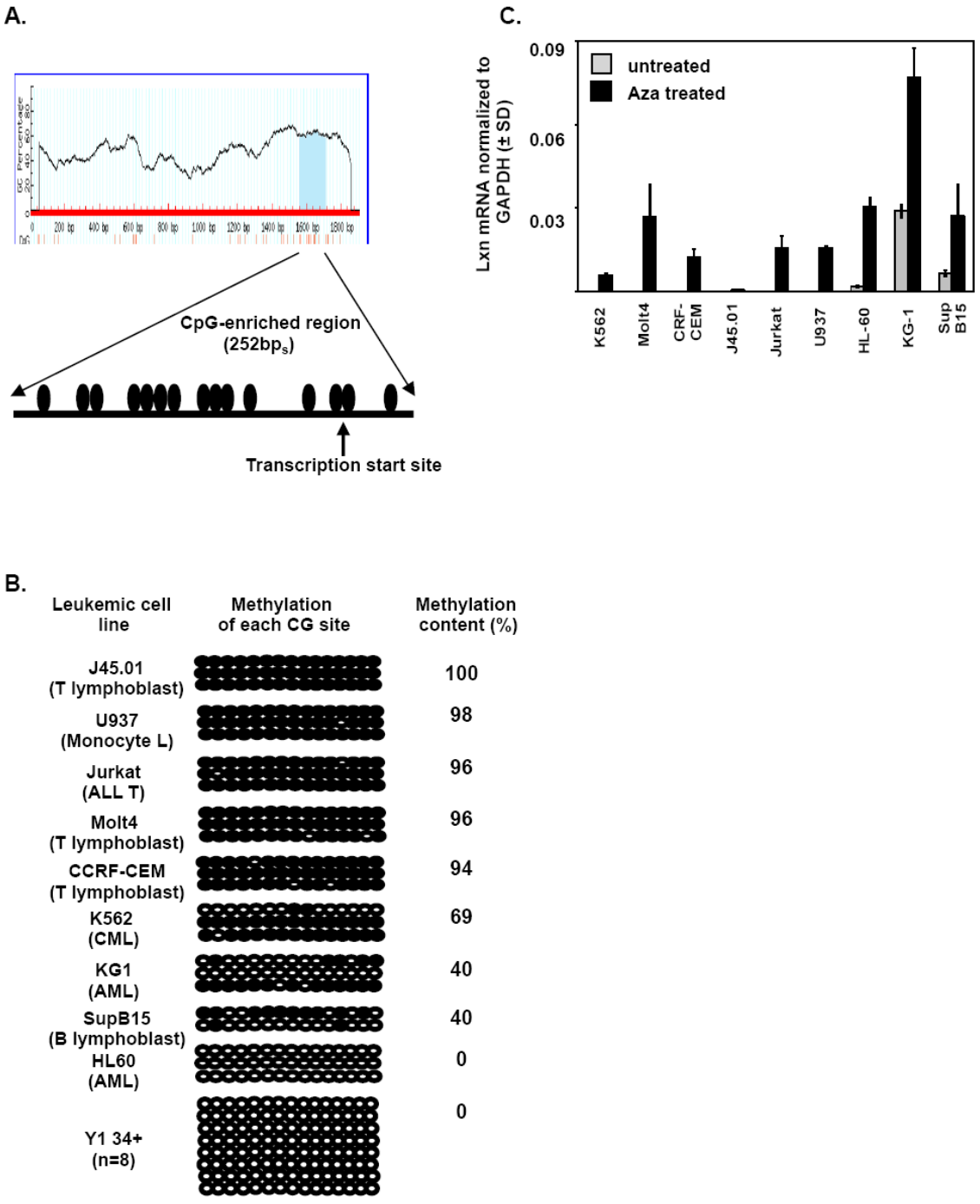

Figure 5.2. Hypermethylation of *Lxn* promoter CpG sites in leukemic cell lines.

(A) CpG-enriched region in *Lxn* promoter. Sequence from 1500 base pairs

upstream regulatory region to the first three exons was analyzed for CpG-enriched sites (top). A CpG island with 252 base pairs (bp_s) length was identified. The transcription starting site is indicated. Each filled circle represents a CpG dinucleotide, and there are 15. (B) Bisulfite sequencing for *Lxn* promoter CpG island methylation analysis in leukemic cell lines. Files are each of the 15 CpGs and ranks are replicate clones sequenced for each CpG (n=3). Open circles indicate unmethylated CpG (n=3) dinucleotides. Filled circles indicate methylated CpG dinucleotides. The methylation content was quantified by dividing the number of methylated CpGs with total numbers of analyzed CpGs. (C) Restoration or up-regulation of *Lxn* expression by 5-aza-2'-deoxycytidine. *Lxn* mRNA was measured by quantitative real-time PCR in leukemic and lymphoma cell lines exposed with or without 2uM 5-aza-2'-deoxycytidine for 4 days. Expression levels were normalized to endogenous control, *Gapdh*. Results shown are mean± SD of 12 replicates from 3 independent experiments.

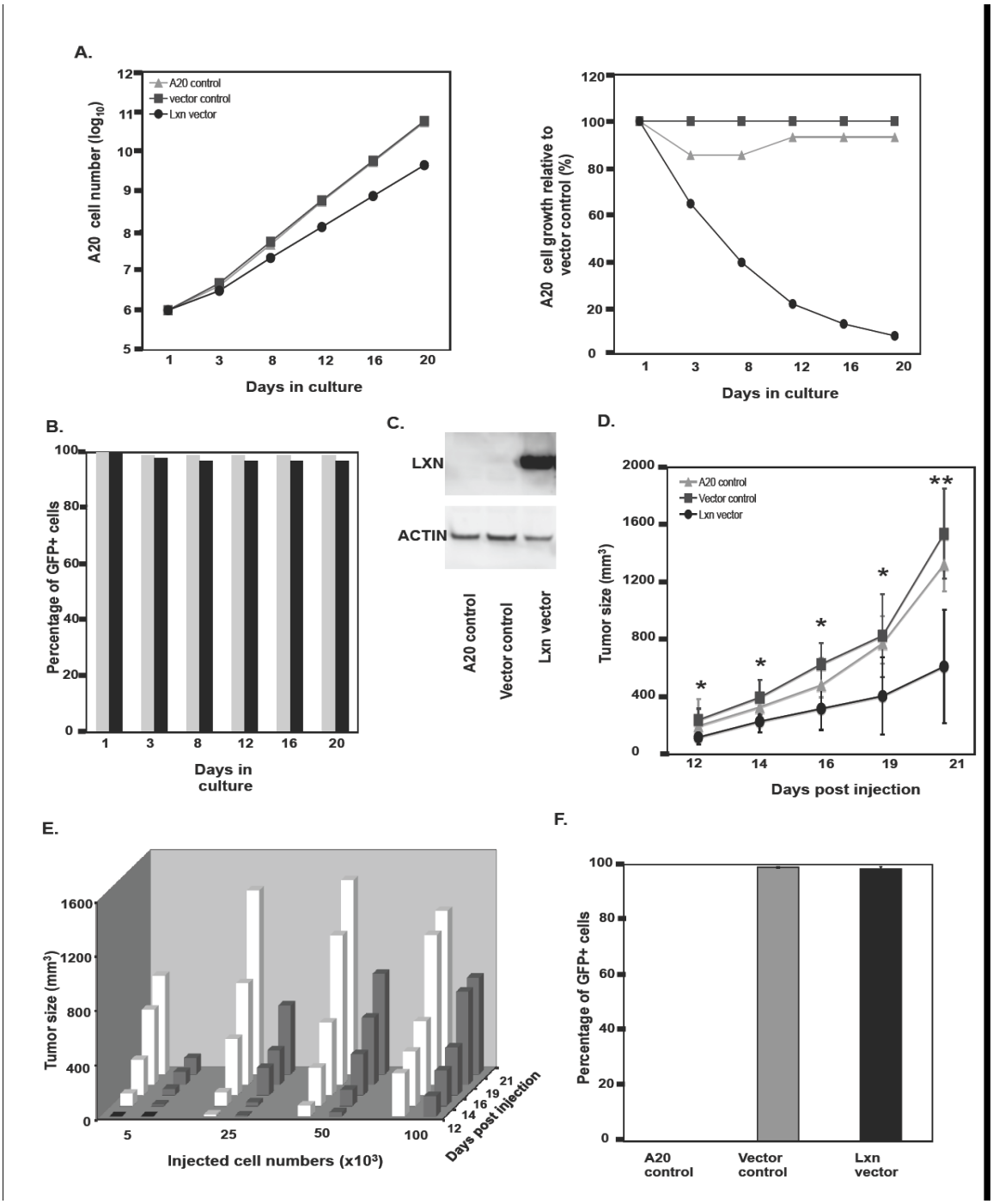

Figure 5.3. Overexpression *Lxn* suppresses growth of A20 lymphoma cell lines.

(A) *In vitro* growth inhibitory effects of *Lxn* overexpression on A20 cells. A20 cells uninfected (A20 control) or infected with empty (vector control) or *Lxn*-containing

vector (Lxn vector) were cultured for 20 days and counted by the trypan blue exclusion method. The absolute cell numbers at indicated time-points (X axis) were represented as log scale (Y axis) and were shown in left panel. The relative tumor growth in *Lxn*-overexpression A20 cells to controls was shown in the right panel. One representative experiment out of 3 independent ones is shown. (B) Proportion of GFP+ A20 cells infected with empty (light grey column) and *Lxn*-containing vector (black column) throughout 20 days of culture. Flow cytometric analysis was performed to detect GFP signal. (C) Western blot analysis with LXN antibody in total protein lysate from A20 cells at day 20 culture showing durable LXN overexpression. (D) *In vivo* tumor formation and growth with injection of 100,000 A20 cells. A20 cells were subcutaneously injected and tumor growth was monitored and measured by all three dimensions of tumors (Y axis) on days indicated on X axis. Shown is the compilation of 2 independent experiments with ± SD (n=12). The statistical significance is represented by * ($p<0.005$) and ** ($p<0.05$). (E) *In vivo* tumor formation and growth with injection of graded doses of A20 cells. Graded doses of A20 cells (X axis) were subcutaneously injected and tumor growth was monitored and measured in all three tumor dimensions (Y axis) on days indicated on Z axis. Unfilled columns represent A20 cells infected with empty vector and filled columns represent cells with *Lxn*-containing vector. A representative experiment is shown (n=4/group). (F) The fraction of GFP-expressing A20 cells in tumors biopsied at 21 days. Single tumor cell suspensions were made on day 21 post injection and subject to flow cytometric analysis for GFP-expressing cells.

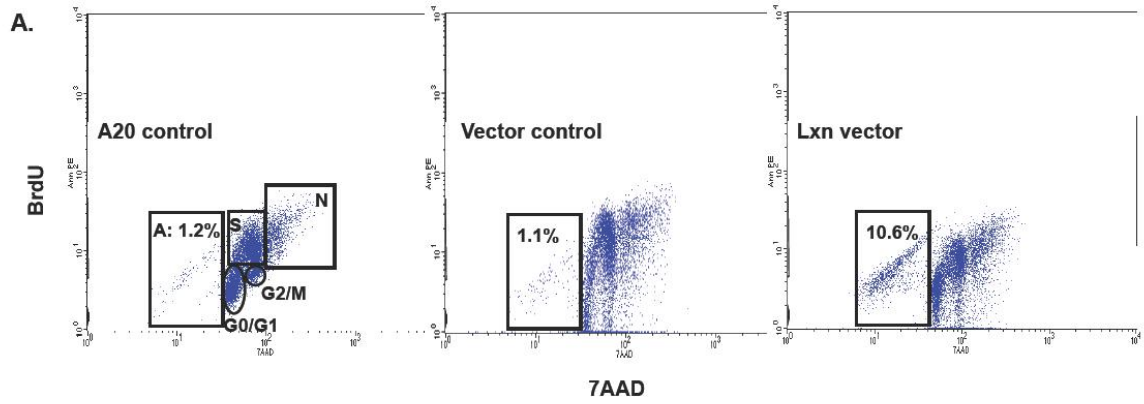

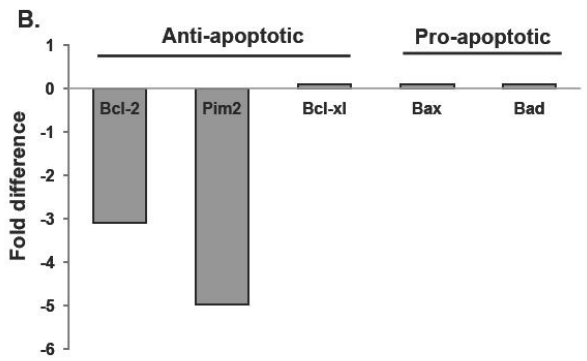

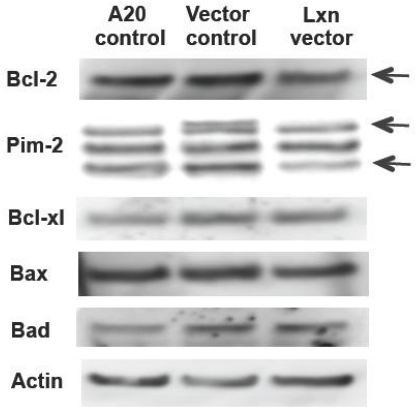

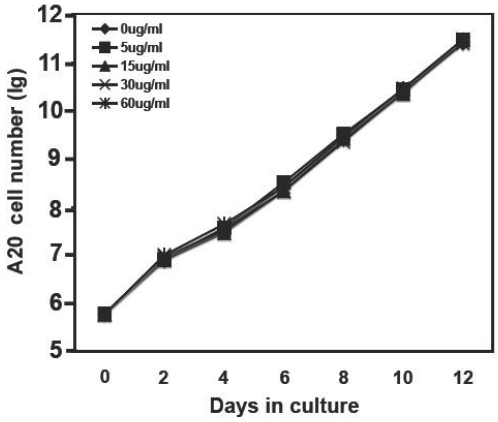

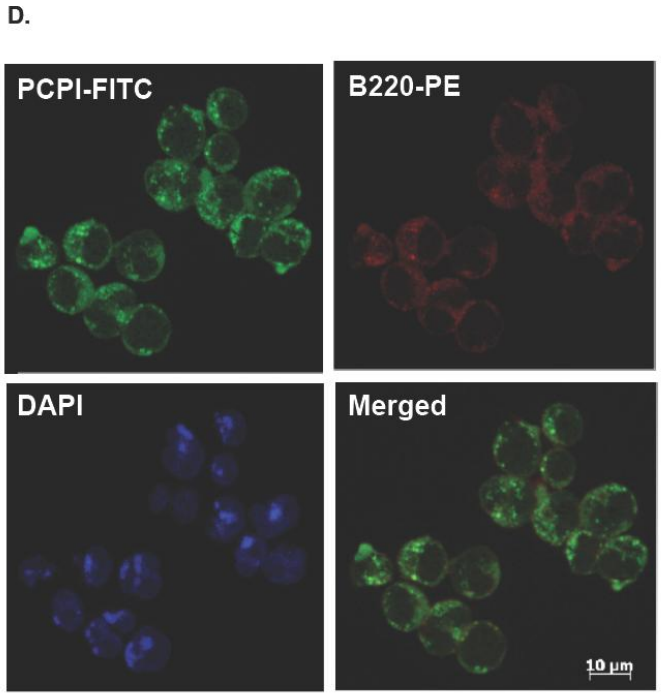

Figure 5.4. Ectopic Lxn expression increases apoptosis of A20 cells.

(A) Flow cytometric analysis of cell cycle and apoptosis in cultured A20 cells. A20 cells without (A20 control) or with empty (vector control) or *Lxn*-containing vector (Lxn vector) were cultured for 21 days. BrdU and 7AAD staining and flow cytometric analysis was used for detecting different phases of the cell cycle (G0/G1, S, G2/M) and apoptotic (A) and necrotic (N) population. A representative flow cytometric file from Day 5 of culture is shown. (B) Down-regulation of anti-apoptotic genes by *Lxn* overexpression. Apoptosis PCR arrays were performed on A20 cells infected with empty or *Lxn*-expressing vectors. Left panel shows the fold changes in the mRNA expression of several selected genes (as indicated in X axis) in *Lxn*-overexpressing cells compared to the control. Western blot confirms the decreased expression of Bcl-2 and two isoforms of Pim-2 at the protein level in *Lxn*-overexpressing cells (arrowhead). The other apoptosis-related genes, such as Bcl-xl, Bax and Bad, did not show significant difference in mRNA and protein expression. (C) The growth curve of A20 cells treated with graded doses of potato carboxypeptidase inhibitor (PCPI). No significant difference is detected between the control and any of the doses of PCPI. (D) Internalization of PCPI to cytosol of A20 cells. A20 cells were cultured with fluorescein isothiocyanate (FITC) labeled PCPI. Shown is a three-color micrograph with PCPI in green (FITC), the B220 lymphoid cell surface marker in red (phycoerythrin, PE), the nucleus in blue (DAPI), and merged image of red and green as indicated.

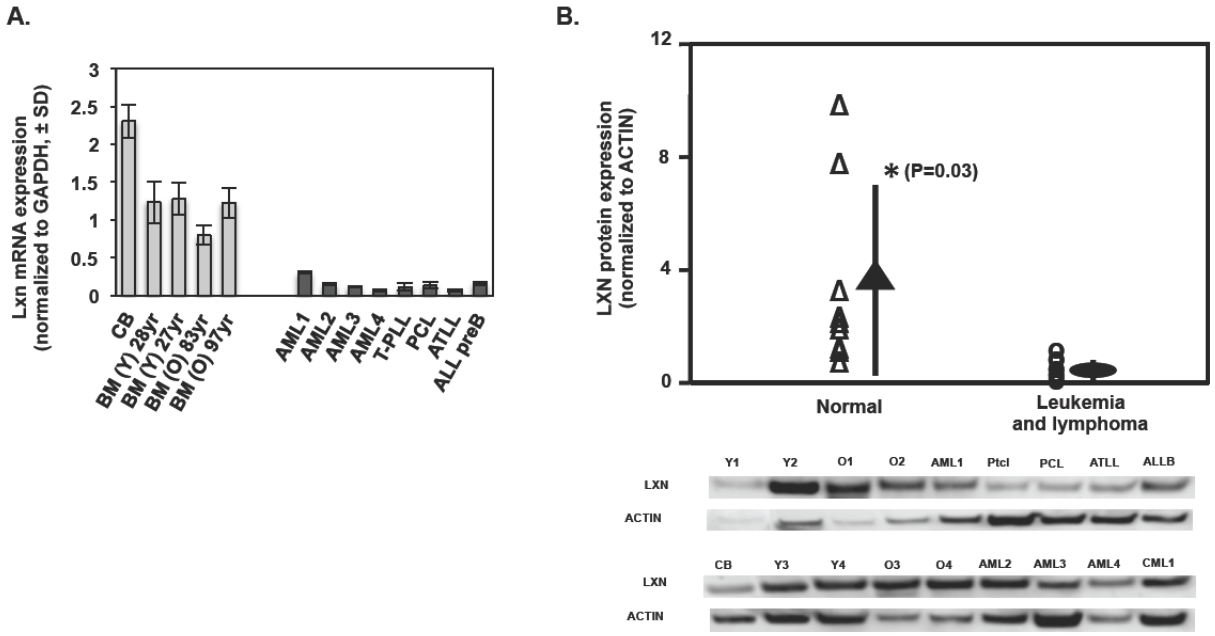

Figure 5.5. Decreased *Lxn* expression in stem/progenitor-enriched CD34+ cells in patients with leukemia and lymphoma.

(A) *Lxn* mRNA expression in bone marrow and peripheral blood CD34+ cells from leukemia and lymphoma patients and normal individuals. *Lxn* mRNA level was measured by quantitative real-time PCR and shown as mean (± 1 SD) (n=12). Normal samples were derived from cord blood (CB), bone marrow (BM) of young at 31 (Y1) and 39 (Y2) years old and old at 85 (O1) and 97 (O2) years old people. The patient samples include acute myeloid leukemia (AML), T cell pro-lympho leukemia (Pctl), plasma cell leukemia (PCL), acute T cell lymphoma (ATLL) and acute lymphoid leukemia (ALL, preB phenotype). (B) LXN protein expression in bone marrow and peripheral blood CD34+ cells from leukemia and lymphoma patients and normal individuals. Western blot was performed on the corresponding samples shown in panel (A) plus five more samples, including two young (Y3 and Y4; at 40 and 31 years old respectively), two old (O3 and O4; at

80 and 87 years old respectively) and chronic myeloid leukemia (CML). The blots (bottom) and their quantification (top) profiles demonstrate the significantly decreased Lxn protein level in leukemic CD34+ and lymphoma cells (P=0.03).

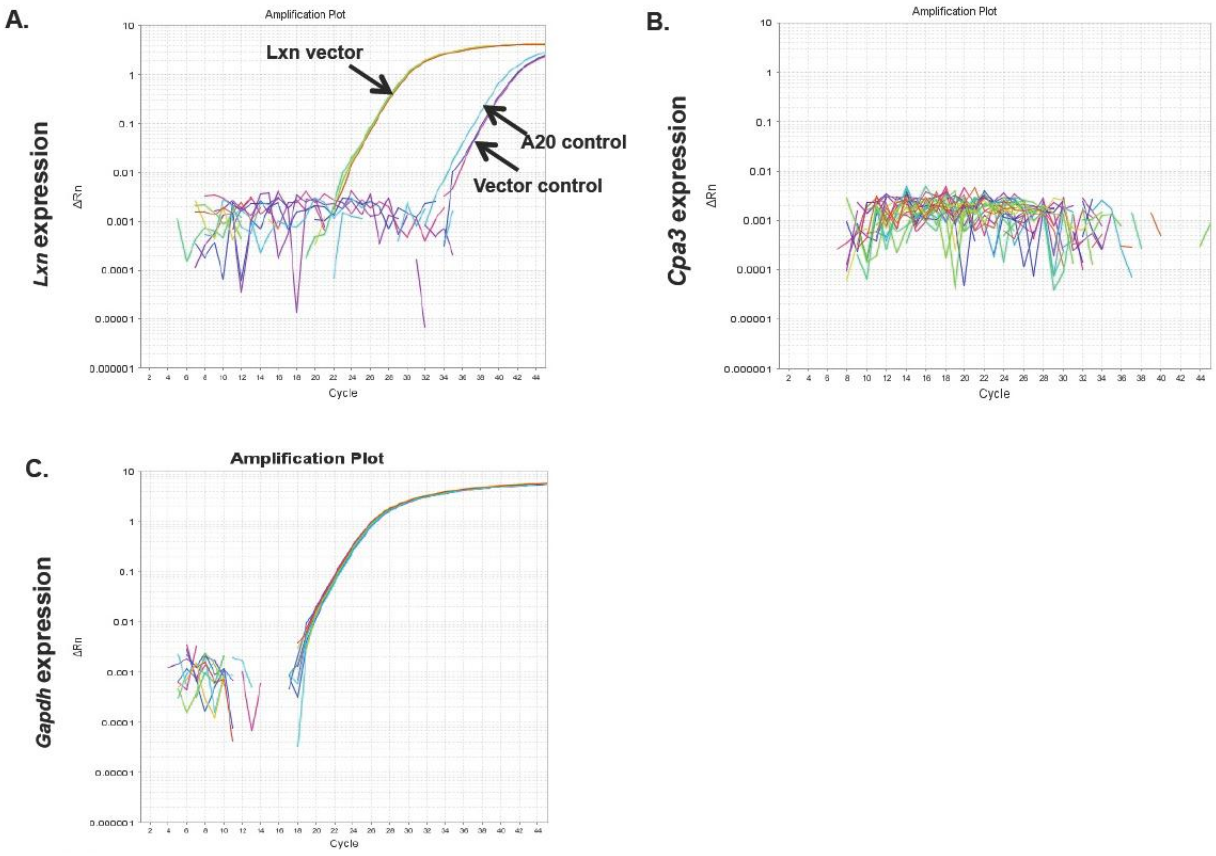

Figure 5.6 Cpa3 is not expressed in A20 cells.

Real-time PCR was performed on A20 cells that were either uninfected (A20 control) or infected with empty (vector control) or *Lxn* expression vector (Lxn vector) to quantify *Cpa3* mRNA expression. The amplification plots for *Lxn* (A), *Cpa3* (B) and *Gapdh* (C) transcript show that *Lxn* is highly expressed in A20 cells infected with *Lxn* expression vector whereas A20 and vector controls have very low expression levels, consistent with the results in Fig. 5.3c. *Cpa3* transcript is not amplified in all types of cells, indicating it is not expressed in A20 cells. These figures show the amplification plots of four individual biological replicates (n=4) for each gene.

Table 5.1 Carboxypeptidase A3 (Cpa3) is highly expressed in stem/progenitor cells.

Probeset	1418625_s_at	1448730_at	1453770_at	1427995_at	1440617_at
Gene Title	glyceraldehyde-3-phosphate dehydrogenase	carboxy-peptidase A3, mast cell	carboxy-peptidase A4	carboxy-peptidase A5	carboxy-peptidase A6
Gene Symbol	GAPDH	Cpa3	Cpa4	Cpa5	Cpa6
Chromosomal Location	6 C 59.3cM	3 A2|3 13.2 cM	6 A3.3	6 A3.3	1 A2
Entrez Gene	14433	12873	71791	74649	329093
mean_y_B6	11982.87	391.33	20.43	16.17	11.43
GO Biological Process Description	glucose metabolism /// glycolysis	proteolysis and peptidolysis	proteolysis and peptidolysis	proteolysis and peptidolysis	proteolysis and peptidolysis
GO Cellular Component Description	cytoplasm /// mitochondrion	extracellular space	extracellular space	---	---

Expression level of CPAs were measured by microarray on a bone marrow population null for cell markers characteristic of lineage-specific differentiated blood cells (Lin-negative), and positive for the Sca-1 and c-Kit cell markers (LSK) cells, enriched for hematopoietic stem/progenitor cells in mouse. The isolation of LSK cells as well as microarray analysis was performed as previously described [158] except the array platform is mouse Genome 430 2.0 Array (Affymetrix). Three biological samples were assayed, and the mean expression value (mean_y_B6) for each gene in the table is the average of three readings. Cpa3 (highlighted in gray) is the only *Cpa* gene that is highly enriched in LSK cells. *Gapdh* is the endogenous control.

CHAPTER 6: General Discussion and Conclusions

Adult stem cells in a variety of organs are responsible for replenishing short-lived, mature cells as they become senescent. The proliferative and regenerative capacities of adult stem cells make them ideal therapeutic tools for treating the degenerative diseases and severe stresses such as tissue injury or prevention of infection.

Our lab has uncovered novel features of adult hematopoietic stem cells, by implementing a forward genetic approach. Using this approach, our lab has identified several genes affecting stem cell population size and aging by correlating phenotypic variation to genotypic variation. Recent studies in our lab have demonstrated that endogenous stem cell numbers in young C57BL/6 (B6) and DBA/2(D2) mice are regulated by several candidate genes including *Lxn*[93], *Slit2* and *p107* (manuscript in preparation). We learned that *Lxn* regulates hematopoietic stem cell pool size through balancing apoptosis, proliferation and self-renewal[93]. The studies outlined in this dissertation were designed to further elucidate the functions of *Lxn* in regulating hematopoietic stem cell biology. To serve this purpose, we generated a constitutive knockout mouse model in which the *Lxn* gene was ablated in the entire organism. Several biological features were analyzed in the *Lxn* null mouse model: First, I studied the phenotypes of *Lxn* null cells in peripheral blood, spleen and bone marrow. A hyperproliferative hematopoiesis was found in *Lxn-/-* mice. Experiments using an apoptotic marker identified decreased apoptotic frequency in *Lxn-/-* BM cells. Thus, I hypothesize that decreased apoptotic frequency was the primary mechanism underlying the

expanded leukocytes and BM progenitor cell population in *Lxn-/-* mice (see in chapter 2). Next, I explored the function of *Lxn* under genotoxic stress using ionizing radiation as the stressor. Ionizing radiation breaks chemical bonds, produce free radicals, and causes DNA damages[167]. DNA repair machinery is triggered to amend the DNA damage; however, when the damage is too severe to repair, apoptotic mechanisms are used to eliminate the damaged cells[118]. Apoptosis is beneficial to retain chromosome integrity, but can also induce cytopenia in hematopoiesis[118]. Pro-apoptotic genes such as *p53* and *Puma* are common pharmaceutical targets for treating radiation exposure because reduced apoptotic activities accelerate hematological and immune recoveries[168-173]. In the current studies, I found that *Lxn-/-* mice were more resistant to lethal and sub-lethal doses of radiation due to greatly accelerated hematological and immune recoveries at one to six weeks after radiation[50]. The recovery advantage was resulted from a reduction in apoptosis in stem and progenitor cell populations (see in chapter 3). In another set of experiments, I studied the tumor suppressor function of *Lxn* by overexpressing *Lxn* in B cell lymphoma cells. The overexpression of *Lxn* up-regulated apoptotic frequencies in the lymphoma cells[107]. High levels of *Lxn* inhibited tumor formation by these cells in vivo and hindered tumor cell growth in vitro by inducing apoptosis (see in chapter 5)[107]. From the studies described above, I hypothesize that *Lxn* negatively regulates homeostatic cell expansion and radio-sensitivity of hematopoietic cells, and suppresses hematological malignancies by mediating apoptosis. *Lxn* expression levels are positively correlated with apoptotic activity (Fig. 6.1): High levels of *Lxn*

increase apoptotic frequency in tumor cells and therefore inhibit tumor cell growth. The down-regulation or absence of *Lxn* expression decreases apoptotic frequency in the peripheral blood and BM leading to a proliferative hematopoiesis. Loss of *Lxn* also confers radio-resistance by decreasing apoptotic frequency (Fig. 6.1). Thus, *Lxn* is an important mediator in response to hematological stresses, and a potential recovery treatment for chemotherapy, radio-therapy and hemorrhage.

As described above, apoptosis is one of the major mechanisms that eliminates undesired and cancer-prone cells. However, a novel role of apoptosis in controlling stem progenitor cell numbers and effecting stem cell-dependent regeneration has been identified by Elaine Fuchs and Hermann Steller's group in hair follicle stem cells. They found that mice deficient for a pro-apoptotic gene *Sept4/ARTS* have elevated numbers of hair follicle stem cells and remarkable improvement in wound healing and regeneration of hair follicles[174]. Our *Lxn* deficient mice an advantage in hematopoietic regeneration after severe oxidative stress (radiation) or after stem cell transplantation. There may be due to elevated apoptosis in stem and progenitor cells by loss of *Lxn* as a pro-apoptotic regulator.

My studies did not definitively uncover the downstream signaling pathways which underlie the altered apoptotic frequencies in *Lxn-/-* mice or in cancer cells with *Lxn* overexpression. Two anti-apoptotic genes, *Bcl-2* and *Pim-2*[107], were significantly down-regulated in murine lymphoma cells with *Lxn* overexpression. Apoptosis is controlled by a balance between positive (pro-apoptotic) and negative (anti-apoptotic) signals[124]. Decreased levels of Bcl-2 allow other pro-

apoptotic proteins to aggregate, therefore, inducing apoptosis[107]. The tumor suppressor *p53* is a negative regulator of *Bcl-2* and the *p53* signaling pathway is central in ionizing radiation-induced apoptosis[125, 126]. It is possible that the mechanisms underlying *Lxn* induced-programmed cell death are involved in *p53* and *Bcl-2* mediated apoptotic signaling pathways.

Another potential candidate involved in *Lxn* induced-apoptosis is *Thbs-1*. I found that the expression level of *Thbs-1* was decreased in the *Lxn-/-* multipotent progenitor cell population, in which the absolute number of cells increased significantly (see in chapter 2). *Thbs-1* null mice display a radio-resistance, similar to what I observed in *Lxn-/-* mice[130]. Further, it has been reported that *Thbs-1* is involved in regulating radiation-induced apoptosis through a CD47-mediated signaling pathway[112, 117]. To test this hypothesis, I will overexpress *Thbs-1* in *Lxn-/-* HSCs and transplant them into lethally irradiation recipients. Three to four months post transplantation (when hematopoiesis is fully reconstituted), the radio-resistance of the recipients will be examined. If, as I hypothesize, overexpressing *Thbs-1* in *Lxn-/-* cells will cause them to lose their recovery advantage and become more sensitive to radiation exposure due to an increased apoptotic frequency compared to empty vector transduced *Lxn-/-* cells.

In a final set of experiments, I demonstrated the effects of *Lxn* on HSC migration activities and identified potential target gene(s) of *Lxn* that may regulate HSPC mobilization (see in chapter 4). As described above, *Thbs-1* is down-regulated in the MPP population in *Lxn-/-* mice. *Thbs-1* is an adhesive glycoprotein that mediates cell-to-cell and cell-to-ECM adhesions. It binds to

various adhesive molecules including fibrinogen, fibronectin, intergrin and collagen[10]. It is possible that *Thbs-1* mediates BM cell retention and mobilization, and further regulates MPP cell numbers by influencing stem cell trafficking and localization.

In conclusion, although yet far away from clinical application, my studies in this dissertation have identified various novel functions of *Lxn* including inducing proliferative hematopoiesis, responding to hematopoietic stresses, mediating tumor formation, and regulating stem cell and progenitor mobilization. My studies described the phenotypes of *Lxn* deficient animals; however, the mechanisms and signaling pathways underlying these phenotypes have yet to be definitively undetermined. In future experiments, I will study *Lxn* downstream signaling pathways, focusing on the potential target genes of *Lxn* identified by microarray analysis. I will examine the RNA expression profiles of candidate genes along the developmental hierarchy, and determine the effects of *Thbs-1* overexpression in stem and progenitor cells using a retroviral vector. I hypothesize that performing CAFC assays with *Lxn-/-* cells in which *Thbs-1* is overexpressed will result in decreased frequency of the primitive day 35 or later CAFC progenitor population. Further, I speculate that overexpressing *Thbs-1* in *Lxn-/-* cells will lead to increased adhesion to stromal cells.

Ultimately, I would like to translate these findings in the mouse to the treatments for human hematopoietic disorder. I hope these studies will aid in the clinical practice of hematopoietic cell expansion in which expanded cells may be used for accelerating hematologic and immunologic recoveries in patients

exposed to high energy radiation, as well as in transplantation procedures for the treatment of hematologic malignancies. My studies also discovered a novel role for *Lxn* as a putative tumor suppressor gene. This role of *Lxn* could be used in treatments designed to suppress the tumor cell growth and tumor formation in hematologic diseases. The potential roles of *Lxn* in clinical and pharmaceutical applications call for a detailed examination of the signaling pathways and downstream regulators of the gene. For example, agonists of the *Lxn* signaling pathway (which may stimulate downstream partners of *Lxn*) may promote apoptosis in cancer cells; whereas antagonists (which block the *Lxn* signaling pathway) may be utilized in expanding hematopoietic progenitor cells for radiation victims, or facilitating hematopoietic reconstitution following stem cell transplantation. The treatments of hematologic disorders using stem cell therapies have advanced greatly in recent years. In this dissertation, I studied various functions of *Lxn* in hopes of aiding the development of such therapies.

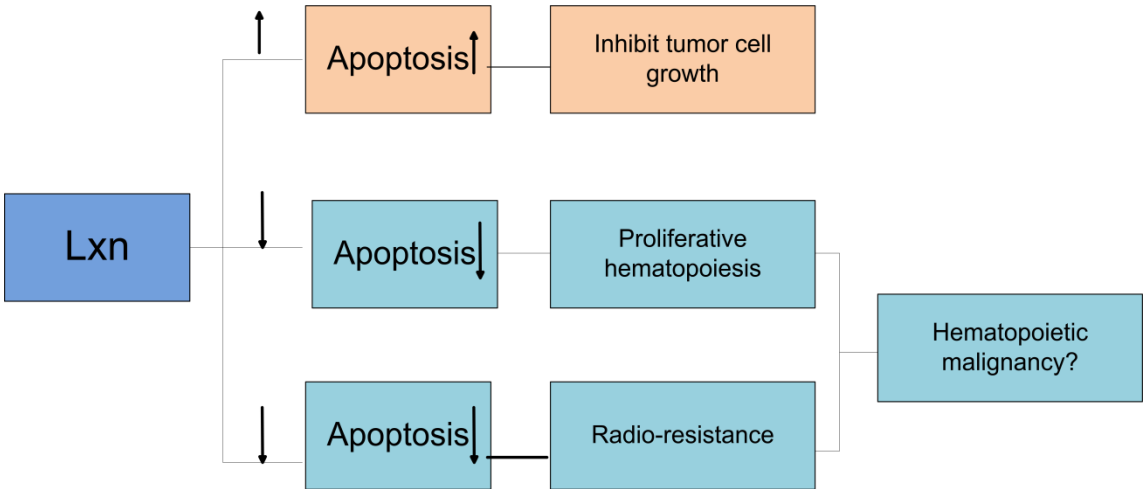

Figure 6.1 Mechanisms of *Lxn* in influencing hematopoietic biology through regulating apoptosis.

The expression of *Lxn* is positively correlated with apoptotic activities. Elevated expression levels of *Lxn* increase apoptotic frequency in tumor cells and inhibit tumor cell growth both in vitro and in vivo. Down-regulation of *Lxn* decreases apoptotic frequencies in the peripheral blood and BM and results in a proliferative hematopoiesis under homeostatic condition in *Lxn-/-* mice. Loss of *Lxn* expression also confers a radio-resistance to *Lxn-/-* mice by decreasing radiation-induced apoptosis.

APPENDIX

Abbreviations

ALL	Acute lymphoid leukemia
AML	Acute myeloid leukemia
ATLL	Acute T cell lymphoma
B6	C57BL/6 mouse
BM	Bone marrow
BrdU	5-bromo-2-deoxyuridine
CAFC	Cobblestone-forming cell assay
CB	Cord blood
CFU	Colony-forming cell unit
CLP	Common lymphoid progenitor
CMP	Common myeloid progenitor
CPA	Carboxypeptidase A
CR	Competitive repopulation
ECM	Extracellular matrix
FBS	Fetal bovine serum
G-CSF	Granulocyte-colony stimulating factor
Gfm-1	G-elongation factor, mitochondria-1
GMP	Granulocyte/monocyte progenitor
HPC	Hematopoietic progenitor cell
HSC	Hematopoietic stem cell
HSPC	Hematopoietic stem and progenitor cell
LK	Lineage-c-Kit+
LS	Lineage-Sca-1+
LSK	Lineage-c-Kit+Sca-1+
LT-HSC	Long term-hematopoietic stem cell
Lxn	Latexin
MEP	Megakaryocyte/erythroid progenitor
MPP	Multipotent progenitor
PBS	Phosphate buffered saline
PCPI	Potato carboxypeptidase inhibitor
PGE_2	Prostaglandin E_2
PI	Propidium iodide
PSGL-1	P-selectin glycoprotein ligand-1
PTH	Parathyroid hormone
SCF	Stem cell factor
SDF-1	Stromal derived factor-1
SP	Side population
ST-HSC	Short term-hematopoietic stem cell
T-PLL	T cell pro-lymphocytic leukemia
TBI	Total body irradiation
TIG-1	Tazarotene-induced gene1

REFERENCE

1. Bryder, D., Rossi, D.J. & Weissman, I.L. Hematopoietic stem cells: the paradigmatic tissue-specific stem cell. *Am J Pathol* **169**, 338-46 (2006).
2. McCulloch, E.A. & Till, J.E. The radiation sensitivity of normal mouse bone marrow cells, determined by quantitative marrow transplantation into irradiated mice. *Radiat Res* **13**, 115-25 (1960).
3. Till, J.E. & Mc, C.E. A direct measurement of the radiation sensitivity of normal mouse bone marrow cells. *Radiat Res* **14**, 213-22 (1961).
4. Van Zant, G., de Haan, G. & Rich, I.N. Alternatives to stem cell renewal from a developmental viewpoint. *Exp Hematol* **25**, 187-92 (1997).
5. Allsopp, R.C. & Weissman, I.L. Replicative senescence of hematopoietic stem cells during serial transplantation: does telomere shortening play a role? *Oncogene* **21**, 3270-3 (2002).
6. Trentin, J.J. Determination of bone marrow stem cell differentiation by stromal hemopoietic inductive microenvironments (HIM). *Am J Pathol* **65**, 621-8 (1971).
7. Wolf, N.S. & Trentin, J.J. Hemopoietic colony studies. V. Effect of hemopoietic organ stroma on differentiation of pluripotent stem cells. *J Exp Med* **127**, 205-14 (1968).
8. Schofield, R. The relationship between the spleen colony-forming cell and the haemopoietic stem cell. *Blood Cells* **4**, 7-25 (1978).
9. Doan, P.L. & Chute, J.P. The vascular niche: home for normal and malignant hematopoietic stem cells. *Leukemia* **26**, 54-62 (2011).

10. Mackie, E.J. Osteoblasts: novel roles in orchestration of skeletal architecture. *Int J Biochem Cell Biol* **35**, 1301-5 (2003).

11. Sipkins, D.A. et al. In vivo imaging of specialized bone marrow endothelial microdomains for tumour engraftment. *Nature* **435**, 969-73 (2005).

12. Visnjic, D. et al. Hematopoiesis is severely altered in mice with an induced osteoblast deficiency. *Blood* **103**, 3258-64 (2004).

13. Yamazaki, S. et al. Nonmyelinating Schwann cells maintain hematopoietic stem cell hibernation in the bone marrow niche. *Cell* **147**, 1146-58 (2011).

14. Naveiras, O. et al. Bone-marrow adipocytes as negative regulators of the haematopoietic microenvironment. *Nature* **460**, 259-63 (2009).

15. Kopp, H.G., Avecilla, S.T., Hooper, A.T. & Rafii, S. The bone marrow vascular niche: home of HSC differentiation and mobilization. *Physiology (Bethesda)* **20**, 349-56 (2005).

16. Calvi, L.M. et al. Osteoblastic cells regulate the haematopoietic stem cell niche. *Nature* **425**, 841-6 (2003).

17. Stier, S. et al. Osteopontin is a hematopoietic stem cell niche component that negatively regulates stem cell pool size. *J Exp Med* **201**, 1781-91 (2005).

18. Zhang, J. et al. Identification of the haematopoietic stem cell niche and control of the niche size. *Nature* **425**, 836-41 (2003).

19. Orkin, S.H. & Zon, L.I. Hematopoiesis: an evolving paradigm for stem cell biology. *Cell* **132**, 631-44 (2008).

20. Magnon, C. & Frenette, P.S. Hematopoietic stem cell trafficking. (2008).

21. Abkowitz, J.L., Robinson, A.E., Kale, S., Long, M.W. & Chen, J. Mobilization of hematopoietic stem cells during homeostasis and after cytokine exposure. *Blood* **102**, 1249-53 (2003).

22. Mendez-Ferrer, S., Lucas, D., Battista, M. & Frenette, P.S. Haematopoietic stem cell release is regulated by circadian oscillations. *Nature* **452**, 442-7 (2008).

23. Scadden, D.T. Circadian rhythms: stem cells traffic in time. *Nature* **452**, 416-7 (2008).

24. Katayama, Y. et al. Signals from the sympathetic nervous system regulate hematopoietic stem cell egress from bone marrow. *Cell* **124**, 407-21 (2006).

25. Wright, D.E. et al. Cyclophosphamide/granulocyte colony-stimulating factor causes selective mobilization of bone marrow hematopoietic stem cells into the blood after M phase of the cell cycle. *Blood* **97**, 2278-85 (2001).

26. Schwartzberg, L.S. et al. Peripheral blood stem cell mobilization by chemotherapy with and without recombinant human granulocyte colony-stimulating factor. *J Hematother* **1**, 317-27 (1992).

27. Neben, S., Marcus, K. & Mauch, P. Mobilization of hematopoietic stem and progenitor cell subpopulations from the marrow to the blood of mice following cyclophosphamide and/or granulocyte colony-stimulating factor. *Blood* **81**, 1960-7 (1993).

28. Duhrsen, U. et al. Effects of recombinant human granulocyte colony-

stimulating factor on hematopoietic progenitor cells in cancer patients. *Blood* **72**, 2074-81 (1988).

29. Molineux, G., Pojda, Z., Hampson, I.N., Lord, B.I. & Dexter, T.M. Transplantation potential of peripheral blood stem cells induced by granulocyte colony-stimulating factor. *Blood* **76**, 2153-8 (1990).

30. Sipkins, D.A. et al. Detection of tumor angiogenesis in vivo by alphaVbeta3-targeted magnetic resonance imaging. *Nat Med* **4**, 623-6 (1998).

31. Schweitzer, K.M. et al. Constitutive expression of E-selectin and vascular cell adhesion molecule-1 on endothelial cells of hematopoietic tissues. *Am J Pathol* **148**, 165-75 (1996).

32. Dimitroff, C.J., Lee, J.Y., Rafii, S., Fuhlbrigge, R.C. & Sackstein, R. CD44 is a major E-selectin ligand on human hematopoietic progenitor cells. *J Cell Biol* **153**, 1277-86 (2001).

33. Levesque, J.P. et al. PSGL-1-mediated adhesion of human hematopoietic progenitors to P-selectin results in suppression of hematopoiesis. *Immunity* **11**, 369-78 (1999).

34. Petit, I. et al. G-CSF induces stem cell mobilization by decreasing bone marrow SDF-1 and up-regulating CXCR4. *Nat Immunol* **3**, 687-94 (2002).

35. Levesque, J.P., Hendy, J., Takamatsu, Y., Simmons, P.J. & Bendall, L.J. Disruption of the CXCR4/CXCL12 chemotactic interaction during hematopoietic stem cell mobilization induced by GCSF or cyclophosphamide. *J Clin Invest* **111**, 187-96 (2003).

36. Pelus, L.M. et al. The CXCR4 agonist peptide, CTCE-0021, rapidly mobilizes polymorphonuclear neutrophils and hematopoietic progenitor cells into peripheral blood and synergizes with granulocyte colony-stimulating factor. *Exp Hematol* **33**, 295-307 (2005).

37. Papayannopoulou, T., Priestley, G.V., Nakamoto, B., Zafiropoulos, V. & Scott, L.M. Molecular pathways in bone marrow homing: dominant role of alpha(4)beta(1) over beta(2)-integrins and selectins. *Blood* **98**, 2403-11 (2001).

38. Frenette, P.S., Subbarao, S., Mazo, I.B., von Andrian, U.H. & Wagner, D.D. Endothelial selectins and vascular cell adhesion molecule-1 promote hematopoietic progenitor homing to bone marrow. *Proc Natl Acad Sci U S A* **95**, 14423-8 (1998).

39. Peled, A. et al. Immature leukemic CD34+CXCR4+ cells from CML patients have lower integrin-dependent migration and adhesion in response to the chemokine SDF-1. *Stem Cells* **20**, 259-66 (2002).

40. Cancelas, J.A. et al. Rac GTPases differentially integrate signals regulating hematopoietic stem cell localization. *Nat Med* **11**, 886-91 (2005).

41. Yang, F.C. et al. Rac and Cdc42 GTPases control hematopoietic stem cell shape, adhesion, migration, and mobilization. *Proc Natl Acad Sci U S A* **98**, 5614-8 (2001).

42. Hoggatt, J., Singh, P., Sampath, J. & Pelus, L.M. Prostaglandin E2 enhances hematopoietic stem cell homing, survival, and proliferation. *Blood* **113**, 5444-55 (2009).

43. Ballen, K.K. et al. Phase I trial of parathyroid hormone to facilitate stem cell mobilization. *Biol Blood Marrow Transplant* **13**, 838-43 (2007).

44. Garrett, R.W. & Emerson, S.G. The role of parathyroid hormone and insulin-like growth factors in hematopoietic niches: physiology and pharmacology. *Mol Cell Endocrinol* **288**, 6-10 (2008).

45. Kanaar, R., Hoeijmakers, J.H. & van Gent, D.C. Molecular mechanisms of DNA double strand break repair. *Trends Cell Biol* **8**, 483-9 (1998).

46. Romero-Weaver, A.L. & Kennedy, A.R. Comparison of Two Methods for the Determination of the Effects of Ionizing Radiation on Blood Cell Counts in Mice. *Int J Biomed Sci* **8**, 7-15.

47. Pluzanska, A. et al. [Early effects of treatment with radium and cobalt-60 gamma radiation on the proportions and absolute counts of T and B lymphocytes in peripheral blood of women with cervical carcinoma]. *Nowotwory* **27**, 225-32 (1977).

48. Haimovitz-Friedman, A. Radiation-induced signal transduction and stress response. *Radiat Res* **150**, S102-8 (1998).

49. Meng, A., Wang, Y., Brown, S.A., Van Zant, G. & Zhou, D. Ionizing radiation and busulfan inhibit murine bone marrow cell hematopoietic function via apoptosis-dependent and -independent mechanisms. *Exp Hematol* **31**, 1348-56 (2003).

50. Wang, Y., Schulte, B.A., LaRue, A.C., Ogawa, M. & Zhou, D. Total body irradiation selectively induces murine hematopoietic stem cell senescence. *Blood* **107**, 358-66 (2006).

51. Budworth, H. et al. DNA repair and cell cycle biomarkers of radiation exposure and inflammation stress in human blood. *PLoS One* **7**, e48619.

52. Wu, H. et al. The role of DNA damage repair and Chk2 protein in hyper-radiosensitivity of lung adenocarcinoma A549 cells. *J Huazhong Univ Sci Technolog Med Sci* **32**, 750-4.

53. Huh, W.J., Pan, X.O., Mysorekar, I.U. & Mills, J.C. Location, allocation, relocation: isolating adult tissue stem cells in three dimensions. *Curr Opin Biotechnol* **17**, 511-7 (2006).

54. Morrison, S.J., Uchida, N. & Weissman, I.L. The biology of hematopoietic stem cells. *Annu Rev Cell Dev Biol* **11**, 35-71 (1995).

55. Muller-Sieburg, C.E., Whitlock, C.A. & Weissman, I.L. Isolation of two early B lymphocyte progenitors from mouse marrow: a committed pre-pre-B cell and a clonogenic Thy-1-lo hematopoietic stem cell. *Cell* **44**, 653-62 (1986).

56. Spangrude, G.J., Heimfeld, S. & Weissman, I.L. Purification and characterization of mouse hematopoietic stem cells. *Science* **241**, 58-62 (1988).

57. Spangrude, G.J. & Brooks, D.M. Mouse strain variability in the expression of the hematopoietic stem cell antigen Ly-6A/E by bone marrow cells. *Blood* **82**, 3327-32 (1993).

58. van de Rijn, M., Heimfeld, S., Spangrude, G.J. & Weissman, I.L. Mouse hematopoietic stem-cell antigen Sca-1 is a member of the Ly-6 antigen family. *Proc Natl Acad Sci U S A* **86**, 4634-8 (1989).

59. Ikuta, K. & Weissman, I.L. Evidence that hematopoietic stem cells express mouse c-kit but do not depend on steel factor for their generation. *Proc Natl Acad Sci U S A* **89**, 1502-6 (1992).

60. Ikuta, K., Ingolia, D.E., Friedman, J., Heimfeld, S. & Weissman, I.L. Mouse hematopoietic stem cells and the interaction of c-kit receptor and steel factor. *Int J Cell Cloning* **9**, 451-60 (1991).

61. Morrison, S.J. & Weissman, I.L. The long-term repopulating subset of hematopoietic stem cells is deterministic and isolatable by phenotype. *Immunity* **1**, 661-73 (1994).

62. Morrison, S.J., Lagasse, E. & Weissman, I.L. Demonstration that Thy(lo) subsets of mouse bone marrow that express high levels of lineage markers are not significant hematopoietic progenitors. *Blood* **83**, 3480-90 (1994).

63. Osawa, M., Hanada, K., Hamada, H. & Nakauchi, H. Long-term lymphohematopoietic reconstitution by a single CD34-low/negative hematopoietic stem cell. *Science* **273**, 242-5 (1996).

64. Yang, L. et al. Identification of Lin(-)Sca1(+)kit(+)CD34(+)Flt3- short-term hematopoietic stem cells capable of rapidly reconstituting and rescuing myeloablated transplant recipients. *Blood* **105**, 2717-23 (2005).

65. Blank, U., Karlsson, G. & Karlsson, S. Signaling pathways governing stem-cell fate. *Blood* **111**, 492-503 (2008).

66. Kiel, M.J., Yilmaz, O.H., Iwashita, T., Terhorst, C. & Morrison, S.J. SLAM family receptors distinguish hematopoietic stem and progenitor cells and

reveal endothelial niches for stem cells. *Cell* **121**, 1109-21 (2005).

67. Yilmaz, O.H., Kiel, M.J. & Morrison, S.J. SLAM family markers are conserved among hematopoietic stem cells from old and reconstituted mice and markedly increase their purity. *Blood* **107**, 924-30 (2006).

68. Goodell, M.A., Brose, K., Paradis, G., Conner, A.S. & Mulligan, R.C. Isolation and functional properties of murine hematopoietic stem cells that are replicating in vivo. *J Exp Med* **183**, 1797-806 (1996).

69. Pereira, C., Clarke, E. & Damen, J. Hematopoietic colony-forming cell assays. *Methods Mol Biol* **407**, 177-208 (2007).

70. Bradley, T.R. & Metcalf, D. The growth of mouse bone marrow cells in vitro. *Aust J Exp Biol Med Sci* **44**, 287-99 (1966).

71. Gregory, C.J. & Eaves, A.C. Human marrow cells capable of erythropoietic differentiation in vitro: definition of three erythroid colony responses. *Blood* **49**, 855-64 (1977).

72. Gregory, C.J. & Eaves, A.C. Three stages of erythropoietic progenitor cell differentiation distinguished by a number of physical and biologic properties. *Blood* **51**, 527-37 (1978).

73. Miller, C.L., Dykstra, B. & Eaves, C.J. Characterization of mouse hematopoietic stem and progenitor cells. *Curr Protoc Immunol* **Chapter 22**, Unit 22B 2 (2008).

74. Ichikawa, Y., Pluznik, D.H. & Sachs, L. In vitro control of the development of macrophage and granulocyte colonies. *Proc Natl Acad Sci U S A* **56**, 488-95 (1966).

75. Pluznik, D.H. & Sachs, L. The induction of clones of normal mast cells by a substance from conditioned medium. *Exp Cell Res* **43**, 553-63 (1966).

76. Ploemacher, R.E., van der Sluijs, J.P., Voerman, J.S. & Brons, N.H. An in vitro limiting-dilution assay of long-term repopulating hematopoietic stem cells in the mouse. *Blood* **74**, 2755-63 (1989).

77. Ploemacher, R.E., Van der Loo, J.C. & Van der Sluijs, J.P. In vitro assays for primitive hematopoietic cells. *Blood* **79**, 834-7 (1992).

78. Ploemacher, R.E., van der Sluijs, J.P., van Beurden, C.A., Baert, M.R. & Chan, P.L. Use of limiting-dilution type long-term marrow cultures in frequency analysis of marrow-repopulating and spleen colony-forming hematopoietic stem cells in the mouse. *Blood* **78**, 2527-33 (1991).

79. Ploemacher, R.E., van der Loo, J.C., van Beurden, C.A. & Baert, M.R. Wheat germ agglutinin affinity of murine hemopoietic stem cell subpopulations is an inverse function of their long-term repopulating ability in vitro and in vivo. *Leukemia* **7**, 120-30 (1993).

80. Coulombel, L. Identification of hematopoietic stem/progenitor cells: strength and drawbacks of functional assays. *Oncogene* **23**, 7210-22 (2004).

81. Xing, Z. et al. Increased hematopoietic stem cell mobilization in aged mice. *Blood* **108**, 2190-7 (2006).

82. Harrison, D.E. Competitive repopulation: a new assay for long-term stem cell functional capacity. *Blood* **55**, 77-81 (1980).

83. van Os, R., Kamminga, L.M. & de Haan, G. Stem cell assays: something

old, something new, something borrowed. *Stem Cells* **22**, 1181-90 (2004).

84. Barnes, D.W., Ford, C.E. & Loutit, J.F. [Serial grafts of homologous bone marrow in irradiated mice]. *Sang* **30**, 762-5 (1959).

85. Koller, P.C. & Doak, S.M. Serial transfer of donor marrow in radiation mouse chimaeras. *Int J Radiat Biol* **2**, 1-7 (1960).

86. Pallares, I. et al. Structure of human carboxypeptidase A4 with its endogenous protein inhibitor, latexin. *Proc Natl Acad Sci U S A* **102**, 3978-83 (2005).

87. Aagaard, A. et al. An inflammatory role for the mammalian carboxypeptidase inhibitor latexin: relationship to cystatins and the tumor suppressor TIG1. *Structure* **13**, 309-17 (2005).

88. Takiguchi-Hayashi, K. & Arimatsu, Y. Restricted expression of latexin in dorsal midline cells of developing rat forebrain. *Neuroreport* **6**, 281-3 (1995).

89. Arimatsu, Y. Latexin: a molecular marker for regional specification in the neocortex. *Neurosci Res* **20**, 131-5 (1994).

90. Jin, M. et al. Reduced pain sensitivity in mice lacking latexin, an inhibitor of metallocarboxypeptidases. *Brain Res* **1075**, 117-21 (2006).

91. Uratani, Y. et al. Latexin, a carboxypeptidase A inhibitor, is expressed in rat peritoneal mast cells and is associated with granular structures distinct from secretory granules and lysosomes. *Biochem J* **346 Pt 3**, 817-26 (2000).

92. de Haan, G. Latexin is a newly discovered regulator of hematopoietic stem

cells. *Nat Genet* **39**, 141-2 (2007).

93. Liang, Y., Jansen, M., Aronow, B., Geiger, H. & Van Zant, G. The quantitative trait gene latexin influences the size of the hematopoietic stem cell population in mice. *Nat Genet* **39**, 178-88 (2007).

94. Pelus, L.M. Peripheral blood stem cell mobilization: new regimens, new cells, where do we stand. *Curr Opin Hematol* **15**, 285-92 (2008).

95. Pelus, L.M. & Fukuda, S. Peripheral blood stem cell mobilization: the CXCR2 ligand GRObeta rapidly mobilizes hematopoietic stem cells with enhanced engraftment properties. *Exp Hematol* **34**, 1010-20 (2006).

96. Chambers, S.M. et al. Aging hematopoietic stem cells decline in function and exhibit epigenetic dysregulation. *PLoS Biol* **5**, e201 (2007).

97. Peled, A. et al. The chemokine SDF-1 stimulates integrin-mediated arrest of CD34(+) cells on vascular endothelium under shear flow. *J Clin Invest* **104**, 1199-211 (1999).

98. Svinareva, D.A., Nifontova, I.N., Chertkov, I.L. & Drize, N.I. Changed homing of hemopoietic precursor cells after long-term treatment with parathyroid hormone. *Bull Exp Biol Med* **142**, 86-9 (2006).

99. Sackstein, R. et al. Ex vivo glycan engineering of CD44 programs human multipotent mesenchymal stromal cell trafficking to bone. *Nat Med* **14**, 181-7 (2008).

100. Christopherson, K.W., 2nd, Hangoc, G., Mantel, C.R. & Broxmeyer, H.E. Modulation of hematopoietic stem cell homing and engraftment by CD26. *Science* **305**, 1000-3 (2004).

101. Peranteau, W.H. et al. CD26 inhibition enhances allogeneic donor-cell homing and engraftment after in utero hematopoietic-cell transplantation. *Blood* **108**, 4268-74 (2006).

102. Takiguchi-Hayashi, K. In vitro clonal analysis of rat cerebral cortical neurons expressing latexin, a subtype-specific molecular marker of glutamatergic neurons. *Brain Res Dev Brain Res* **132**, 87-90 (2001).

103. Takiguchi-Hayashi, K. et al. Latexin expression in smaller diameter primary sensory neurons in the rat. *Brain Res* **801**, 9-20 (1998).

104. Mouradov, D. et al. Modelling the structure of latexin-carboxypeptidase A complex based on chemical cross-linking and molecular docking. *Protein Eng Des Sel* **19**, 9-16 (2006).

105. Garcia-Castellanos, R. et al. Detailed molecular comparison between the inhibition mode of A/B-type carboxypeptidases in the zymogen state and by the endogenous inhibitor latexin. *Cell Mol Life Sci* **62**, 1996-2014 (2005).

106. Youssef, E.M. et al. Hypermethylation and silencing of the putative tumor suppressor Tazarotene-induced gene 1 in human cancers. *Cancer Res* **64**, 2411-7 (2004).

107. Liu, Y. et al. Latexin is down-regulated in hematopoietic malignancies and restoration of expression inhibits lymphoma growth. *PLoS One* **7**, e44979.

108. Wu, X. et al. The haploinsufficient hematopoietic microenvironment is critical to the pathological fracture repair in murine models of neurofibromatosis type 1. *PLoS One* **6**, e24917.

109. Walkley, C.R. et al. A microenvironment-induced myeloproliferative syndrome caused by retinoic acid receptor gamma deficiency. *Cell* **129**, 1097-110 (2007).

110. Casanova-Acebes, M. et al. Rhythmic modulation of the hematopoietic niche through neutrophil clearance. *Cell* **153**, 1025-35.

111. Clezardin, P., Frappart, L., Clerget, M., Pechoux, C. & Delmas, P.D. Expression of thrombospondin (TSP1) and its receptors (CD36 and CD51) in normal, hyperplastic, and neoplastic human breast. *Cancer Res* **53**, 1421-30 (1993).

112. Isenberg, J.S. et al. Thrombospondin-1 and CD47 limit cell and tissue survival of radiation injury. *Am J Pathol* **173**, 1100-12 (2008).

113. Soto-Pantoja, D.R. et al. CD47 deficiency confers cell and tissue radioprotection by activation of autophagy. *Autophagy* **8**, 1628-42.

114. Soula-Rothhut, M. et al. The tumor suppressor PTEN inhibits EGF-induced TSP-1 and TIMP-1 expression in FTC-133 thyroid carcinoma cells. *Exp Cell Res* **304**, 187-201 (2005).

115. Lawler, J. et al. Thrombospondin-1 gene expression affects survival and tumor spectrum of p53-deficient mice. *Am J Pathol* **159**, 1949-56 (2001).

116. Nor, J.E. et al. Thrombospondin-1 induces endothelial cell apoptosis and inhibits angiogenesis by activating the caspase death pathway. *J Vasc Res* **37**, 209-18 (2000).

117. Maxhimer, J.B. et al. Radioprotection in normal tissue and delayed tumor growth by blockade of CD47 signaling. *Sci Transl Med* **1**, 3ra7 (2009).

118. Watters, D. Molecular mechanisms of ionizing radiation-induced apoptosis. *Immunol Cell Biol* **77**, 263-71 (1999).

119. Peslak, S.A. et al. EPO-mediated expansion of late-stage erythroid progenitors in the bone marrow initiates recovery from sublethal radiation stress. *Blood* **120**, 2501-11.

120. Wagemaker, G. Heterogeneity of radiation sensitivity of hemopoietic stem cell subsets. *Stem Cells* **13 Suppl 1**, 257-60 (1995).

121. van Bekkum, D.W. Radiation sensitivity of the hemopoietic stem cell. *Radiat Res* **128**, S4-8 (1991).

122. Lutgens, L.C. et al. Citrulline: a physiologic marker enabling quantitation and monitoring of epithelial radiation-induced small bowel damage. *Int J Radiat Oncol Biol Phys* **57**, 1067-74 (2003).

123. Thames, H.D., Bentzen, S.M., Turesson, I., Overgaard, M. & Van den Bogaert, W. Time-dose factors in radiotherapy: a review of the human data. *Radiother Oncol* **19**, 219-35 (1990).

124. Kelly, P.N. & Strasser, A. The role of Bcl-2 and its pro-survival relatives in tumourigenesis and cancer therapy. *Cell death and differentiation* **18**, 1414-24 (2011).

125. Miyashita, T., Harigai, M., Hanada, M. & Reed, J.C. Identification of a p53-dependent negative response element in the bcl-2 gene. *Cancer Res* **54**, 3131-5 (1994).

126. Miyashita, T. et al. Tumor suppressor p53 is a regulator of bcl-2 and bax gene expression in vitro and in vivo. *Oncogene* **9**, 1799-805 (1994).

127. Tokalov, S.V., Pieck, S. & Gutzeit, H.O. Varying responses of human cells with discrepant p53 activity to ionizing radiation and heat shock exposure. *Cell Prolif* **40**, 24-37 (2007).

128. Fei, P. & El-Deiry, W.S. P53 and radiation responses. *Oncogene* **22**, 5774-83 (2003).

129. Smith, M.L. et al. p53-mediated DNA repair responses to UV radiation: studies of mouse cells lacking p53, p21, and/or gadd45 genes. *Mol Cell Biol* **20**, 3705-14 (2000).

130. Soto-Pantoja, D.R., Isenberg, J.S. & Roberts, D.D. Therapeutic Targeting of CD47 to Modulate Tissue Responses to Ischemia and Radiation. *J Genet Syndr Gene Ther* **2**.

131. Bolstad, B.M., Irizarry, R.A., Astrand, M. & Speed, T.P. A comparison of normalization methods for high density oligonucleotide array data based on variance and bias. *Bioinformatics* **19**, 185-93 (2003).

132. Subramanian, A. et al. Gene set enrichment analysis: a knowledge-based approach for interpreting genome-wide expression profiles. *Proc Natl Acad Sci U S A* **102**, 15545-50 (2005).

133. Forsberg, E.C. & Smith-Berdan, S. Parsing the niche code: the molecular mechanisms governing hematopoietic stem cell adhesion and differentiation. *Haematologica* **94**, 1477-81 (2009).

134. Bergstrom, S.E., Bergdahl, E. & Sundqvist, K.G. A Cytokine-Controlled Mechanism for Integrated Regulation of T Lymphocyte Motility, Adhesion and Activation. *Immunology*.

135. Dick, J.E. & Lapidot, T. Biology of normal and acute myeloid leukemia stem cells. *Int J Hematol* **82**, 389-96 (2005).

136. Marx, J. Molecular biology. Cancer's perpetual source? *Science* **317**, 1029-31 (2007).

137. Huntly, B.J. & Gilliland, D.G. Leukaemia stem cells and the evolution of cancer-stem-cell research. *Nat Rev Cancer* **5**, 311-21 (2005).

138. Hatanaka, Y. et al. Intracortical regionality represented by specific transcription for a novel protein, latexin. *Eur J Neurosci* **6**, 973-82 (1994).

139. Arimatsu, Y., Ishida, M., Takiguchi-Hayashi, K. & Uratani, Y. Cerebral cortical specification by early potential restriction of progenitor cells and later phenotype control of postmitotic neurons. *Development* **126**, 629-38 (1999).

140. Arimatsu, Y., Kojima, M. & Ishida, M. Area- and lamina-specific organization of a neuronal subpopulation defined by expression of latexin in the rat cerebral cortex. *Neuroscience* **88**, 93-105 (1999).

141. Arimatsu, Y., Ishida, M., Kaneko, T., Ichinose, S. & Omori, A. Organization and development of corticocortical associative neurons expressing the orphan nuclear receptor Nurr1. *J Comp Neurol* **466**, 180-96 (2003).

142. Aagaard, A. et al. An inflammatory role for the mammalian carboxypeptidase inhibitor latexin: relationship to cystatins and the tumor suppressor TIG1. *Structure (Camb)* **13**, 309-17 (2005).

143. Jing, C. et al. Tazarotene-induced gene 1 (TIG1) expression in prostate carcinomas and its relationship to tumorigenicity. *J Natl Cancer Inst* **94**,

482-90 (2002).

144. Kwong, J. et al. Silencing of the retinoid response gene TIG1 by promoter hypermethylation in nasopharyngeal carcinoma. *Int J Cancer* **113**, 386-92 (2005).

145. Zhang, J., Liu, L. & Pfeifer, G.P. Methylation of the retinoid response gene TIG1 in prostate cancer correlates with methylation of the retinoic acid receptor beta gene. *Oncogene* **23**, 2241-9 (2004).

146. Termini, L. et al. Characterization of global transcription profile of normal and HPV-immortalized keratinocytes and their response to TNF treatment. *BMC Med Genomics* **1**, 29 (2008).

147. Li, Y. et al. Latexin expression is downregulated in human gastric carcinomas and exhibits tumor suppressor potential. *BMC cancer* **11**, 121 (2011).

148. Mitsunaga, K., Kikuchi, J., Wada, T. & Furukawa, Y. Latexin regulates the abundance of multiple cellular proteins in hematopoietic stem cells. *Journal of cellular physiology* **227**, 1138-47 (2012).

149. Muthusamy, V. et al. Epigenetic silencing of novel tumor suppressors in malignant melanoma. *Cancer research* **66**, 11187-93 (2006).

150. Feinberg, A.P., Ohlsson, R. & Henikoff, S. The epigenetic progenitor origin of human cancer. *Nat Rev Genet* **7**, 21-33 (2006).

151. Fraga, M.F. et al. Epigenetic differences arise during the lifetime of monozygotic twins. *Proc Natl Acad Sci U S A* **102**, 10604-9 (2005).

152. Fraga, M.F. & Esteller, M. Epigenetics and aging: the targets and the

marks. *Trends Genet* **23**, 413-8 (2007).

153. Fraga, M.F., Agrelo, R. & Esteller, M. Cross-talk between aging and cancer: the epigenetic language. *Ann N Y Acad Sci* **1100**, 60-74 (2007).

154. Shames, D.S., Minna, J.D. & Gazdar, A.F. DNA methylation in health, disease, and cancer. *Curr Mol Med* **7**, 85-102 (2007).

155. Oakley, E.J. & Van Zant, G. Unraveling the complex regulation of stem cells: implications for aging and cancer. *Leukemia* **21**, 612-21 (2007).

156. Toyota, M. & Issa, J.P. Epigenetic changes in solid and hematopoietic tumors. *Semin Oncol* **32**, 521-30 (2005).

157. Sahab, Z.J. et al. Tumor suppressor RARRES1 interacts with cytoplasmic carboxypeptidase AGBL2 to regulate the alpha-tubulin tyrosination cycle. *Cancer research* **71**, 1219-28 (2011).

158. Gururajan, M. et al. c-Jun N-terminal kinase (JNK) is required for survival and proliferation of B-lymphoma cells. *Blood* **106**, 1382-91 (2005).

159. Blanco-Aparicio, C. et al. Potato carboxypeptidase inhibitor, a T-knot protein, is an epidermal growth factor antagonist that inhibits tumor cell growth. *J Biol Chem* **273**, 12370-7 (1998).

160. Dykstra, B., Olthof, S., Schreuder, J., Ritsema, M. & de Haan, G. Clonal analysis reveals multiple functional defects of aged murine hematopoietic stem cells. *The Journal of experimental medicine* **208**, 2691-703 (2011).

161. Greaves, M. & Maley, C.C. Clonal evolution in cancer. *Nature* **481**, 306-13 (2012).

162. Yan, B. et al. The PIM-2 kinase phosphorylates BAD on serine 112 and

reverses BAD-induced cell death. *The Journal of biological chemistry* **278**, 45358-67 (2003).

163. Macdonald, A. et al. Pim kinases phosphorylate multiple sites on Bad and promote 14-3-3 binding and dissociation from Bcl-XL. *BMC cell biology* **7**, 1 (2006).

164. Gomez-Abad, C. et al. PIM2 inhibition as a rational therapeutic approach in B-cell lymphoma. *Blood* **118**, 5517-27 (2011).

165. Lin, Y.W. et al. A small molecule inhibitor of Pim protein kinases blocks the growth of precursor T-cell lymphoblastic leukemia/lymphoma. *Blood* **115**, 824-33 (2010).

166. Agrawal-Singh, S. et al. Pim2 cooperates with PML-RARalpha to induce acute myeloid leukemia in a bone marrow transplantation model. *Blood* **115**, 4507-16 (2010).

167. Wang, Y. et al. Total body irradiation causes residual bone marrow injury by induction of persistent oxidative stress in murine hematopoietic stem cells. *Free Radic Biol Med* **48**, 348-56.

168. Ahmed, M.M. et al. Ionizing radiation-inducible apoptosis in the absence of p53 linked to transcription factor EGR-1. *J Biol Chem* **272**, 33056-61 (1997).

169. Norimura, T., Nomoto, S., Katsuki, M., Gondo, Y. & Kondo, S. p53-dependent apoptosis suppresses radiation-induced teratogenesis. *Nat Med* **2**, 577-80 (1996).

170. Erlacher, M. et al. BH3-only proteins Puma and Bim are rate-limiting for

gamma-radiation- and glucocorticoid-induced apoptosis of lymphoid cells in vivo. *Blood* **106**, 4131-8 (2005).

171. Mustata, G. et al. Development of Small-Molecule PUMA Inhibitors for Mitigating Radiation-Induced Cell Death. *Curr Top Med Chem*.

172. Qiu, W. et al. PUMA regulates intestinal progenitor cell radiosensitivity and gastrointestinal syndrome. *Cell Stem Cell* **2**, 576-83 (2008).

173. Shao, L. et al. Deletion of proapoptotic Puma selectively protects hematopoietic stem and progenitor cells against high-dose radiation. *Blood* **115**, 4707-14.

174. Fuchs, Y. et al. Sept4/ARTS regulates stem cell apoptosis and skin regeneration. *Science* **341**, 286-9.

VITA

Yi Liu was born in Xianyang, Shaanxi, China

Education
Fall 2008 to Spring 2009: Graduate Student, Integrated Biomedical Science (IBS) Ph.D. Program, University of Kentucky, Lexington, KY

Fall 2005 to Spring 2007: Master of Science, College of Agriculture and Biotechnology, Zhejiang University, Hangzhou, Zhejiang, China

Fall 2001 to Spring 2005: Bachelor of Science, Department of Plant Protection, Northwest A &F University, Xi'an, Shaanxi, China

Scholastic Honors

2012	ASH Abstract Achievement Award
2012	Graduate School Travel Award
2011-2012	Kentucky Opportunity Fellowship
2011	Graduate School Travel Award

Poster and Oral Presentations (selected)

2012 Annual meeting of American Society of Hematology, Atlanta, GA: Yi Liu, Carol Swiderski, Barry Grimes, Chi Wang, Ying Liang, and Gary Van Zant; A Cell-Autonomous Myeloproliferatvie phenotype Caused by Loss of Latexin In Stem and Progenitor Cells. (Poster)

2012 Midwest Blood Club Symposium, Indianapolis, IN; Yi Liu, Ying Liang and Gary Van Zant; Latexin expression in hematopoietic malignancies and its inhibition of lymphoma growth as a novel tumor suppressor. (Poster)

2011 Keystone Symposium, Big Sky, MT; Yi Liu, Erin J. Oakley, Kyle Rector and Gary Van Zant. Age and mouse strain variation in the functional capacity of highly purified hematopoietic stem cells. (Poster)

2010 Markey Cancer Center Research Day, Lexington, KY; Yi Liu, Ying Liang and Gary Van Zant; Latexin expression in hematopoietic malignancies and its inhibition of lymphoma growth as a novel tumor suppressor. (Poster)

Publications

1. Yi Liu, Diana Howard, Kyle Rector, Carol Swiderski , Jason Brandon, Lawrence Schook, Jayesh Mehta, J. Scott Bryson, Subbarao Bondada and Ying Liang. Latexin is down-regulated in hematopoietic malignancies and restoration of expression inhibits lymphoma growth. ***Plos One*** 7(9):e41796.

2. Kyle Rector, Yi Liu, and Gary Van Zant. Hematopoietic stem cell isolation methods. ***Aging and Stem Cells: Methods and Protocols***

3. Chenjun Ding, Ling Qing, Zhenghe Li, Yi Liu, Yajuan Qian, Xueping Zhou. 2009. Genetic determinants of symptoms on viral DNA satellites. ***Applied and Environmental Microbiology*** 75(16)：5380-5389

4. Yajuan Qian, Zhong Tian, Yi Liu, Rob Briddon, Xueping Zhou. 2008. Size revision of a truncated DNAβ associated with *Tobacco curly shoot virus*. ***Virus Research*** 131(2) : 288-292